AN ATLAS OF CENOZOIC CLIMATE ZONES

by

CLINTON WHITAKER CROWLEY

Presented to the Faculty of the Graduate School of

The University of Texas at Arlington in Partial Fulfillment

of the Requirements

for the Degree of

MASTER OF SCIENCE IN GEOLOGY

THE UNIVERSITY OF TEXAS AT ARLINGTON

May 2012

ACKNOWLEDGEMENTS

I would like to thank Dr. Scotese for making me a part of the PALEOMAP Project. Our collaboration put my artwork in the National Geographic—the magazine that introduced science and discovery to me as a child.

I thank Dr. Arne Winguth and Dr. Harry Rowe for their work reviewing this thesis. Dr. Winguth's own work is relevant to this topic, and I refer to it in these pages. Dr. Gary Upchurch of Texas State University, though not a committee member, has worked with Dr. Scotese. He gave me a great deal of his research to use in this atlas.

Thanks to Derek Main, of the Arlington Archosaur Site, I can now say my art is on the cover of an international scientific journal, and has been printed in other periodicals as well. Thanks also to Dean Williams and Mark Kalpakis at Joint Resources Company. They gave me the resources and the time to complete this degree, and a concurrent education in the oil business.

Many other people in the department helped me out through my graduate student career. My compliments to all of you—Dr. John Wickham, Beth Ballard, Kim Gray, Paula Burkhart, Wanda Slagle, Pat Cowan, Dr. Gloria Eisenstadt, and Dr. Larry Standlee.

My parents sparked my interest in geology. Claude and Carolyn Crowley took their children outdoors to see streams and roadcuts at a very early age. They told us of the long-ago worlds that made the rocks we lived on in Tennessee and Texas. When I found out that the continents themselves were moving, my vocation became clear.

I'm fortunate to have known Dr. Donald Reaser, who took a lively interest in my career, turbocharging my interest in local geology. We agreed that a worthy geologist should die clutching a rock hammer, or while looking down a microscope. I intend to go out like that, myself.

April 9, 2012

ABSTRACT

AN ATLAS OF CENOZOIC CLIMATE ZONES

Clinton W. Crowley, M.S.

The University of Texas at Arlington, 2012

Supervising Professor: Christopher Scotese

This atlas illustrates global climatic zones in five major turning points of Cenozoic climate history: the K/T, the Paleocene/Eocene Thermal Maximum (PETM), the Eocene/Oligocene Transition (EOT), the Late Miocene (Messinian), and the Last Glacial Maximum (LGM). The maps were produced from a combination of climate simulations (FOAM, CCSM, ECHAM, BESTGUESS, GENESIS and others) and climatic zone reconstructions based on lithologic data. Paleogeographic base maps of the time intervals from the PALEOMAP Project were then illustrated with an artist's rendition of the Earth's appearance. The color scheme was based on NASA's Blue Marble images. An overview of the conditions that shaped global climate zones in each time interval accompanies the atlas: plate tectonics, paleogeography, configuration of ocean basins and currents, greenhouse gas concentration, plant life, and other climate forcing mechanisms.

TABLE OF CONTENTS

LIST OF ILLUSTRATIONS

Figure Page

LIST OF TABLES

CHAPTER 1

INTRODUCTION

1.1 Global Climates of the Cenozoic Era

During the Cenozoic Era, global climate changed dramatically. The early Cenozoic was a continuation of the Cretaceous Hot House World. Global temperatures rapidly increased across the Paleocene/Eocene boundary—the Paleocene/Eocene Thermal Maximum (PETM) (Zachos et al., 2008). Hot House conditions persisted until the end of the Eocene, when global climate began to rapidly cool. During the late Cenozoic, global climate plunged into the depths of the current Ice House. Antarctica was glaciated in the Oligocene, and full bipolar Ice House glaciation began in the Miocene.

To better understand these global climatic changes, I have visualized the Earth's appearance in a series of artistically rendered paleoclimate reconstructions. The images are most similar to climatic zone maps, such as the Köppen-Geiger map of the modern world's vegetation zones. Climate reconstructions for the following 5 time intervals have been produced: Last Glacial Maximum (20 Ka), Late Miocene (6 Ma), Eocene-Oligocene boundary (34 Ma), Paleocene-Eocene Thermal Maximum (55 Ma), and K/T boundary (65 Ma) (Table 1.1).

Each chapter in this thesis describes the paleoclimate reconstruction of one of the five time intervals in Table 1.1. Each map is accompanied by a chapter with appropriate documentation and discussion of the relevant scientific issues. Examples of these points of discussion are the Paleocene/Eocene Thermal Maximum, the Eocene/Oligocene Transition, the Miocene beginnings of the Ice House World, and the Ice Age World of the Pliocene/Pleistocene.

Table 1.1 Important Moments In Cenozoic Climate History.

Time interval	Stage	Age
Present-day	Holocene	Today
Last Glacial Maximum	Late Pleistocene	20,000 Ka
Late Miocene	Messinian	6 Ma
Eocene/Oligocene	Priabonian/Rupelian	34 Ma
Paleocene/Eocene Thermal Maximum (PETM)	Thanetian/Ypresian	55 Ma
Cretaceous/Tertiary boundary (K/T)	Maastrichtian/Danian	65 Ma

In the past few decades, global climate models (GCM) have made increasingly accurate simulations of past climates, made possible by improved computing power and better-constrained input data. These paleoclimate simulations are not equally accurate in all parts of the globe. Neither should paleoclimate simulations be used as a true representation of paleoclimate. All paleoclimate maps, like all paleogeographic maps, will contain some error. These errors can be minimized by comparing results of the paleoclimate simulation with independently run simulations, or better yet by checking the results of paleoclimate simulations with geological proxies for climate such as: coals, evaporites, bauxites, and fossil leaf-shape analysis.

Using paleogeographic maps and paleoclimate simulations provided by the PALEOMAP Project, I have reconstructed Equatorial Wet, Arid, Warm Temperate, Cool Temperate, and Polar Paleoclimatic Zones for each of the selected time intervals. Some maps include paleoclimatic zones peculiar to that time interval. For example, warm temperate grasslands, first appearing in the Miocene map, appear slightly different from warm temperate forest. For the late Cenozoic, other unique climates include tundra and cool temperate grassland, or steppe.

Maps produced by climate simulations were compared with paleoclimatic zone maps, based on evidence from the rock record: evaporites, coal, till, fossil flora and fauna, etc. The best available data was used, with lithology-based data taking precedence. When paleoclimatic zone maps had information about climate, that information was used. When no lithologic data were found, climate simulation data was used. Because the fossil record is very incomplete, even in the relatively recent Cenozoic Era, climate simulation data were crucial to "connecting the dots" of isolated fossil evidence.

The K/T Event (Alvarez et al., 1980) ended a brief cool interval at the end of the Mesozoic Hot House world and introduced a warmer Cenozoic Hot House world (Upchurch et al., 1999, 2007). Paleobotanical analysis from leaf macrofossils has shown that a very shallow temperature gradient existed between Equator and Poles in the Paleocene. Today, that temperature gradient is much steeper. The events that brought about this change are known—events that punctuate the long cooling trend of Cenozoic climate history. The isotope ratios $\delta^{18}O$ and $\delta^{13}C$, measured over the entire Era, record the sudden climate shifts and long optimum intervals (Zachos et al., 2001, Zachos et al., 2008). Figure 1.1 shows the important events in Cenozoic climate history.

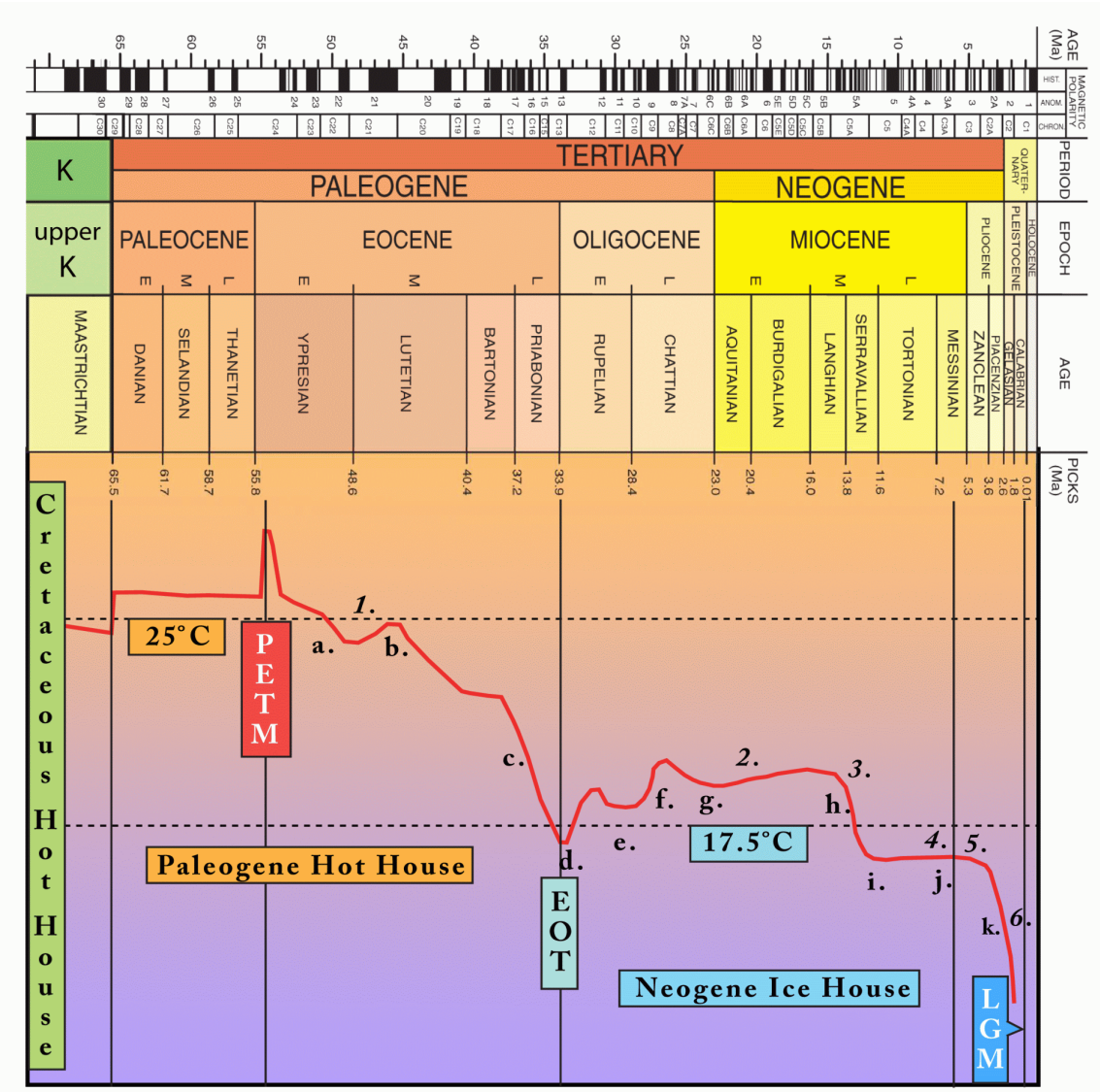

ANTARCTIC REGION

a. Antarctica unglaciated, 55-50 Ma
b. Antarctic ice sheets above 1000 m, 40 Ma
c. Major accumulation of ice on Antarctica, 34 Ma
d. First ice-rafted debris around Antarctica, 33-28 Ma
e. Some parts of Antarctica still forested, 32-23 Ma
f. Continental glaciers in West Antarctica, 27 Ma
g. Glaciers at sea level in West Antarctica, 25-23 Ma
h. Circum-Antarctic Current well-established, 23-16 Ma
i. Build-up of massive, permanent Antarctic Ice Cap, 14-12 Ma
j. Earliest mountain glaciers in high Andes, 7-4 Ma
k. Great expansion of Antarctic Ice Cap, 5 Ma

ARCTIC REGION

1. Local glaciers in Svalbard, 56-34 Ma
2. No permanent ice cap in Arctic, 20 Ma
3. Glaciers in Alaska, 12 Ma
4. Greenland Ice Cap grows, 7-3 Ma
5. Arctic polar ice cap expands, 4-3 Ma
6. Ice sheets cover large parts of North America and Eurasia, 2.6-0.01 Ma

Fig. 1.1 A graph showing the long cooling trend of the Cenozoic, and the time intervals mapped (Scotese, 2008). Note that the steep declines in global temperature are associated with periods of rapid polar icecap accumulation.

Seafloor spreading rate affects the carbon cycle, and thus strongly affects global climate (Lasaga et al., 1983; Brady and Gislason, 1997; Tajika, 1998; Kashiwagi et al., 2008). Spreading rate affected Cenozoic global climate, as when the Iceland Hotspot became quiet at the Eocene/Oligocene Transition (Abelson et al., 2008). Other important changes in paleogeography that affected climate in the Cenozoic are:

a.) The isolation of Antarctica and the inception of the Circum-Antarctic Current. Opening of the Drake Passage and Tasman Sea, coincident with reduced greenhouse gas concentration (Mikolajewicz et al., 1993), resulted in the refrigeration of Antarctica at the Eocene/Oligocene boundary. This was the beginning the Cenozoic Ice House world.

b.) The collision of India with Eurasia, and the rise of the Himalayas and Tibetan Plateau. This event may have enhanced global cooling by making large amounts of silicate rock available to combine with atmospheric CO_2.

c.) The isolation of the Mediterranean from Tethys. This led to the Messinian Salinity Crisis, and contributed to cooler temperatures in Europe.

d.) The separation of the Atlantic and Pacific oceans by the Panama land bridge. This closure triggered a sequence of events that resulted in the growth of Northern Hemisphere ice sheets, marking the beginning of the full, i.e. bi-polar, Ice House world of the late Cenozoic.

Inspired by today's warming global climate, the natural process of climate change has become a primary area of research in Earth Science. The geologic past provides a frame of reference that helps us understand modern and future climate change. These maps combine data and conclusions from descriptive and computational climate science. These maps may help provide insights to climate scientists researching any time interval in the Cenozoic, including the Holocene and Earth's immediate future.

CHAPTER 2

GEOLOGICAL EVIDENCE AND PREVIOUS WORK

2.1 Types of Data Assembled

These maps are based on paleoclimate simulations and paleoclimatic zone maps derived from lithologic data. This chapter is an overview of types of paleoclimate models and the types of data used to make paleoclimatic zone maps.

In order to produce meaningful climate simulations, climate modelers must amass data about the factors that force climate change, listed in Table 2.1.

Table 2.1 Climate Forcing Mechanisms

Mechanism	Aspects of climate affected by mechanism
Greenhouse gas (GHG) concentration (CO_2, CH_4, H_2O vapor, N_2O, O_3)	Temperature, precipitation, weathering rate
Solar radiation output	Insolation
Orbital cycles	Insolation
Vegetation cover	Albedo of landmasses, transpiration rate, GHG concentration
Global plate tectonics/ Paleogeography	GHG concentration, sea level, oceanic and atmospheric circulation
Airborne particles	Insolation
Weathering	GHG concentration

2.2 Climate Models

In this section, the main types of paleoclimate models are described, along with the varieties of data they use, and the types of maps produced by the models.

Climate models such as Combined Community Systems Model (CCSM) (Collins et al., 2006), European Centre Hamburg (ECHAM) (Roeckner et al., 2003), and the Fast Ocean Atmosphere Model (FOAM) (Jacob et al., 2001), simulate the circulation of the Earth's oceans and atmosphere, and are called General Circulation Models (GCMs). A climate model is the computer program which produces climate simulations. These models are composed of sub-models of ocean and atmosphere that run simultaneously. These "coupled" sub-models influence each other as the simulation runs. (Here, a climate model refers to the program itself, and a climate simulation is the result of a particular run of the program.) New versions of the same basic types of GCM are developed for use in different paleoclimate reconstructions.

2.2.1 CCSM

The National Center for Atmospheric Research (NCAR) developed the GENESIS Global Climate Model, based on its Community Climate Model, version 1 (CCM1). It was used (Upchurch et al., 1999, Upchurch et al., 2007) to simulate latest Cretaceous (Maastrichtian) climate and the influence of vegetation upon it. This climate simulation supported their hypothesis that forested landmasses around the Arctic were an important factor in warming the Cretaceous and Paleogene Arctic Ocean.

Winguth et al., (2010) used CCSM-3 to model the Paleocene-Eocene Thermal Maximum (PETM). These simulations included variables such as atmospheric CO_2 in concentrations of 4X, 8X, and 16X Holocene (pre-industrial) values. The simulation produced global maps of surface air temperature (SAT), precipitation, wind and sea level pressure, ocean circulation and overturning, sea surface salinity, and ocean mixing and temperature at depth.

2.2.2 ECHAM

Arpe et al., (2011) used three versions of ECHAM to make three simulations of the Last Glacial Maximum (LGM). Their purpose was to identify refugia in Southern Europe where warm-loving deciduous trees (chestnuts, olives, buckthorns, some oaks) might have survived during the maximum extent of glaciation in Europe. These results were compared with LGM biome maps derived from plant macrofossils and pollen data, to judge which simulation best matched the floral data. Late Miocene (Tortonian) climates were simulated and compared with proxy data using ECHAM (Micheels et al., 2007). The Late Miocene climate simulation is mostly consistent with proxy data, but the temperatures in high latitudes are predicted to be −2.4 ℃ too cool.

2.2.3 FOAM

Donnadieu et al (2006) used FOAM to estimate the influence of paleogeography on Cretaceous climates. Their three simulations (Aptian, Cenomanian, and Maastrichtian) added new details, including tectonically-forced sea level changes, topographic highs, and epicontinental seas.

Scotese et al., (2009) used FOAM to model numerous paleoclimatic phenomena related to the formation of hydrocarbon source rocks. Some of the resulting simulations illustrate: rainfall, drainage patterns, winds, ocean currents, seasonal land and sea temperatures, and the upwelling zones that fuel primary productivity in the oceans.

2.3 Isotopic data

Isotopes of common elements can be used as proxies for paleoclimatic conditions if the chemical signature of the sample has not been altered by diagenetic processes. The record of $\delta^{18}O$, and of $\delta^{13}C$, are useful indicators of climatic factors, CO_2 content of the atmosphere, and relative amount of water sequestered in ice sheets. The equations for finding these values are shown in Fig 2.1:

$$\delta^{18}O = \left[\frac{\left(\frac{^{18}O}{^{16}O}\right)_{sample}}{\left(\frac{^{18}O}{^{16}O}\right)_{standard}} - 1 \right] (1000\ ‰) \qquad \delta^{13}C = \left[\frac{\left(\frac{^{13}C}{^{12}C}\right)_{sample}}{\left(\frac{^{13}C}{^{12}C}\right)_{standard}} - 1 \right] (1000\ ‰)$$

Fig. 2.1 Equations for $\delta^{18}O$, and of $\delta^{13}C$.

Less-common isotope values, such as the ratio of $^{143}Nd/^{144}Nd$, can be used to estimate circulation patterns of ocean water, and rates of erosion from nearby landmasses.

2.3.1 Oxygen isotopes

The Cenozoic time intervals in this atlas were primarily chosen from notable excursions or knickpoints of $\delta^{18}O$ in the oxygen isotope/paleotemperature curve from the seminal work of Zachos et al., 2001 (Fig. 2.2). ^{16}O and ^{18}O occur in varying proportions in sea water through geologic time; the Holocene ratio is called Vienna Standard Mean Ocean Water (VSMOW). ^{18}O is heavier than ^{16}O; it is less likely to evaporate. ^{18}O more likely to fall as precipitation, so meteoric waters are relatively enriched in ^{16}O. Thus greater proportions of ^{18}O in the bodies of marine fauna indicates that large amounts of water are sequestered in ice sheets. Ocean salinity can also affect the $\delta^{18}O$ value, so an oceanic sample enriched in ^{18}O does not necessarily prove the existance of ice sheets without corroborating evidence.

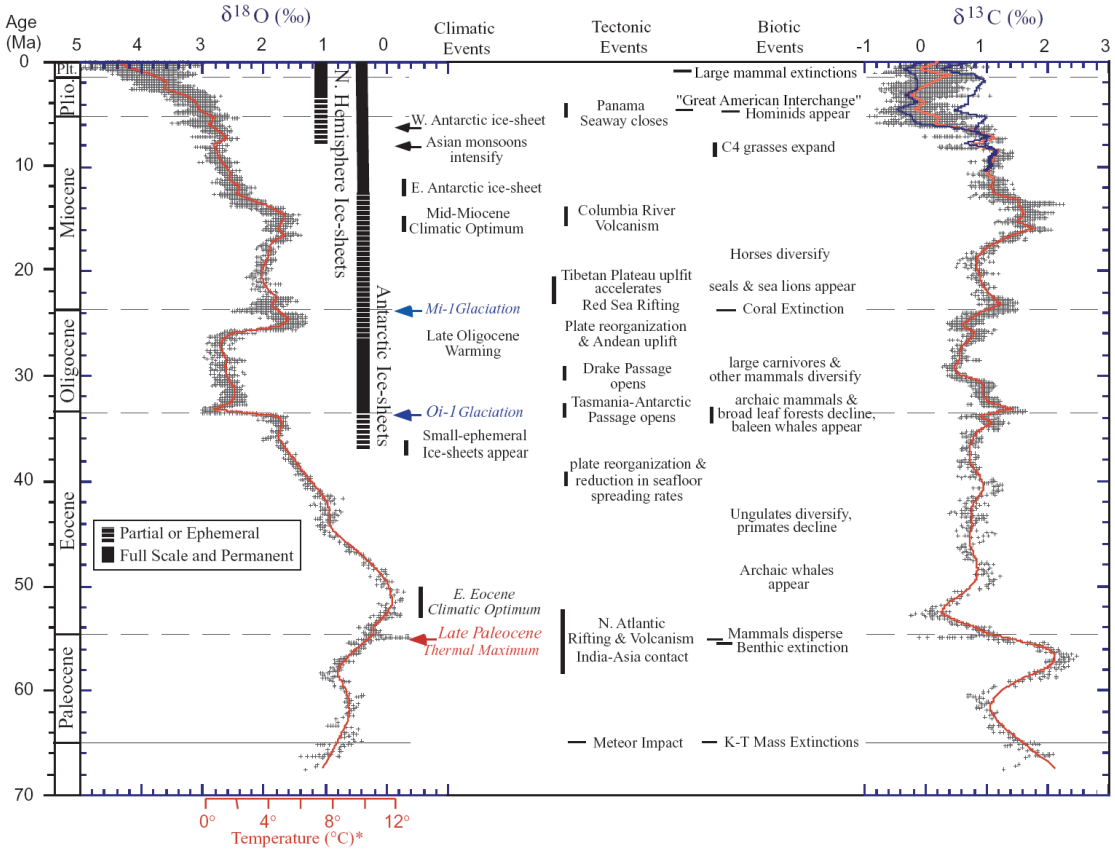

Fig. 2.2 Isotope curves spanning Cenozoic time, from Zachos et al., 2001. The data was compiled from DSDP and ODP sites.

Oxygen isotope data can be used to identify very short intervals of climate change, such as identifying the PETM (Kennett and Stott, 1991), or finding a cooling trend in the Late Maastrichtian from the $\delta^{18}O$ values in the final 20 cm. of the Cretaceous section (Habib and Saeedi, 2007). The $\delta^{18}O$ value may come from microfossils, such as foraminifera and dinoflagellate cysts (Kennett and Stott, 1991, Beerling, et al., 2002). It may also be found in calcareous paleosols (Dworkin et al., 2005), fossil woods (Richter et al., 2008) and for Pleistocene/Holocene studies from calcareous speleothems (Ruddiman, 2006, Cosford et al., 2010) and ice cores from polar ice sheets (Rasmussen, 2008, Suwa and Bender, 2008). If fossil teeth are abundant enough, the $\delta^{18}O$ value can be estimated from tooth enamel of fish (Pucéat et al., 2007) or land mammals (Bryant et al., 1996).

2.3.2 Carbon isotopes

Carbon takes the form of carbonate ions in seawater, carbonate minerals in soil and rock, and greenhouse gases such as CO_2 and CH_4 (methane). The volume of all the forms of carbon available for chemical reactions in the atmosphere and ocean is called the carbon budget. Cenozoic fluctuations of CO_2 and methane gas have been studied extensively (Zachos et al., 2008; 2005; Pancost et al., 2007). Fluctuations in $\delta^{13}C$ indicate changes in plant productivity and the size of the carbon budget.

The Calcite Compensation Depth (CCD) is the depth in the ocean at which mineral calcium carbonate ($CaCO_3$) dissolves at the same rate at which it forms. Several factors influence the CCD: pressure, temperature, and acidity of ocean waters. Above the CCD, $CaCO_3$ can exist; below the CCD, $CaCO_3$ dissolves. Deepening of the CCD and lowered acidity of ocean water indicates a climate cooled by a diminishing atmospheric CO_2 concentration. Varying values of $\delta^{13}C$ in contemporaneous samples from different ocean basins indicate that the basins were isolated from each other.

Volcanic activity increases the atmospheric concentration of CO_2. Uncertainties in the geologic record make it difficult to quantify rates of CO_2 emissions for a specific time interval (Boucot and Gray, 2001). But in a general sense, atmospheric CO_2 concentration is elevated in times of increased plate tectonic activity (seafloor spreading and subduction-related magmatism) (Lasaga et al., 1984; Berner, 1994). Atmospheric CO_2 concentrations fall as spreading and subduction are replaced by collisional mountain-building. In the Cenozoic, rapid erosion of silicate rocks in rising mountain belts, particularly the Himalayas and the Tibetan Plateau, contributed to lowering atmospheric concentration of CO_2.

Beginning at 15 Ma, the $\delta^{13}C$ gradients of the Atlantic and Pacific basins began to diverge. This event is thought to represent the time when Central America blocked the interchange of water between the Atlantic and Pacific basins (Zachos et al., 2001). Varying levels of ^{13}C in paleosols have been used to map the changing vegetation coverage in the Amazon

basin; C_4 grasses are enriched in ^{13}C, whereas C_3 forests are depleted in ^{13}C (Anhuf et al., 2006). It is also interesting to note that a negative carbon isotope excursion at the K-T boundary is cited as evidence for global wildfires (Upchurch et al., 2007).

2.3.3 Less-common isotopes

Neodymium (Nd) has been used as an ocean circulation tracer (Thomas et al., 2003; Scher and Martin, 2006), Continentally-derived neodymium is also taken up by fossil fish teeth during diagenesis, and has been used to measure increased glacial weathering across the Eocene/Oligocene boundary in Antarctica (Scher et al., 2011). The $^{87}Sr/^{86}Sr$ ratio was used to identify the extent of the Mediterranean during the Miocene, and its connectivity with Paratethys and the world ocean (Flecker and Ellam, 2006).

2.4 Paleobotany

Plant fossils are the most useful evidence for paleoclimatic reconstructions. There are many localities of Cenozoic age with well-preserved macrofossils of leaves, cuticle, seeds, spores, and pollen. Assemblages of plant species show how the West Siberian Seaway helped warm the Boreal and Arctic portions of Eurasia (Akhmetiev and Beniamovsky, 2009). When enough leaf macrofossils can be found, the CLAMP methodology (Climate Leaf Analysis Multivariate Program) can be used to estimate temperature, rainfall, and other aspects of climate (Spicer, 2000, Upchurch et al., 2008).

Recently, the CLAMP methodology has been updated by Peppe et al., (2011). Digital leaf physiognomy (DLP) is used to estimate mean annual temperature (MAT) and mean annual precipitation (MAP). DLP is able to analyze more variables, allowing more fossil localities to be included in paleoclimate studies. The results have been shown to be more consistent than other leaf analysis techniques (Peppe et al., 2011).

Palynology is an especially useful tool for paleoclimatology, because pollen grains are widely dispersed. Most importantly, pollen is borne on wind currents far into the ocean basins.

Pollen samples can also be obtained for landmasses that are now inaccessible, such as Antarctica and Greenland. Pollen samples from deep-ocean cores are used to constrain plant assemblages on nearby landmasses, provided that the paleowinds and paleocurrents are adequately understood. Pollen from deep-ocean cores can be cross-referenced with microfauna to accurately date samples. Good pollen samples from land areas are less common, but are sometimes quite well-preserved (Wheeler and Lehman, 2005).

2.5 Micropaleontology

Foraminifera provide valuable information about paleoclimates. Their shells, made of calcium carbonate from sea water, record $\delta^{18}O$ and $\delta^{13}C$, and can be used to plot global climatic trends (Zachos et al., 2001). Their appearance or disappearance up-section in core samples can indicate profound changes in oceanic chemistry and temperature (Kennett and Stott, 1991). Foraminiferal assemblages also may indicate some of the consequences of those changes in seawater composition, such as changes in the calcite compensation depth (CCD) (Coxall et al., 2005), or salinity (Nunes and Norris, 2006). Surface-dwelling marine plankton record important changes in ocean conditions. A good example is the remarkable global bloom of the dinoflagellate Apectodinium during the Paleocene-Eocene Thermal Maximum (PETM) (Crouch et al., 2001). This dinoflagellate is known to favor warm water, so its global extent is evidence of rapid global warming at the Paleocene/Eocene boundary.

2.6 Lithology

Bauxites, generated in warm, rainy climates, appear in the Eocene Ob and Yenisei basins (Akhmatiev, 2010), and in the Cretaceous of Romania (Melinte-Dobrinescu and Bojar, 2010). Laterite, a paleosol that results from very rainy paleoclimates, is found in the Early Eocene of India, capturing India's transit across the Equatorial Wet Belt (Kent and Muttoni, 2008).

Coal, a product of wet temperate and wet tropical climates, is found at high latitudes at times of Hot House global warming. Examples include Cretaceous coals in Alaska and

Saskatchewan (Upchurch et al., 2007, Williams et al., 2010), Eocene coals in Alaska (Tomisch et al., 2010), Eocene coals in Siberia and Svalbard (Schloemer-Jaeger, 1958, Schweitzer, 1974, 1980, Spicer et al., 2008, Spielhagen and Tripati, 2009).

Ratios of physically-weathered to chemically-weathered clays, and different types of clays, have been used as a proxy for temperature and precipitation in the Cretaceous of the Spanish Pyrenees (Arostegi et al., 2011). The presence of smectite indicates a warm climate with seasonal rainfall (Eocene of Antarctica, Roberts and Kennett, 1994).

Evaporites, primarily halite and gypsum, indicate warm climates where evaporation exceeds precipitation, corresponding to a paleolatitude in the Northern or Southern Arid Belt. Evaporites appear in the Paleocene of Spain (Arostegi et al., 2011), the Eocene of China (Abels et al., 2011), and in great thicknesses in the late Miocene of the Mediterranean Basin—the Messinian Salinity Crisis (Hsu et al., 1973, Krijgsman et al., 2010).

2.7 Previous Climatic Reconstructions

Climatic maps show one or several of the aspects of global climate. Some of the important aspects that can be graphically represented include: mean average temperature (MAP), seasonal high and low temperatures in Northern and Southern Hemispheres, rainfall, winds, currents, evaporation, and salinity. The temperature differential between a time in the past and the present day can be mapped. Climate maps are produced by entering boundary conditions into a climate model and running the simulation. These boundary conditions are climatic variables such as: CO_2 concentration in the atmosphere, insolation in response to Milanković cycles, among other parameters.

Climatic zone maps, also called biome maps, were introduced by Köppen and Geiger. The maps of Köppen and Geiger use regional variations in temperature and precipitation to map distinct climatic zones. The climatic zones are thought to represent major biomes or vegetation

assemblage types. These maps look similar to climate simulation results, but are made by field observations of vegetation and climate.

Climatic zones of the modern world can be researched in person; therefore climatic zone maps of the modern world can be made to show a high degree of complexity. Paleoclimatic zone maps are based on far more limited geological data sets, and consequently, have a lower degree of accuracy. Paleoclimatic zone maps cannot be based on climate simulations, which provide no direct evidence of vegetation assemblages. Though these maps must contain some error, they are invaluable in checking the accuracy of climate simulation maps. The classic example for the Cenozoic is that while climate simulations predict an early onset of Arctic glaciation, as early as the Eocene/Oligocene Transition (EOT), fossil plants prove the Arctic was still home to cool temperate forests at that time.

CHAPTER 3

METHODOLOGY

In this chapter, I describe the methods and information that was used to produce the paleoclimate reconstructions. This section is intended to read as a "how-to guide," which outlines the steps taken to draw the maps using standard rendering software such as Adobe Photoshop©.

3.1 Plate Tectonic Basemaps

The plate tectonic and paleogeographic base maps that were used in this thesis were provided by C. R. Scotese, PALEOMAP Project. These maps show the configuration of the ocean basins and continents, topography of landmasses, and bathymetry of oceans. The climatic information was added artistically as layers upon these topographic base maps.

3.2 Visualizing Climatic Zones

Digital art techniques render the climatic zones onto the topographic maps. A palette of colors for each climatic zone was made using Adobe Photoshop, and using NASA's Blue Marble rendering of the Earth as seen from space.

3.3 The Mapmaking Process: A Step by Step Description

1) Open a digital elevation model (DEM) of Earth from the PALEOMAP Project Earth History series in Photoshop (Fig. 3.1). The map is similar to DEMs in GIS datasets: Lower elevations appear as darker grays, higher elevations are lighter. There is a range of 256 grays in each DEM.

2) Open the color table tool.

3) Using the NASA Blue Marble map colors as a reference, observe the colors of the climate belt to be represented. Select a range of values in the color table dialog box, and assign two endpoint colors to the range. This will make a gradation from one endpoint color to the other across all pixels of that range of color values (Fig. 3.2). For each map, make one image for each climatic zone color palette. This means there will be six images for each map: a world made entirely of equatorial wet colors, one of arid colors, and one each for the color palettes used to represent semiarid, warm temperate, cool temperate, and polar ice (Fig. 3.3). For maps of the Neogene, more palettes were made to represent tundra, grassland, tropical grassland, and montane parkland colors. The same color palettes will be used for similar climatic zones throughout the atlas. This will give the whole atlas a similar appearance even though the climatic zones shift and change size from map to map.

4) Open the DEM image of the time interval and convert it to RGB (red/green/blue) color mode. This is now the main map that will be artistically rendered. Add the Equatorial Wet Zone color image as a second layer. The color image is hidden beneath the untouched gray of the main image.

5) Add a guide image on top of the main image (Fig. 3.4). Make it 50% transparent. This image shows the boundaries of the climatic zones. Lock this image so it can't be modified.

6) Return to the main image, and choose the eraser tool. Erase the main image layer within the boundaries of the equatorial climate belt, allowing the equatorial wet layer to show through.

7) Combining the visible elements of the picture is called flattening. After the Equatorial Wet Zone has been fully represented, flatten the image, save, and apply the next climatic zone. Apply all 6 zones, flattening that zone image with the main image after each zone is applied (Fig. 3.5).

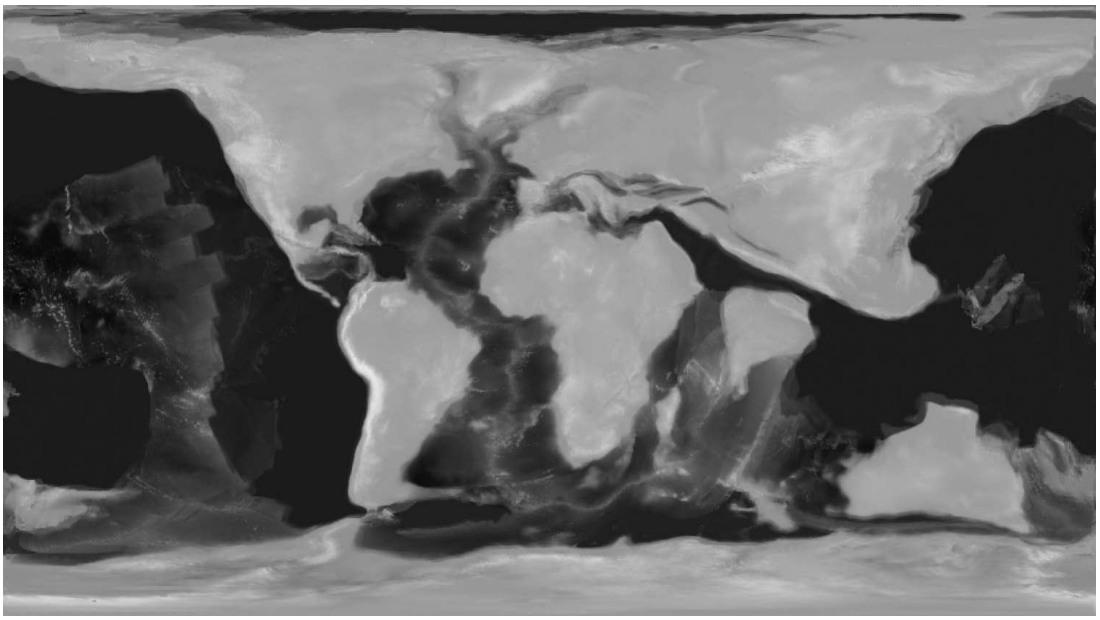

Fig. 3.1 A digital elevation model (DEM) of the Paleocene/Eocene world.

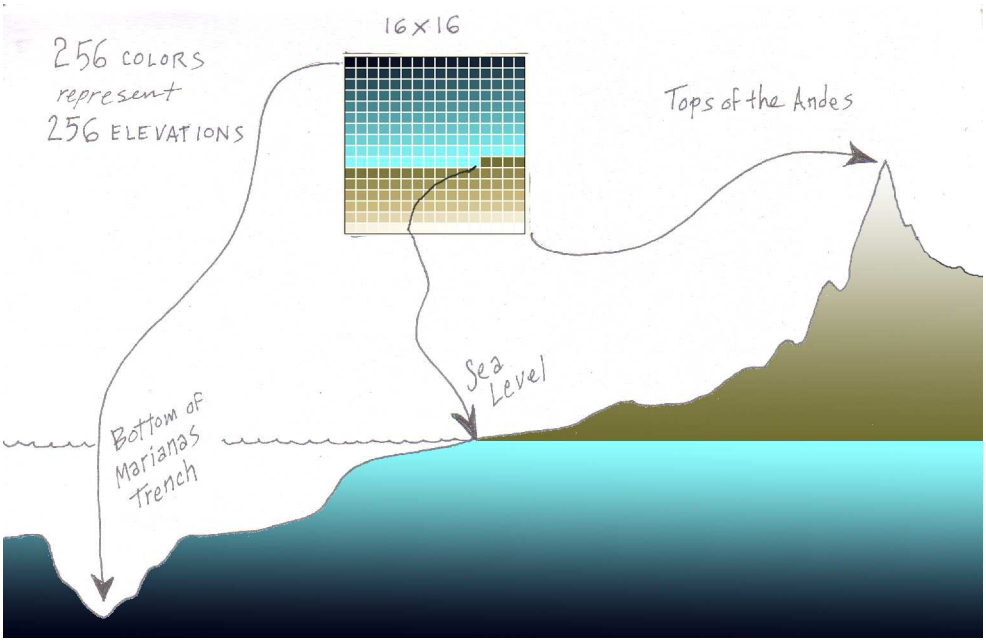

Fig. 3.2 How a color table approximates elevation in a DEM.

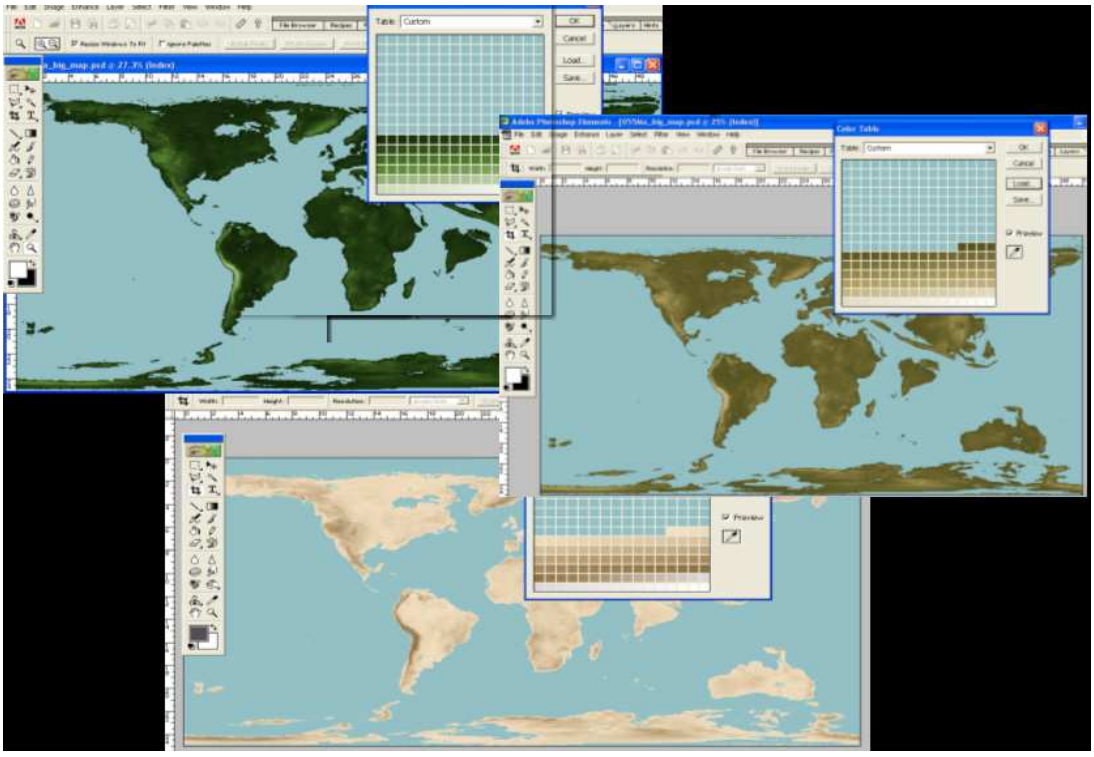

Fig. 3.3 Color tables for 3 climatic zones, Equatorial Wet, Semiarid, and Arid.

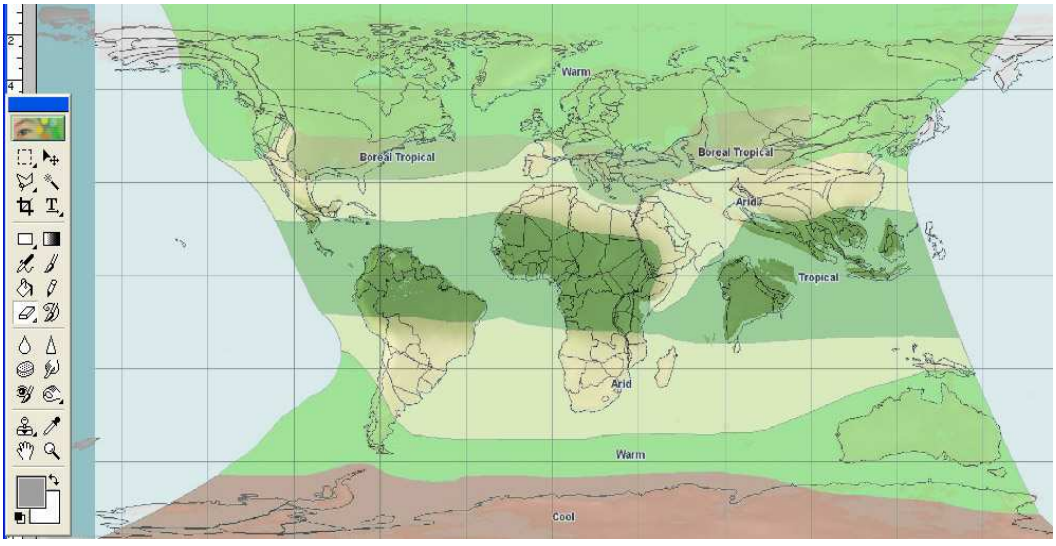

Fig. 3.4 Guide image superimposed over map. Equatorial Wet Zone has been colored in beneath it.

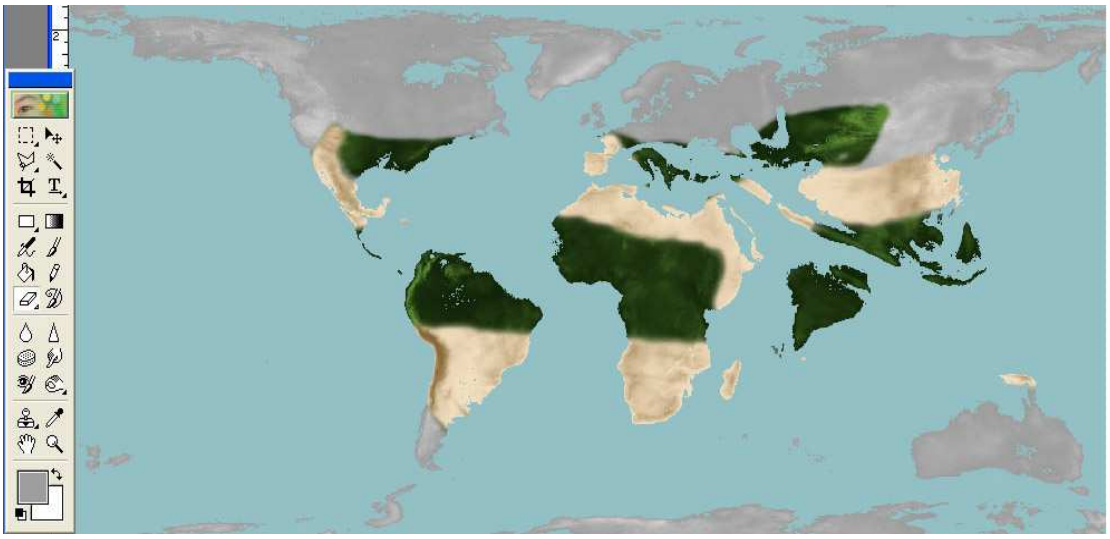

Fig. 3.5 Main map with Equatorial Wet, Arid, and Boreal Tropical Zones colored in.

Steps 1-7 complete the primary coloring of the maps. The boundaries between the climatic zone are in place, but they do not resemble the earth from space—the boundaries are all equally sharp. Using the present as the key to the near geologic past, adjust the boundaries realistically using the high-resolution Blue Marble image (Fig. 3.6).

Fig. 3.6 Retouching climatic zone boundaries using modern Earth imagery.

8.) Make new high-resolution images that are pastiches of each type of today's climate boundaries. Using a realistic mock-up of a climate boundary keeps recognizable modern features—such as the Nile or the Tibesti mountains—from appearing on the paleoclimate map.

9.) Choose the rubber stamp tool, which copies parts of one image to another. Open a mock-up boundary image and the main image. Cover the low-resolution spray-painted boundary with high-resolution mock-up boundary. The line of the boundary should be the same, but it now resembles a modern climate boundary extending over photo-realistic terrain appropriate to the area.

10.) After the image is complete, save the file and proceed to the next interval. The final images are presented in Plates I-V that accompany this thesis.

CHAPTER 4

CRETACEOUS/TERTIARY (K/T) CLIMATE

4.1 Introduction to the K/T

A single definition of Hot House world climate does not necessarily fit every potential Hot House world. The final moment of the Mesozoic Era, the Maastrichtian Epoch of the Late Cretaceous, looks nothing like the Hot House worlds that preceded or followed it (Francis et al., 2008). The great tropical rainforests of the early Cenozoic are missing. Instead of lush vegetation at the Equator, prominent swathes of brush country covered the high and dry hinterlands of low-latitude continents.

Open dry forest in the Temperate and Arid Zones received only occasional rain. Unlike today's savannas, these forests had no grassland component.

The phrase "ice-free world" is often used to describe Earth's climates of the past when forests grew near the poles. But "ice-free" does not mean "snow-free," "glacier-free," or "sea-ice free." A more accurate term, though less easy to say, would be "ice-sheet-free world."

The Maastrichtian is well within the evolutionary limitations of Climate Leaf Analysis Multivariate Program (CLAMP), and leaf shape from macrofossils from the Maastrichtian are a dependable proxy for Maastrichtian climate.

4.1.1 Plate Tectonics

By the Late Cretaceous, no supercontinents remained on Earth. Only Antarctica's tenuous connections with Australia and South America hinted at Gondwana's former proportions. All over the globe, oceans surrounded the continents, widening like the Atlantic, or shrinking like Tethys (Fig. 2.1).

Fig.2.1 Paleogeographic Base Map for the K/T. Scotese, 2008.

Active rifting continued in the Central and Southern Atlantic. The North Atlantic was beginning to tear apart, even as the Labrador Sea lay cooling and relatively motionless to the west. Rift shoulders stood above the newborn North Atlantic, the youthful South Atlantic, and across the reach of new Southern Ocean between West Antarctica and South Australia (Scotese 2008).

New ocean floor spread south of Gondwana's last remnants, India and Australia (Scotese 2008). Hot spots active in the late Cretaceous included the Mongolian Hot Spot Chain, Iceland, Reunion, and Ascension (Scotese 2008).

Andean margins stretched along the western margins of the Americas, the Pacific margin of Antarctica, and northeastern Asia—Kamchatka, the Kuriles, and Japan (Scotese 2008).

Continental collisions raised mountains in Central and East Asia. The Stanovoy Mountains now stood where the Amurian Seaway had been (Zonenshain et al., 1990), and the Verkhoyansk Mountains marked the collision of the Kolyma and Omolon terranes. (Zonenshain et al.,1990). A mountainous heartland stood uplifted in Central Asia, where numerous small tectonic plates had piled into the southern margin of Kazakhstan and the Siberian Craton (Scotese PaleoAtlas)

Subduction consumed Pacific crust below the American Cordilleras, new Southern Ocean crust under West Antarctica, and Pacific Ocean crust along the coast of northeast Asia. Tethys seafloor, rich in carbonate (Kent & Muttoni, 2008) slid beneath strips of South Asian continent that were themselves colliding with Asia. Those blocks' collision with Asia closed the last vestiges of Paleotethys' ocean floor. In Central and Eastern Europe, small ocean basins closed (names of basins). Between the Americas, the Caribbean Plate had begun to bulldoze its way into the Central Atlantic (Scotese 2008).

Rift shoulders stood above the newborn North Atlantic, the youthful South Atlantic, and across the reach of new Southern Ocean between West Antarctica and South Australia (Scotese 2008).

Paleozoic mountain belts (Appalachians, Caledonides, Hercynides and Urals) were much lower and less widespread than the Andes and later Cenozoic orogenies. Even so, they influenced climatic zone boundaries, as they do today.

4.1.2 Paleogeography

In Maastrichtian time, global sea levels had been on the retreat since the Cenomanian/Turonian high-water mark. Sea levels had fallen 100m, but were still 150m above the present (Haq et al., 1987). This K/T map is based on paleogeographic maps by Scotese (2004, 2008), Upchurch et al. (1999), Horrell (1991), Zonenshain et al., (1990) and Kazmin and Natapov (1998).

The Arctic Ocean had no deep-water communication with other world oceans. Open channels along the Equator allowed currents to flow westward through Tethys, between the Americas, and between Australasia and Southeast Asia.

Laramide uplift and eustatic sea level fall (Haq et al., 1987) had caused continental seas to withdraw from the interior of North America, save for southeast Texas and the Cannonball Sea in North Dakota and Canada's prairie provinces. The Arctic Ocean, while still warm, no longer had access to warm surface currents from the Gulf of Mexico (Herman and Spicer, 1996). Continental shelves lay beneath shallow seas across northern Siberia, Central and South Asia, eastern Arabia, the Tarim Basin, and the Ross Sea in Antarctica. Shallow seawater stretched across the Paris Basin, the Rhineland, and Bavaria. Shallow seas covered eastern Iberia, and the Atlas Mountain trough. Florida and Yucatan had partially emerged from the sea, isolating the Gulf of Mexico (Scotese et al., 2008).

The rising Andes had begun to act as the same orographic barrier they are today (Aragon et al., 2011). Even so, rainfall from Equatorial easterlies did not result in an Amazonian rainforest (Upchurch et al., 1998, Sewall et al., 2007).

Australia and South America, and the Antarctic Peninsula, prevented a Circum-Antarctic Current currents from encircling Antarctica. The Southern Ocean did not yet exist as it is known today.

Both island continents of the Late Cretaceous—India and Australia—lay far south of their modern tropical and subtropical latitudes. Rainforest conifer pollen is found in India, but plant remains from Australia are from temperate evergreen coniferous and broad-leaved forest (Upchurch et al., 1999).

4.1.3 Paleoclimate of the K/T in Context of the Late Cretaceous

A Hot House world exists when average global temperature rises above 20° C, and no permanent ice covers the poles. Permanent ice sheets at one or both poles, and an average global temperature of 12° C, defines an ice house world (Frakes et al, 1992). Tropical coal swamps can flourish in an ice house world, as in the Pennsylvanian (Eros et al., 2012); and seasonal snow can blanket high latitude landmasses in a Hot House world (Morris et al., 2008, Flögel et al., 2011). The Late Cretaceous is a very well-documented Hot House world, with deciduous plants and reptiles living north of the Arctic Circle—clear evidence of poles without permanent ice (Wolfe, 1987; Parrish and Spicer, 1988; Horrell, 1991; Herman and Spicer, 1996; Frakes, 1999; Spicer et al., 2008; Spicer and Herman, 2010; Boucot et al., 2011). Oxygen isotopic composition of pedogenic carbonates, compared with global mean annual temperature estimates, indicates a Maastrichtian world climate cooling from the last peak of Cretaceous greenhouse warming (Dworkin et al., 2005). Oxygen isotope data from a population spike in Manumiella seelandica dinoflagellate cysts correlates with this cooling trend in the final 20 cm. of the Maastrichtian section (Habib and Saeedi, 2007).

4.2 Discussion of K/T Paleoclimate Reconstruction

In this section, we review the climatic zones of the Maastrichtian, starting with Equatorial Wet and moving toward the Poles. Similar zones, such as the Northern and Southern hemispheres' Arid Zones, are discussed in the same section.

In general, warm green colors indicating wet climate and broad tan to brown patches indicating semiarid climate cover the majority of the Late Maastrichtian world map. No huge deserts or continent-sized rainforests existed, nor did broad areas of tundra, except in high elevations in Antarctica. On the map, the light blue-green of shallow seas color continental shelf on both sides of Tethys, eastern Arabia, and the now-subducted northern portion of India. A startling green Antarctica shows spots of continental ice in the Transantarctic Mountains, but the Southern Ocean and Arctic Ocean are bordered in rich green in summer. Winter snow cover reaches far into lower latitudes, but widespread glaciation is not possible in this Hot House world.

4.2.1 Description of Climatic Zones

4.2.1.1 Equatorial Wet Climatic Zone

Although the Maastrichtian was a Hot House world, large swaths of rainforest did not stretch across the Equatorial landmasses as they do t6oday (Upchurch et al., 1998, 2007). Orbital-driven changes in insolation narrowed the Intertropical Convergence Zone (ITCZ) in the Late Cretaceous, just as the ITCZ has been observed to shift and change shape in the present day (Flögel and Wagner, 2006). Warm, dry shrubland or dry deciduous forest covered Amazonia and the Congo (Sewall et al., 2007). Mixed coniferous/deciduous forests rimmed northwestern South America and the Guinea coast of Africa, and many other parts of the globe (Van der Ham et al., 2003).

4.2.1.1.1 Lithologic and Paleontologic Data for the Equatorial Wet Zone

The Late Cretaceous Hot House was drier than the Cenozoic Hot House that was to follow, but coal deposits are found along the Guinea coast of Africa—Benin and Dahomey, Nigeria and Senegal—(De Swardt and Casey, 1961, Scotese et al., 1999), and are also found in areas considered to be dry forest in other climate simulations, namely the coasts of Africa (Horrell, 1990; Scotese et al., 1999), and the northwest coast of South America (Scotese et al., 1999).

4.2.1.2 Arid and Semiarid Climatic Zones

On the map, a similar pattern of Arid to Semiarid Climatic Zones can be seen in South America and Africa (Sewall et al., 2007). Dry scrubland, surrounded by sparse dry forest, grew in the central and southwestern coasts of each continent. This core area was surrounded by closed-canopy dry deciduous forest. These dry deciduous forests also grew in the southern regions of North America and Europe, and in northern India.

4.2.1.2.1 Lithologic and Paleontologic Data for the Arid and Semiarid Zones

An increase in the number of physically-weathered clays, and an increase in the smectite/kaolinite ratio, are proxies for increasing aridity in Spain (Arostegi et al., 2011). Evaporites rim the pre-Mediterranian Tethys shore of North Africa, in Algeria and Libya (Boucot, 2012, Horrell, 1990), and elsewhere in Africa in Niger and Mozambique (Horrell, 1990). Evaporites also appear in China (Mateer and Pei-ji, 1992).

4.2.1.3 Warm Temperate Climatic Zone

The Warm Temperate Climatic Zone was the most extensive climatic zone of the Maastrichtian Epoch. The majority of warm temperate forests, i.e. deciduous, coniferous, and mixed coniferous/deciduous, lay across the parts of North America and Europe that bordered the Central Atlantic and Tethys Oceans. Less extensive Warm Temperate Zones crossed the

southern regions of South America, Africa, and India, and northern Australia (Sewall et al., 2007). Leaf macrofossils and CLAMP analysis support a picture of widespread warm temperate forests on all major continents (Upchurch et al., 1999, 2007).

Mountainous Central Asia rose high enough to experience a significantly cooler and wetter climate. The orographic barrier caused by the Central Asian ranges produced large semiarid scrublands and dry forests to the west and southwest. Note the contrast on the map between Asia and the recently separated South America and Africa, each with their own large central highlands. Zones of savanna ring the highlands in Asia, but the southern continents' high plateaus are warm and dry (Sewall et al., 2007).

4.2.1.3.1 Lithologic and Paleontologic Data for the Warm Temperate Zone

Angiosperm and conifer forests covered North America in the Maastrichtian, with palms and cycads found as far north as the Canadian Arctic (Wolfe and Upchurch, 1987, Lomax et al., 2001). Fossilized stands of angiosperm and conifer communities are found grouped in separate layers in West Texas (Wheeler and Lehman, 2005). Well-preserved fossils of warm temperate conifer forest growth has been found in the Maastrictian of the Netherlands (van der Ham et al., 2003).

4.2.1.4 Cool Temperate Climatic Zone

Leaf macrofossils of known species and CLAMP analysis of leaves show that cool temperate forests ringed the North Pacific Ocean from the Sea of Okhotsk to British Columbia. Inland, these forests which were similar to the evergreen, coniferous woodlands in present-day southern Wisconsin, stretched across Canada, southern Greenland, and bordered the Barents and Kara Seas. A narrower belt of cool temperate forest crossed Siberia between 50° and 60° North latitude. A broad stripe of cool temperate forest crossed Australia, and appeared locally in spots in the outlying regions of Antarctica (Francis and Poole, 2001, Upchurch et al, 1998, Francis et. al., 2002, Hayes et al., 2006). These fossils are convincing proof that temperatures

were significantly warmer near the poles during the Cretaceous. They do not, however, disprove the occurrence of minor alpine or continental glaciation during cooler episodes during the Cretaceous (Flögel et al, 2011).

4.2.1.4.1 Lithologic and Paleontologic Data for the Cool Temperate Zone

CLAMP analysis applied to floral assemblages from the lower Cantwell Formation in Central Alaska indicates a cool temperate climate (Tomsich et al., 2010). Spores, pollen, and plant fossils in Australia and Antarctica reveal a “Valdivian” community of southern beeches (Nothofagaceae), myrtles, (Myrtaceae), laurels, (Lauraceae) and broadleaf shrubs of the Monimiaceae. Junipers and redwoods (Cupressaceae) shared this ecosystem, along with Podocarps and Araucariaceae (monkey-puzzle pines) (Poole et al., 2003).

4.2.1.5 Polar Climatic Zone

Because it was a Hot House world, there was no polar climate in any modern sense. The pole and surrounding regions experienced a variety of cool temperate climate, modified by polar seasonal day-night cycles. No climate like this exists on Earth today.

Mixed coniferous/deciduous forest ringed the enclosed Arctic Ocean in the Late Cretaceous (Upchurch et al., 1999). Forest ringed Antarctica’s rim (Dettman 1989; Francis et al., 2008), but a clear picture of flora in Antarctica’s interior is not currently available.

4.2.1.5.1 Lithologic and Paleontologic Data for the Polar Zone

Tropical plant fossils and coal are found near and above the Arctic Circle in rocks of Late Cretaceous age (Wolfe, 1987; Parrish and Spicer, 1988; Horrell, 1991; Herman and Spicer, 1996; Frakes, 1999; Spicer and Ahlberg, 2008; Spicer and Herman, 2010; Boucot et al., 2012). Fossils of deciduous forest vegetation are found in K/T sections in the Brackett Basin, Northwest Territories, and the Alaskan North Slope (Upchurch et al., 2007). On the Amur River, and in

Kolyma, Maastrichtian sections reveal abundant angiosperm species in a forest assemblage grown in a humid climate (Herman et al., 2009).

Fossil angiosperms and conifers are found in rocks of Antarctica's Late Cretaceous (Poole et al., 2005) Angiosperm and conifer pollen is found in ocean sediment cores from around Antarctica (Ross Ice Shelf, Weddell Sea, Shackleton Ice Shelf) (Truswell, 1983). Angiosperm pollen includes lilies, irises, soapberries, myrtles, Bombacaceae (modern examples are the balsa and ceiba trees), laurels (sassafras), myrtles, southern beeches (Nothofagus) and palms (Poole et al., 2005). Conifer pollen includes the ubiquitous araucaria and podocarps. Other common Cretaceous plants, the ginkos and cycads, appear as well in the polar fossil record.

4.3 Summary of K/T Global Climate

An Earth without ice caps would look strange to us, revealing details of Arctic and Antarctic landmasses and coastlines hidden in brilliant ice today. The Maastrichtian forests grew unbroken from the Arctic Ocean to Yucatan, and from Germany to Kolyma—no steppe environments existed.

The Maastrichtian, at the end of the Cretaceous Hot House world, is a logical place to begin a series of reconstructions of Cenozoic climates. This was a Hot House world, but it was not a world of extreme climates. No Sahara or Australian Western deserts, or large Amazon/Congo type of rainforests appear. But both of these types of climatic zones will appear in the next Hot House world, only 10 Ma in the future.

Simulations of Maastrichtian climate have been run as if the continents were covered with bare soil (GENESIS climate model, Upchurch et al., 1999). This resulted in temperatures far too cold for the fossil plants found at middle and high latitudes (Wolfe and Upchurch, 1987). Therefore vegetation is thought to have a strong impact on polar climates.

Results of climate simulations for the Maastrichtian Hot House world still produce polar climates that are too cold (Scotese, personal communication, 2011). FOAM results indicate -40 C

at the Pole, yet as noted above, cycads and gingkoes along with broad-leaved deciduous trees survived there. Thus, there is overwhelming evidence for a much warmer climate at the poles than climate simulations suggest. Even seasonal ice is problematic (Scotese, personal communication, 2011).

CHAPTER 5

PALEOCENE/EOCENE THERMAL MAXIMUM (PETM) CLIMATE

5.1 Introduction to the PETM

The Paleocene-Eocene Thermal Maximum was a brief interval (<300 kyr) of elevated temperatures that occurred in the late Paleocene/early Eocene (Kennett and Stott, 1991). The authors described seafloor sediments marked by a sudden excursion in oxygen and carbon isotope values, extinctions of benthic fauna, and the disappearance of carbonate minerals. This horizon was overlain by a sequence of unbioturbated seafloor sediments, with a return of carbonate minerals further up-section. Other research supports Kennett and Stott's conclusions about global warming and changes in seawater chemistry at the PETM. injection of vast amounts of methane into the atmosphere from dissolved clathrates (Dickens et al., 1995), orbital forcing of climate (Lourens et al., 2005), acidification of seawater (Zachos et al., 2005), and the effect of a freshwater Arctic ocean on global oceanic circulation (Nunes and Norris, 2006, Brinkhuis et al., 2006, Cope and Winguth, 2009). In a world already in greenhouse conditions (Beerling et al., 2002), a rapid rise in global temperature over a few thousand years heated the climate to hotter than normal greenhouse conditions (Zachos et al., 2001; Zachos et al., 2010). Other phenomena associated with this sudden change in climate were shallowing of the calcite compensation depth (CCD) (Leon-Rodriguez and Dickens, 2010), extinction of many foraminiferal faunas (Schmitz et al., 1996), and the rapid speciation of others (Kennett, Stott 1991, Schmitz et al., 1996, Kelly et al., 1996, Crouch et al., 2001). Sluijs et al. (2011) report a bloom of the subtropical dinoflagellate Apectodinium, which is a proxy for warmer temperatures, that predates the carbon isotope excursion (CIE). This indicates that global climate was already warming before the CIE.

The PETM world has been described through paleogeographic reconstructions (Scotese, PALEOMAP Project), lithologic data (Robert and Kennett, 1994), paleontology (Dawson et al,

1976; Markwick 1997; Markwick, 2007), palynology (Wing and Harrington, 2001; Utescher and Mosbrugger, 2007; Smith et al, 2007; Akhmetiev and Beniamovsky, 2009), and climate simulations (Huber and Sloan, 2001; Huber and Cabellero, 2003; Cope and Winguth, 2009; Heinemann et al., 2009; Winguth et al, 2010).

Why does the PETM matter? Global climates have not been in greenhouse conditions since the Eocene (Zachos et al., 2001). The abrupt onset of the PETM may be the best analogue to the rapid warming observed in today's climate. (Leng et al., 2010, Leon-Rodriguez et al., 2010). Modern evidence for a warming climate invites a comparison with the PETM.

The PETM is the best-known example of super-greenhouse climates, or hyperthermals (Kennett and Stott, 1991; Thomas et al, 2003; Lourens et al., 2005; Zachos et al, 2006; Zachos et al, 2010). During the early Eocene, there were several hyperthermal events triggered by volcanism, ocean warming, and release of GHG from carbon sinks (Sluijs et al., 2007), most likely clathrates (Kennett and Stott, 1991), and/or Antarctic permafrost (McInerney and Wing, 2011). Hyperthermals subsequent to the PETM are called H1/ETM-2 (~53.7 Ma), I1 (~53.2 Ma), and K/X (~52.5 Ma). The effect of orbital cycles combined with perturbations of the carbon cycle may have amplified the climatic changes (Lourens et al, 2005; Röhl et al, 2007).

The PETM is dated at or near the 55.8 Ma boundary between the Thanetian stage of Paleocene time and ended in the early Ypresian stage of Eocene time. It lies within magnetochron 24 (reversed). It has chiefly been described from deep-sea boreholes of the Ocean Drilling Program (ODP), and its boundaries are defined in seafloor sediments by this evidence:

- A large negative carbon isotope excursion (CIE) detected in carbonate shells of microfossils: benthic foraminifera, coccolithophores, and dinoflagellate tests (Kennett and Stott 1991, Zachos et al., 2001, Smith et al, 2007).
- A global mass extinction of benthic foraminifera (Kennett and Stott, 1991).

- A global bloom of the dinoflagellate Apectodinium (Crouch et al., 2001)
- Clay-rich sediments that record dissolution of carbonates in a rapidly-acidified ocean (Roberts and Kennett 1994).
- An upper boundary marked by a carbonate-rich layer (Zachos et al., 2001), marking sudden plunges in the calcite compensation depth (CCD) (Leon-Rodriguez et al, 2010).
- Proxies used to estimate sea temperatures when seafloor conditions do not favor preservation of carbonate-shelled taxa: TEX_{86} (tetraether index of lipids consisting of 86 carbon atoms) and the alkenone unsaturation index $(U^{k'}_{37})^{8}$ (Bijl et al., 2009).

The base of the PETM has been dated at 54.93 Ma to 54.98 Ma (Norris and Rohl, 1999), 55.5 Ma (Kennett and Stott, 1991), 55.8 Ma (Robinson, 2011), 56 Ma (Bowen and Zachos, 2010) and variously at 55.5, 55.9, or 56.6 Ma (Westerhold and Rohl, 2009). Duration of the PETM has been set at 150 to 220 ka (Norris and Rohl, 1999)

5.1.1 Plate Tectonics

The paleogeography of the PETM world had not changed significantly from the K/T Boundary, only 10 million years before. The North Atlantic ocean basin was just beginning to open in Paleocene/Eocene time, but had not yet widened enough to allow deep ocean currents into the Arctic Ocean (Fig. 5.1) (Brinkhuis et al., 2006). As the Tethys Ocean closed, a collisional assembly of continental blocks was forming the southern Eurasian margin from Spain to India, with India just beginning to collide with Asia (Scotese 2008). The Drake Passage and Tasman Sea were beginning to open up, but ocean currents could not yet flow through them (Scotese, 2008).

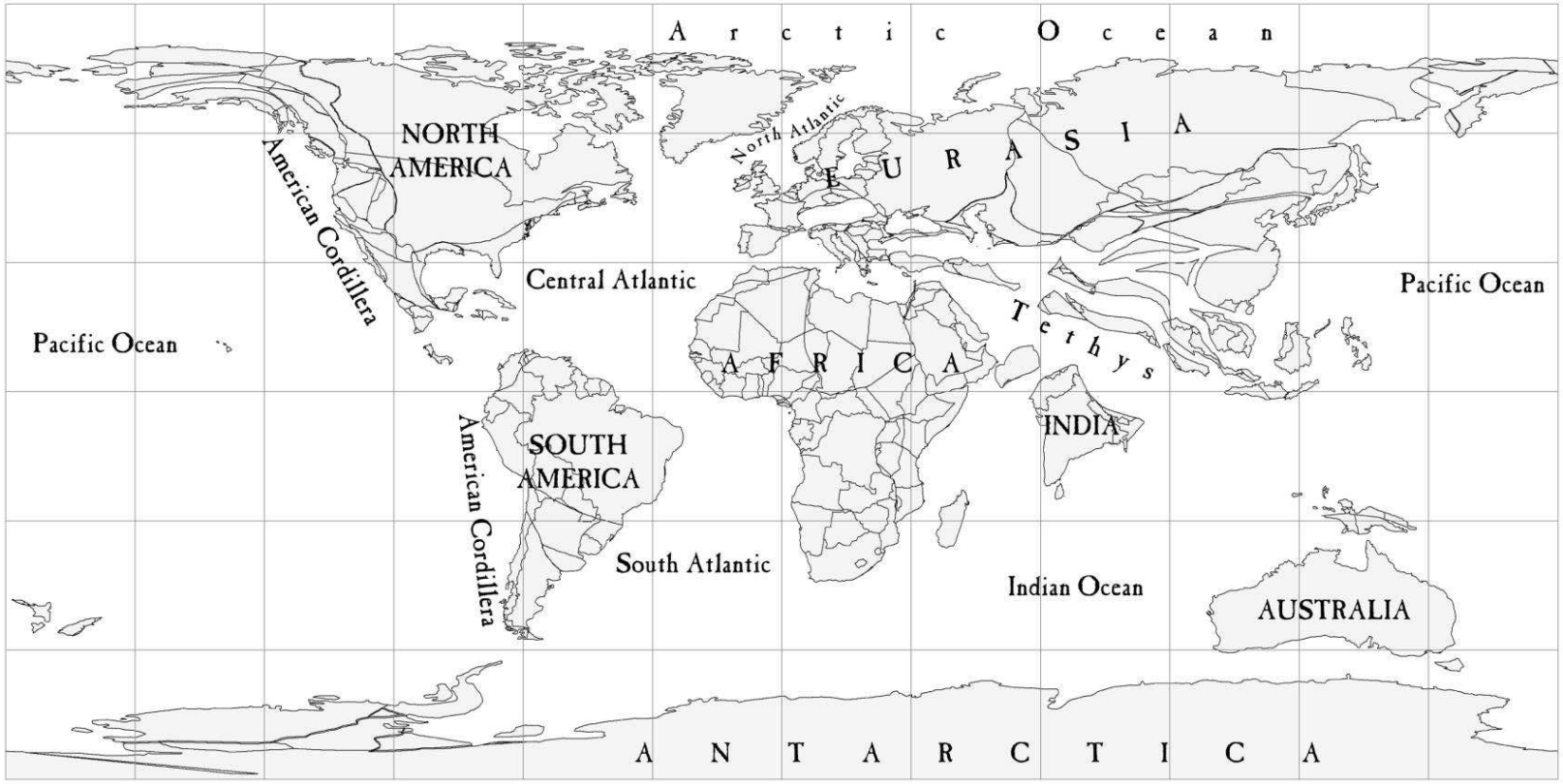

Fig. 5.1 Paleogeographic Base Map for the Paleocene/Eocene World. Scotese, 2008.

5.1.2 Paleogeography

Global sea level was high in the Paleocene relative to today (Golonka 2004, Scotese 2008). Shallow seas flooded large areas of Eurasia, Western Europe, North Africa, South America, New Guinea and the southern United States. (Scotese 2008, Akhmatiev and Beniamovsky 2009). No known ice caps existed, even small ones, so all the water that now covers Antarctica and Greenland was then in the oceans. The Arctic Ocean was still restricted enough to where it would have become brackish to fresh from precipitation, particularly during the increased precipitation thought to have fallen during the PETM (Brinkhuis et al., 2006).

Carbon isotope records indicate that like today, the Southern Ocean was the source for deep ocean currents (Pak and Miller, 1992; Thomas et al, 2003). Higher precipitation at high latitudes reduced salinity of polar ocean waters, making them less dense and preventing them from sinking and transporting cool, polar water to low latitudes (Miller et al., 1987). But freshwater in polar oceans, and the global pattern of δ13C values before, during, and after the CIE, may be evidence for a drastic shift in ocean circulation during the PETM (Nunes and Norris, 2006). The same greenhouse conditions that freshened the Southern Ocean also increased evaporation rates—and thus salinity and density of surface waters—in northern ocean basins. The source of deep ocean currents may have switched from the southern to northern hemisphere in as little as 5 kyr. Warmer waters at depth would have hastened the dissolution of clathrates, injecting vast amounts of methane into the atmosphere. More methane led to an increased greenhouse effect, which led to increased evaporation in northern ocean surface waters and increased rainfall in the Antarctic regions—a classic greenhouse feedback loop (Roberts and Kennett, 1995; Dickens et al, 1995; Bice and Marotzky, 2002; Nunes and Norris, 2006).

5.1.3 Paleoclimate of PETM in Context of the Paleogene

The Warm Temperature Climatic Zones in the Early to Middle Paleogene world were extended poleward from the equator, with no boreal forest or continental glaciers in evidence (Fig 5.2) (Utescher and Mossbrugger, 2007, Boucot et al., 2012).

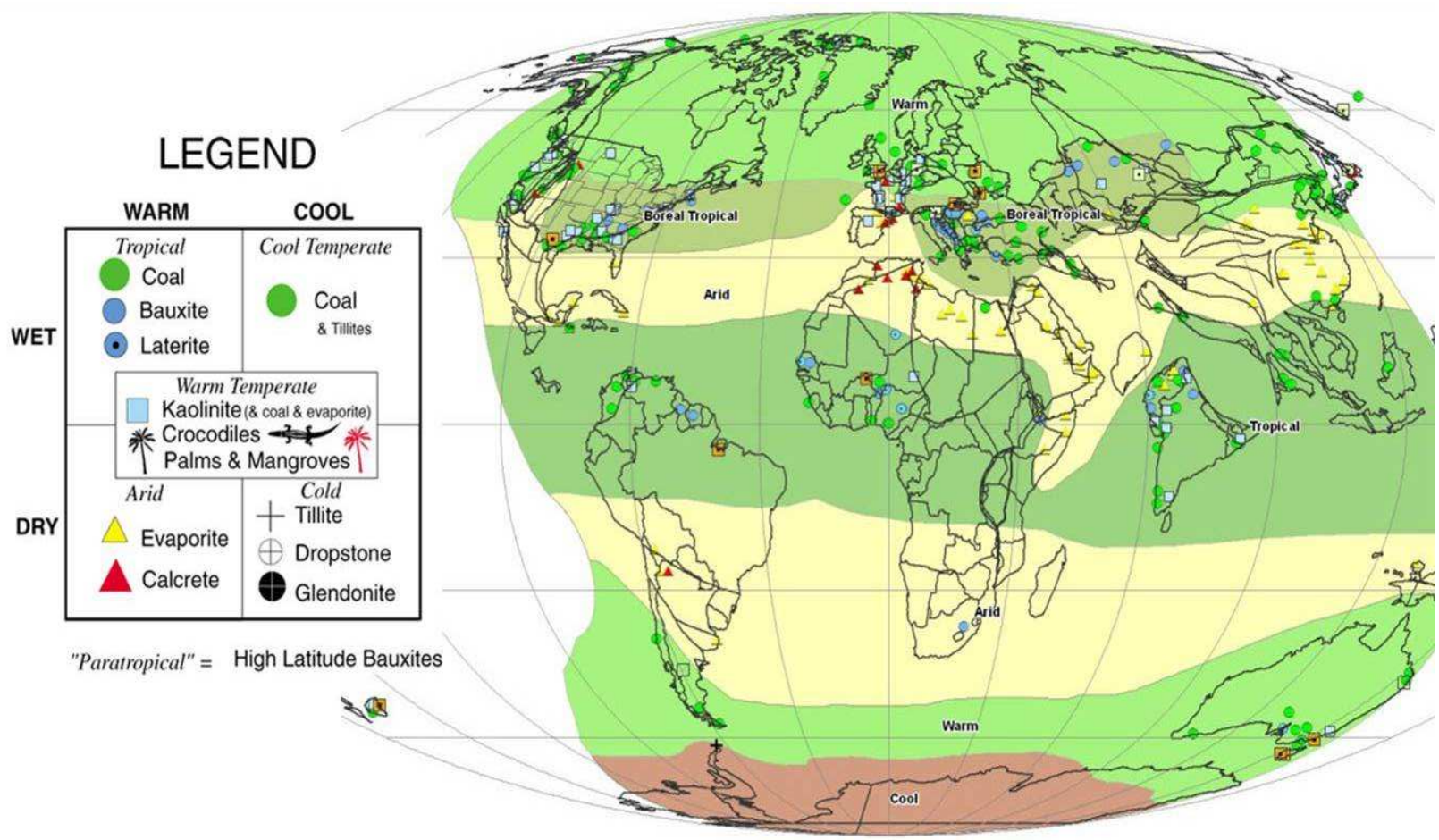

Fig. 5.2 PETM Climate Belts. Boucot et al., 2012

In this Hot House world, the PETM was the interval with the highest global average temperature. The equatorial wet belt expanded across what is today the Sahara and the Sahel, caused by a possible northern shift of the Intertropical Convergence Zone (ITCZ) (Winguth et al., 2010). Neither India nor Australia lay in the arid belts they are in today (Scotese 2008). An unusual boreal tropical belt stretched across the southern United States, southern Europe, and into central Asia (Utescher and Mossbrugger, 2007; Boucot et al., 2012). Kaolinite in deep-sea boreholes in the Southern Ocean are evidence that Antarctica had a cool temperate/rainy climate at this time (Robert and Kennett, 1994; Tripati et al., 2001,). There was enough climatic variability to produce both coals and sea ice in Svalbard in Paleocene and Eocene times (Spielhagen and Tripati, 2009).

Deep-sea oxygen and carbon isotope studies have provided an outline of climate history throughout the Cenozoic (Zachos et al, 2001; Tripati and Elderfield, 2005). A large negative oxygen isotope excursion at the PETM indicates warmer waters circulated throughout the oceans (Kennett and Stott 1991; Zachos et al., 2001; Bijl et al., 2009; Stap et al., 2010). In the PETM oceans, the global mass extinction event among benthic foraminifera is strong evidence for a tremendous change in ocean temperature, chemistry, or both (Kennett and Stott 1991; Kelly et al., 1996).

A large negative carbon isotope excursion at the PETM coincides with an oxygen excursion (Kennett and Stott 1991). It may be evidence of an injection of huge amounts of light carbon into the atmosphere from dissasociated clathrates (Dickens et al., 1995; Zachos et al, 2001). Biochemical markers in terrestrial sediments indicate that this carbon isotope excursion may be due in part to increased production of methane in wetlands (Pancost et al., 2007).

Deep-sea cores show a sudden disappearance of carbonate minerals at the base of the PETM. The calcium carbonate content of some cores dropped to 0% for a brief interval (Roberts and Kennett 1994, Zachos et al., 2005). Coincidental with the CIE, this is evidence for

acidification of seawater resulting from increased atmospheric CO_2 dissolved in seawater (Zachos et al., 2005, Leon-Rodriguez and Dickens 2010).

Concentrations of extraterrestrial ^{3}He have been observed to coincide with the CIE and lithologic evidence of the PETM (Murphy et al, 2009). A new age model has been proposed by Murphy et al., (2009) that includes a longer, sustained ^{13}C excursion that ended rapidly.

Evidence of seasonal/multiyear rhythms such as fossil tree rings or varved sediments could provide supporting evidence for models of changing climate patterns. CCSM models of the early Eocene ocean show an El Nino-Southern Oscillation (ENSO)-like rhythm, but supporting evidence is not yet available (Huber and Caballero, 2003).

5.2 Discussion of Paleoclimate Reconstruction

In this section, we review the climatic zones of the PETM world, starting with Equatorial Wet and moving toward the poles. Similar zones, such as the Northern and Southern hemispheres' Arid Zones, are discussed in the same section.

5.2.1 Description of Climatic Zones

5.2.1.1 Equatorial Wet Climatic Zone

If one includes the Boreal Tropical Climatic Zone in North America and Europe, the warm, wet Equatorial Zone spanned ~65 degrees from 45 N latitude in Russia to 20 S latitude in East Africa. India and Southeast Asia bore dark green rainforests, as did the Lhasa block (Utescher and Mossbrugger, 2007).

5.2.1.1.1 Lithologic and Paleontologic Data for the Equatorial Wet Zone

Warm, rainy climates increased the chemical weathering of silicate minerals, forming bauxite deposits and kaolinite-rich clays in soils. Bauxite deposits formed on the west coasts of Eurasian interior seaways (Akhmetiev, 2010), in Siberia north of Mongolia, and in the

northeastern United States (Boucot et al., 2012). Laterite in Algeria suggest that this part of the Sahara was much wetter than today, at least for a time (Boucot et al., 2012). Coals formed in the southeastern United States, in the Donbas and northern Kazakhstan (Hackley et al., 2006, Akhmetiev, 2010), and in northern Pakistan (Warwick and Shakoor, 1993). Tropical rainforest in northern South America experienced rapid species diversification during the time of elevated temperature and increased CO_2 (Jaramillo et al., 2010).

5.2.1.2 Arid and Semiarid Climatic Zones

In the PETM hot house world, arid landscapes covered much of the low-latitude continents. A wide stripe of desert crossed from the Tethys shore to the Pacific margins in East Asia. Tethys' coasts baked in dry conditions from Iran's Sanandaj-Sirjan Zone to the western coast of Spain. The climate of Africa's Arabian coast, now located in the middle of the Arabian peninsula, resembled today's Persian Gulf climate., All Africa and Madagascar south of 20 degrees S latitude was semiarid to arid. South America's hinterland between 10 and 40 degrees S latitude was also dry to very dry. Southern France and New Guinea, which are not arid today, experienced dry climates during the PETM.

5.2.1.2.1 Lithologic and Paleontologic Data for Arid and Semiarid Zones

Evaporites such as salt, gypsum, sylvite, borax, trona, and others, form in arid to seasonally dry climates. Evaporite deposits are found in Yucatan, Chiapas, and Florida; south of the Rio de la Plata, in New Guinea, and abundantly in eastern China (Boucot et al., 2012). Calcrete is a calcium deposit which occurs in semiarid to arid soils that form at the maximum percolation depth of water. Calcretes appear in Eocene paleosols in southern Europe, western North America, and northern Argentina (Scotese et al., 2009, Boucot et al., 2012). Land plant macrofossils indicating a warm, dry climate are found in the Bighorn Basin in Wyoming (Wing and Harrington, 2001, Wing et al., 2005). Diminished body size in the soil fauna in the Bighorn Basin of North America has been presented as evidence for elevated temperatures (Smith et al., 2009).

5.2.1.3 Warm Temperate Climatic Zone

The forest flora that evolved in the Mesozoic were ready to take advantage of the broad new habitat opened by the PETM warming event. Warm temperate forests of angiosperms and conifers flourished on every continent, including Antarctica. Greenland and southern Australia, that had been cool temperate to polar in the Maastrichtian, now supported broadleaf forest and palms. Subtropical plant life bloomed in Scandinavia, Novaya Zemlya, Kolyma, and the Antarctic Peninsula.

5.2.1.3.1 Lithologic and Paleontologic Data for the Warm Temperate Climatic Zone

A warm, summer-monsoon climate kept Siberia warm and wet enough for bauxite to form on the coast of the West Siberian Sea (Akhmetiev, 2010; Utescher and Mosbrugger 2007). Subtropical plants grew near today's Arctic Circle (Wolfe, 1994; Sluijs, 2006; Akhmatiev, 2010). Tex_{86} analysis indicates sea surface temperatures may have climbed to 24°C in the warmest hot house intervals (Sluijs et al., 2006). The presence of the free-floating fern Azolla shows that surface waters were relatively fresh (Brinkhuis et al., 2006).

Fossil terrestrial animals such as crocodilians and snakes appear north of the Arctic Circle (Dawson et al, 1976; Markwick 1997, 2007). Coal was laid down in Greenland, the south coast of Australia, and Tierra del Fuego (Scotese et al., 2009). Coal deposits in Alaska indicate a warm temperate if not subtopical climate (Williams et al., 2010). PETM-era coal also occurs on Ellesmere Island in Arctic Canada (McIver and Basinger, 1999), and on Svalbard (Spielhagen and Tripati, 2009). Sluijs et al. (2011) reports estimated sea surface temperature (SST) of ~30°C in the Southern Ocean near Antarctica.

5.2.1.4 Cool Temperate Climatic Zone

Antarctic ice now conceals the entire land surface that the Cool Temperate Climatic Zone may have covered. At present, only pollen in Southern Ocean core samples can provide information about the cool temperate climatic zones in the PETM.

5.2.1.4.1 Lithologic and Paleontologic Data for the Cool Temperate Zone

Fossil wood from mixed deciduous/coniferous forests of early Eocene age were found on King George Island, at the point of the Antarctic Peninsula (Poole et al., 2001). Pollen grains and spores of Paleogene age were found in glacial erratics in the Grove Mountains of East Antarctica (Fang et al., 2008). The assemblages include southern beech, pine, araucaria, and podocarps.

5.2.1.5 Polar Climatic Zone

There is no evidence of polar climates, such as boreal forest or tundra,in the PETM (Utescher and Mossbrugger, 2007, Upchurch et al., 2009), so no Polar or Boreal Climatic Zones are shown on the map.

5.3 Summary of PETM Global Climate

Lasting less than a million years, the PETM was a brief abberation from the normal Paleogene Hot House world. Average temperatures were higher than in other Hot House time intervals, especially at high latitudes. The pole-to-equator temperature gradient was much shallower, and Antarctic sea surface temperatures (SST) rose 8-10℃ (Zachos et al., 2003). No significant continental or sea ice was present in the PETM.

Ten million years after the muted hot house world of the Maastrichtian, the PETM climate painted the globe in a bold, contrasting pattern of dark rainforest and light desert surfaces. Bands of color marked the Equatorial Wet and Arid Zones in Africa, South America, and East Asia. The green Antarctica of the Late Cretaceous had become even greener, without continental glaciers. Deciduous trees grew across the interior of Antarctica, and along the shores of the Arctic Ocean. Apulia, India, southeastern North America and southern Siberia were dark with rainforest growth.

In terms of climate alone, the PETM was a hotter, more remarkable world than the Cretaceous Hot House. Even so, the term “hotter” implies extreme heat, which was certainly not the case over most of the world at that time. A greenhouse, after all, does not incinerate the

plants in it. The PETM world is more accurately described as a temperate-dominated world in the high latitudes, whereas extreme temperatures were only common in the tropics.

CHAPTER 6

EOCENE-OLIGOCENE TRANSITION (EOT) CLIMATE

6.1 Introduction to the EOT

The second dramatic climatic event of Paleogene time began near the end of the Eocene and continued through the beginning of the Oligocene Epoch. The Eocene/Oligocene Transition (EOT) marks the beginning of the modern world Ice House, even while Hot House conditions remained in force in middle and low latitudes (Boucot et al., 2012). Off the shores of Antarctica, dropstones litter the seafloor in the Eocene-Oligocene stratigraphic section, marking this epochal change (Zachos et al., 1992). Tropical seafloor sediments of Eocene age, rich in opal grains, change suddenly to a carbonate-rich composition as the calcite compensation depth (CCD) deepened near the Oligocene boundary (Coxall et al., 2005). Lithology, plate tectonics, and positive excursions in the $\delta^{18}O$ and $\delta^{13}C$ curves are strong evidence for a world in which multiple causes worked at the same time toward dramatically cooling the polar climate, and to an extent, the global climate. Climate models generally agree with the rock evidence (Zhang et al., 2011). As high-albedo tundra replaced Antarctica's dark evergreen forest, a vegetation-climate feedback loop may have accelerated the cooling climate (Thorn & DeConto, GENESIS model, 2005). CCSM3 model runs show significant cooling of Antarctic surface waters resulting from lowered atmospheric CO_2 (Liu et al 2009). A FOAM simulation that closed the two tropical oceanic gateways—Tethys and the Central America Seaway—also show strong cooling of Antarctic seas (Zhang et al., 2011). But the Eocene-Oligocene Transition (EOT), while a dramatic climate event, did not end the Hot House conditions all over the world.

6.1.1 Plate Tectonics

The general tectonic theme of post-Pangean continental dispersion continued in the Eocene. The Atlantic Ocean continued to widen. Only the southern border of Eurasia saw extensive collisional mountain-building, where India collided with Asia (Fig 6.1). The last of Tethyan ocean floor was subducted as Africa (including Arabia) collided with Asia, raising the Zagros and Tauride ranges (Yin, 2010). This collision resulted in a slower average seafloor spreading rate (Scotese et al., 2008), which corresponds with prediction models such as the BLAG hypothesis (Lasaga et al., 1983) and GEOCARB II (Berner, 1994).

India's post-collisional northward movement raised Tibet into a very high plateau in the hinterland of the enlarged Asian continent (Yin, 2010). The Tibetan Plateau, and the rising Himalayas, began to alter Asian climate, causing wetter conditions in China that have persisted to the present day (Sun and Wang, 2005, Allen and Armstrong, 2012).

In the Southern Hemisphere, South America and Australia had fully rifted away from Antarctica—opening the Drake Passage and Tasman Straits. These oceanic gateways widened enough to affect oceanic circulation, allowing ocean currents to flow all around Antarctica (Scher, et al. 2006, Katz et al., 2011). South of the Antarctic Circumpolar Current, water masses became restricted in the embayments around Antarctica and formation of cold, deepwater currents was strengthened (Katz et al., 2011).

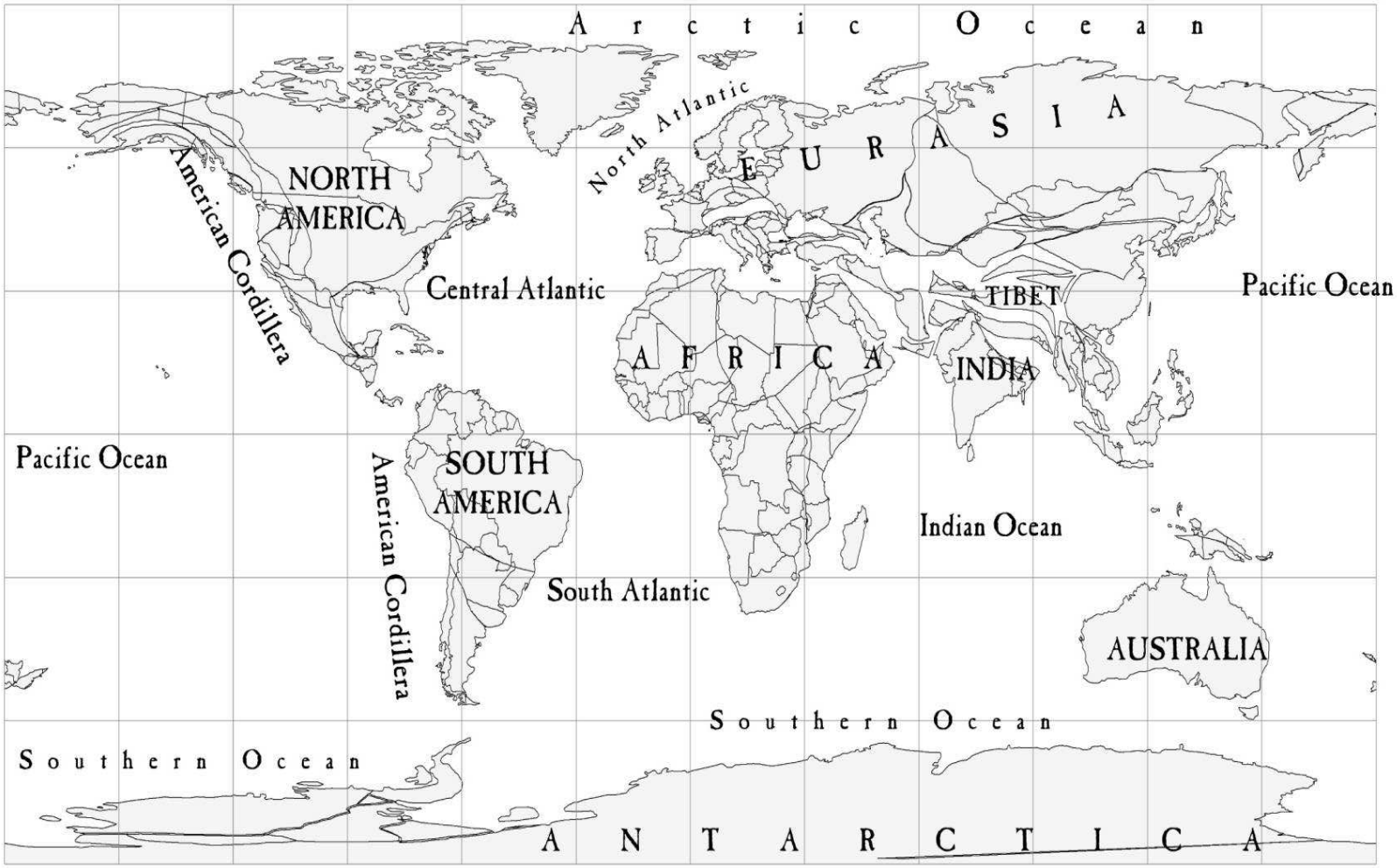

Fig. 6.1 Paleogeographic Base Map for the Early Oligocene World. After Scotese, 2008.

6.1.2 Paleogeography

The continents of Eocene-Oligocene Transition (EOT) time lay in the same relative positions they appear in today. India had met Asia, but its collision was still incomplete. Both South and North Atlantic Oceans were 20% narrower, meaning the Pacific Ocean was correspondingly broader than today. The Southern Ocean was still interrupted at the Drake Passage and the Tasman Sea (Lawver & Gahagan, 2003, Livermore et al., 2005). Australia's position left a passage ~10 degrees wide between the Indian and Pacific Oceans (Lawver & Gahagan, 2003, Scotese 2008).

Changing straits and land bridges opened or strangled the inter-ocean flow of currents. The evolving current flow strongly affected the EOT world, and combined with other factors to cool it dramatically (Katz et al., 2011, Zhang et al., 2011). The restrictions of the Drake Passage and Tasman Sea caused EOT oceanic currents to flow rather differently than they do in modern oceans (Zhang et al., 2011). South America and Antarctica's connection had been tenuous since the late Jurassic. By the late Eocene, it allowed deep currents to pass through a strait ~6 degrees wide (Livermore et al., 2005). Deep waters began to pass south of Australia as it drew rapidly away from Antarctica between 35 and 40 Ma. Near the Equator, the continental crust of Central America and Panama did not yet connect North and South America. But Panama rose high enough, even in its still-submerged sections, to allow only shallow currents to pass between the Pacific and Atlantic Oceans (Zhang et al., 2011). In Europe, the North Sea-Paratethys Seaway narrowed and was divided by a new land bridge between Eurasia, including Scandinavia, and Western Europe. This brought about the extinction event that defined the Eocene-Oligocene boundary—the Grande Coupure (Stehlin, 1910).

Global sea levels were higher than today (Haq et al., 1987, Scotese 2008), as much as 200 m above modern sea level at the Eocene-Oligocene boundary. As the Oligocene began, sea levels immediately dropped to ~25 m above modern sea level at the end of the Rupelian at 28.5 Ma (Haq et al., 1987). This dramatic fall in sea level corresponds with the growth of a large

continental ice cap in Antarctica (Peters et al., 2010). Scandinavia, Greenland, Iceland, and Svalbard were not yet separated by deep ocean basin.

As far back as 40 Ma, continental glaciation on Antarctica is indicated by steadily increasing $\delta^{18}O$ values following the Mid-Eocene Climatic Optimum (MECO) (Zachos et al., 2001). $\delta^{18}O$ increases in in a large knickpoint between 33 and 34 Ma, corresponding with the first appearance of ice-rafted dropstones in the Southern Ocean around Antarctica (Scher et al., 2011). However, evidence for full-scale continental ice sheets is lacking from the Arctic (Eldrett et al., 2007).

6.1.3 Paleoclimate of EOT in Context of Late Paleogene

34 million years ago, cooling climate at the end of the brief MECO (Bohaty and Zachos, 2003) marked the beginning of the end of the most recent global Hot House world. Foraminiferal $\delta^{18}O$ values from ODP Site 689 began rising at 41.5 Ma (Diester-Haass and Zahn, 1996), indicating a cooling climate. Global sea levels fell by 10^1 meters 2 Ma before the cooling began (Peters et al., 2010). The $\delta^{18}O$ curve can indicate either icecap growth or global cooling without icecaps (Liu et al., 2009), but comparison with other proxies ($U^{K'}_{37}$ and TEX_{86}) indicates that an icecap covered much of Antarctica (Liu et al., 2009). Despite the cooling South Pole, the EOT's Warm Climatic Zones still extended far from the Equator in both hemispheres.

A decrease in atmospheric CO_2 is likely to be the cause of icecap growth in Antarctica at the EOT (Pagani et al., 2005, Pearson et al., 2009). The end of Tethyan subduction north of India may have resulted in significantly decreased atmospheric CO_2 levels (Kent & Muttoni, 2008). Weathering of the Deccan and Ethiopian igneous provinces by equatorial rain, as well as weathering of the rising Himalayas, withdrew CO_2 from the atmosphere at the same time (Kent & Muttoni, 2008). $\delta^{13}C$ increased sharply before the EOT (Zachos et al., 1992) and ocean productivity increased during the EOT.

Continental ice caps in Antarctica are indicated by dropstones at ODP site 738 (Scher et al., 2011) and tillites on the Antarctic Peninsula, in Prydz Bay, and in the Ross Sea. Deposition of

ice-rafted debris coincides with the second major plunge of $\delta^{18}O$, but not the first (Scher et al., 2011).

Non-radiogenic neodymium (Nd) isotopes in fossil fish teeth indicate that a new continental source for the element, had entered the marine realm (van de Flierdt et al., 2007, Scher et al., 2011). Angiosperm-dominated forests of the Antarctic Peninsula decreased in diversity, shifting to conifer and beech woodlands that marked the onset of much colder climates (Anderson et al., 2011). The calcite compensation depth (CCD) in the Pacific Ocean deepened by ~1 km (Coxall et al., 2005). The CCD is mainly controlled by dissolved inorganic carbon (DIC) + alkalinity, and only to a lesser extent by temperature. The CCD deepens in CO_2-poor deep water, so the deepened CCD of EOT oceans indicates a decrease in the overall carbon budget of the EOT (Coxall et al., 2005).

Dropstones are reported from ODP 913 off east-central Greenland (Eldrett et al., 2007), but floral assemblages in the Arctic indicate summer temperatures too warm for continental glaciation at this time (Eldrett et al., 2009). Although there is no reason to doubt localized and alpine glaciation in the Arctic highlands, the $\delta^{18}O$ curve can be explained by Antarctic glaciation alone (Liu et al., 2009).

6.2 Discussion of EOT Paleoclimate Reconstruction

In this section, we review the climatic zones of the EOT, starting with Equatorial Wet and moving toward the poles. Similar zones, such as the Northern and Southern hemispheres' Arid Zones, are discussed in the same section.

6.2.1 Description of Climatic Zones

6.2.1.1 Equatorial Wet Climatic Zone

Similar to the PETM 25 million years before, extensive areas of rainforest and wet/dry forest encircled the EOT tropics. Central America had moved southward into the Tropics. Northern South America and Central Africa were covered in rainforest. The African Equatorial Wet Zone lay roughly where it does today, but did not extend as far north as it had in the PETM. India, Southeast Asia, Indonesia and the Phillipine Islands all supported lush forest growth.

The Boreal Tropical Belt persisted into the Oligocene, stretching from France to Mongolia. Apulia and the Balkans lay ~30° North of the Equatorial Wet Zone, but experienced similar climate. The eastern United States had become drier, and no longer was part of the Boreal Tropical Belt.

6.2.1.1.1 Lithologic and Paleontologic Data for the Equatorial Wet Zone

Coal deposits chiefly define the Equatorial Wet Zone in the EOT (Boucot et al., 2012). Numerous coal deposits delineate the European, Southeast Asian, and Indonesian Equatorial Wet Zones. Other evidence includes kaolinites, bauxites, laterites, and crocodilian fossils. Oligocene kaolinites are found in Europe, Kazakhstan, and Japan in the Boreal Tropical Zone, and Colombia near the Equator. Bauxites appear in Apulia, Kazakhstan, Siberia, and French Guiana. Laterites appear in Colombia and Brazil.

6.2.1.2 Arid and Semiarid Climatic Zones

Arid to semiarid climates covered the interior western United States—the Rockies and plains to the East. Northern Mexico and the Greater Antilles were also dry. With Tethys' closure, a desert now spanned from the Atlantic coast of West Africa all the way to the eastern coast of China (Boucot et al., 2012). South America lay within the southern Arid Zone between ~15° and

35° S. Arid climate capped the interior highland of Africa with an extensive desert south of Angola and Zambia. New Guinea lay at ~20° S latitude, with in the Arid Climatic Zone.

6.2.1.2.1 Lithologic and Paleontologic Data for the Arid and Semiarid Zones

In North America, evaporites and calcretes are found in the the Rocky Mountains and in regions east of the mountains. The Arid Zone in North Africa and the Near East is marked by evaporites and calcretes. Many evaporite localities appear across Asia between 25° and 45°N latitude. Evaporites provide a record of increasing aridity in the northeast Tibetan Plateau (Abels et al., 2011). South America contains calcretes and evaporites between ~15° and 35° S.

6.2.1.3 Warm Temperate Climatic Zone

The remainder of North America that was not Alpine or part of the Arctic Ocean seacoast lay in the Warm Temperate Zone. In the newly-assembled Eurasian continent, warm temperate climates stretched from the Bay of Biscay to the Sea of Okhotsk, Korea, and Japan. In the Southern Hemisphere, only Patagonia, Australia, New Zealand and Kerguelen, had warm temperate climates.

6.2.1.3.1 Lithologic and Paleontologic Data for the Warm Temperate Zone

Coal forests blanketed the Pacific coasts of Alaska and Canada. Arctic coals were deposited in Ellesmere Island and Svalbard. Coal deposits were laid down in abundance in Western and Central Europe, the Balkan Peninsula, Manchuria, Korea, and Japan. Bauxites formed around the Adriatic Sea. In South America and Australia, the southern Warm Temperate Zone is marked by the occurrence of coal, kaolinite, and crocodilians.

6.2.1.3 Cool Temperate Climatic Zone

The poleward shift of the Warm Temperate Climatic Zone boundaries resulted in less room for the Cool Temperate Zone in both Northern and Southern Hemispheres.

6.2.1.3.1 Lithologic and Paleontologic Data for the Cool Temperate Zone

Lithologic evidence for the Cool Temperate Climatic Zone has been found on the Antarctic Peninsula in Early Oligocene sediments (Thorn and DeConto, 2006), and some evidence for cool Oligocene climates has been described in the Arctic (Moran et al., 2006; Eldrett et al., 2009)

6.2.1.4 Polar Climatic Zone

For the first time since the Permian, large continental ice sheets covered the South Pole. Antarctica entered the Ice House conditions that persist there to this day (Cooper and O'Brien, 2004, Miller et al., 2007, Liu et al., 2009, Scher et al., 2011). The cool temperate forests of Eocene age retreated to the Antarctic Peninsula, the last part of the continent to be glaciated (Anderson et al., 2011).

6.2.1.4.1 Lithologic and Paleontologic Data for the Polar Zone

Ice-rafted dropstones (IRD) began to accumulate on the Kerguelen Plateau at ~36.3 million years ago (Ehrmann and Mackensen, 1992, Zachos et al., 1992). Pollen of beech and conifer forests has been described in core samples from the Weddell Sea and Joinville Plateau (Anderson et al., 2011). This indicates that the Antarctic Peninsula may have only experienced limited alpine glaciation during EOT time.

6.3 Summary of EOT Global Climate

The isolation and subsequent glaciation of Antarctica at the end of the Eocene was the most important climatic turning point of the Cenozoic. After this plunge into very cold conditions in the Southern Hemisphere, Earth's climate experienced fewer warm intervals. Forests would grow on the shore of the Arctic Ocean into the Neogene. But the events that would lead to the eventual freezing of the Arctic had been put into motion.

India had collided with Asia, leaving only the Mediterranean as the last remnant of Tethys. The Panama and Indonesian gateways were closing. The Himalayas and Tibetan Plateau had risen and the weathering of these highlands began to promote the absorbtion of CO_2. This absorbtion of CO_2 lowered the concentration of the greenhouse gas in the atmosphere, and contributed to global cooling. With continued uplift and erosion, the reduction of CO_2 concentration by the Himalayas and Tibet continued at a more rapid pace.

The Himalayas and Tibet began to affect climate physically as well as chemically. The new highland disturbed the parallel bands of winds and climatic zones circling the Earth from Equator to the poles. The two most important effects of this disturbance was the beginning of tropical seasonality in India, and increased rainfall in eastern China. After the South Asian orogeny, only western China would remain a desert.

Large rain forests and deserts crossed the low latitude lanmasses. Warm temperate forests dominated the northern continents and Australasia. Cool temperate and boreal forests ringed the Arctic Ocean, and covered the highlands of the Russian Far East.

6.3.1 Remaining Questions About Eocene/Oligocene Climate

Climate evidence and models indicate that the world cooled significantly at the Eocene-Oligocene Transition. Questions that remain to be answered include: The extent of Antarctic glaciation at the end of the Eocene (Anderson et al., 2011, Wilson et al., 2011), and the presence of glaciers in Late Eocene Greenland (Eldrett et al., 2007).

CHAPTER 7

MIOCENE (MESSINIAN) CLIMATE

7.1 Introduction to the Messinian

During the Late Miocene, both the Arctic as well as Antarctic were covered by vast continental ice caps. The Messinian Age marks the beginning of full, i.e. bipolar, Ice House conditions on Earth. The continents and ocean basins lay approximately in their modern positions. Three oceanic gateways (Panama, Gibraltar, and Indonesia), that previously connected the world's oceans, were completely closed by the Messinian Age. These barriers greatly altered ocean currents and triggered bipolar Ice House conditions.

Closing of the Panama Strait ended the mixing of Caribbean waters with less-saline Pacific waters (Bartoli et al., 2005). Warm, westward-flowing Central Atlantic currents began to mix with more saline Caribbean waters. Circulating around the Central Atlantic subtropical gyre, these waters entered the newly-formed Gulf Stream. Warm, high-salinity waters began to discharge into the North Atlantic. Once in the North Atlantic, the warmer water evaporated more quickly than the cold water around it, providing abundant water vapor to North Atlantic weather systems. Some of this water vapor fell as snow on Greenland and Baffin Island. Over time, ice sheets formed on these islands as orbital forcing caused cooler summers (Haug and Tiedemann, 1998). Once the ice sheets had formed, they increased the albedo of the North Atlantic area, contributing to cooler temperatures. Increased evaporation caused increased salinity in North Atlantic waters, and escalated the formation of North Atlantic deep water (NADW) (Keigwin, 1982). The alternating advances of polar ice sheets, driven by Milanković forcing, did not begin until the Pliocene, but the important changes to Atlantic currents during the Messinian helped shape these subsequent events.

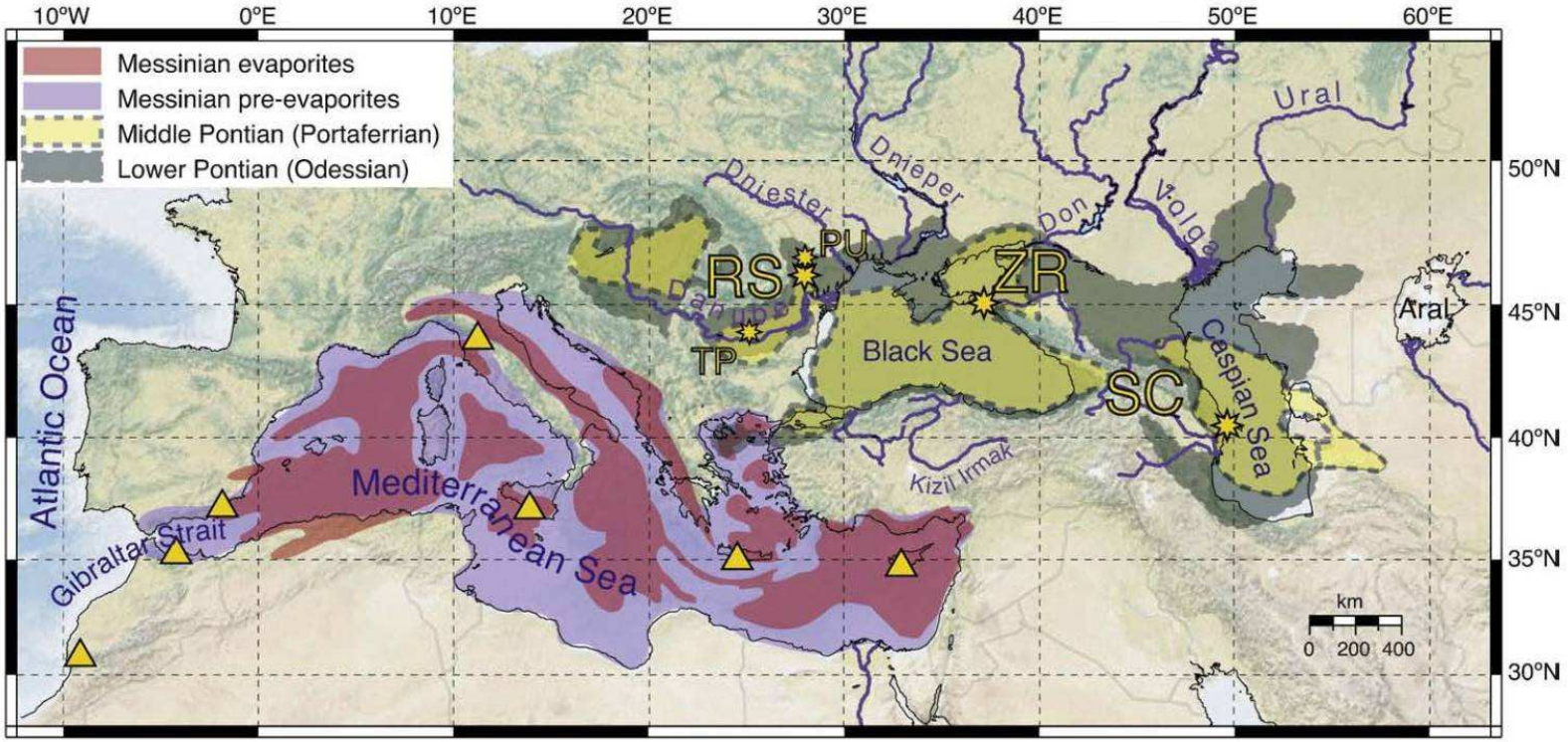

Fig. 7.1 Messinian Evaporites in the Mediterranean and Paratethys Basins. Krijgsman et al., 2010.

Evaporites of Messinian age ring the Mediterranean and Paratethys Basins (Fig. 7.1.). Thick sequences of evaporites buried beneath the floor of the Mediterranean Sea were found by the Deep-Sea Drilling Project (Hsü et al. 1973). These evaporites record the greatest known sea level fluctuations in geologic history, up to 3 km (Hsü et al., 1973). This event is called the Messinian Salinity Crisis (MSC). These evaporites were deposited in a completely enclosed Mediterranean Basin. Previously, the Mediterranean Basin had been connected to the Atlantic and Tethys Oceans. Closing of the Straits of Gibraltar in the Messinian cut off the Mediterranean from the world's oceans.

The processes that closed and opened the Stratis of Gibraltar, the Mediterranean's sole connection with the world ocean, remain a topic of debate. Roll-back tectonics may have allowed hot asthenosphere to lift up the crust under the Betic/Rifean Arc, closing the oceanic gateway (Duggen et al., 2003). A huge ramp may have formed a whitewater river with a slope of 1 to 4% that ate a channel through the Betic Cordillera (Garcia-Castellanos et al., 2009). Irregardless of the cause, the Mediterranean Sea was isolated from the world's oceans between 5-6 Ma. At ~30 degrees N latitude, the Mediterranean lies in the arid climate belt. Once it was isolated, its waters evaporated, leaving their mineral content as evaporite sequences. Disconnected hypersaline seas lay in the bottom of the deepest parts of the basin, which may or may not have dried out entirely at times (Hardie and Lowenstein, 2004). It is interesting to note that if the Mediterranean had lain along the Equator, rainfall would have filled its isolated basin, making a brackish ocean (Scotese, 2011).

C_4 grasses became important parts of Miocene ecologies, possibly caused by cooler, drier climates and lowered CO_2. levels (Osborne, 2008). Grasses spread successfully around the world in the Miocene, modifying existing biomes and causing the appearance of new biomes (steppe/prairie, modern savanna). Grassland biomes spurred animal evolution, most notably in ungulate mammals (Edwards et al., 2010). Charcoal records indicate an increased incidence of wildfires (Keeley and Rundel, 2003, Osborne and Beerling, 2006). Grasses may have evolved ways to profit from dry season fires that reduced forest cover, growing abundantly in the wet

season, retaining dead foliage, and developing fire-resistant seeds (Edwards et al., 2010). Grasslands have a higher albedo than dense forests, and reflect more solar energy back into space. This may have contributed to cooler average temperatures in the Miocene.

7.1.1 Plate Tectonics

In the nearly 30 million years since the Eocene-Oligocene Transition (EOT), significant plate tectonic events had taken place. These changes altered global sea and air circulation, resulting in full Ice House conditions.

Equatorial oceanic gateways were now closed. Central America blocked exchange of warm ocean currents between the Atlantic and Pacific Oceans. In the Western Pacific, Australia and Southeast Asia had begun to collide, blocking equatorial currents flowing between the Indian Ocean and the Pacific Ocean (Fig. 7.2).

Polar oceanic gateways were fully open by the Miocene. At nearly its full modern width, the widening North Atlantic Ocean allowed deep currents to flow in and out of the Arctic Ocean. At the opposite pole, the wide-open Drake Passage and Tasman Sea allowed Southern Ocean currents to move unhindered around Antarctica.

7.1.1.1 Closure of the Mediterranean-Atlantic Oceanic Gateway Through Gibraltar

The Miocene tectonics of the western Mediterranean are complex. During the Miocene, the Betic-Balearic-Kabiliy Arc rifted away from eastern Iberia, opening the Balearic Sea Basin. Also at this time, Corsica and Sardinia rifted away from southern France. As the Betic-Balearic-Kabiliy Arc moved southward, it closed the Mediterranian-Atlantic oceanic gateway.

Until the Miocene, the greater Mediterranean Basin had separated Apulia, Pannonia, and Moesia from northern Europe. By the Messinian, these several continental blocks had joined Europe. New mountain belts rose: the Alps, Carpathians, Dinarides, and the Balkans of Bulgaria.

The Pontides narrowed the oceanic gateway between the Mediterranean and Paratethys Seas, forming the Bosphorus and Dardanelles.

In the western Mediterranean Basin, Sardinia and Corsica had rifted away from southern France. Pulled away from the continent by subduction beneath the Tyrrhenian Sea, they pivoted counterclockwise around an axis in the Ligurian Sea. The Balearic Islands sat on a promontory of the Iberian block as they do today, separated from Catalonia by the Balearic Sea. A small island arc in the shape of the letter C, the Betic-Rifean Arc, almost plugged the western entrance to the Mediterranean. The Atlantic and Mediterranean were connected by a shallow oceanic gateway passing through the center of this arc, which closed in the Messinian.

7.1.1.2 Other Late Miocene Tectonic Events

The largest orographic barrier on Earth, Tibet had achieved its current elevation and extent by 15 Ma in the mid-Miocene (Spicer et al., 2003). Tibet blocked warm, northward-flowing air currents, and caused monsoon climates to develop in South, East, and Southeast Asia. These monsoon climates had been in place since the beginning of the Miocene (Sun and Wang, 2005, Allen and Armstrong, 2012). Tibet's elevation has remained nearly constant since then (Spicer et al., 2003, Currie et al., 2005, Rowley and Garzione, 2007).

During the Miocene, the southern border of Eurasia experienced a series of collisional orogenies similar to the Pangaean collisions of Carboniferous age. Collisions with Africa, India, and Australia pushed up fold-thrust belts that stretched 15,000 km from Spain to Burma. Turkey was extruded westward as Arabia pushed northwards into Eurasia.

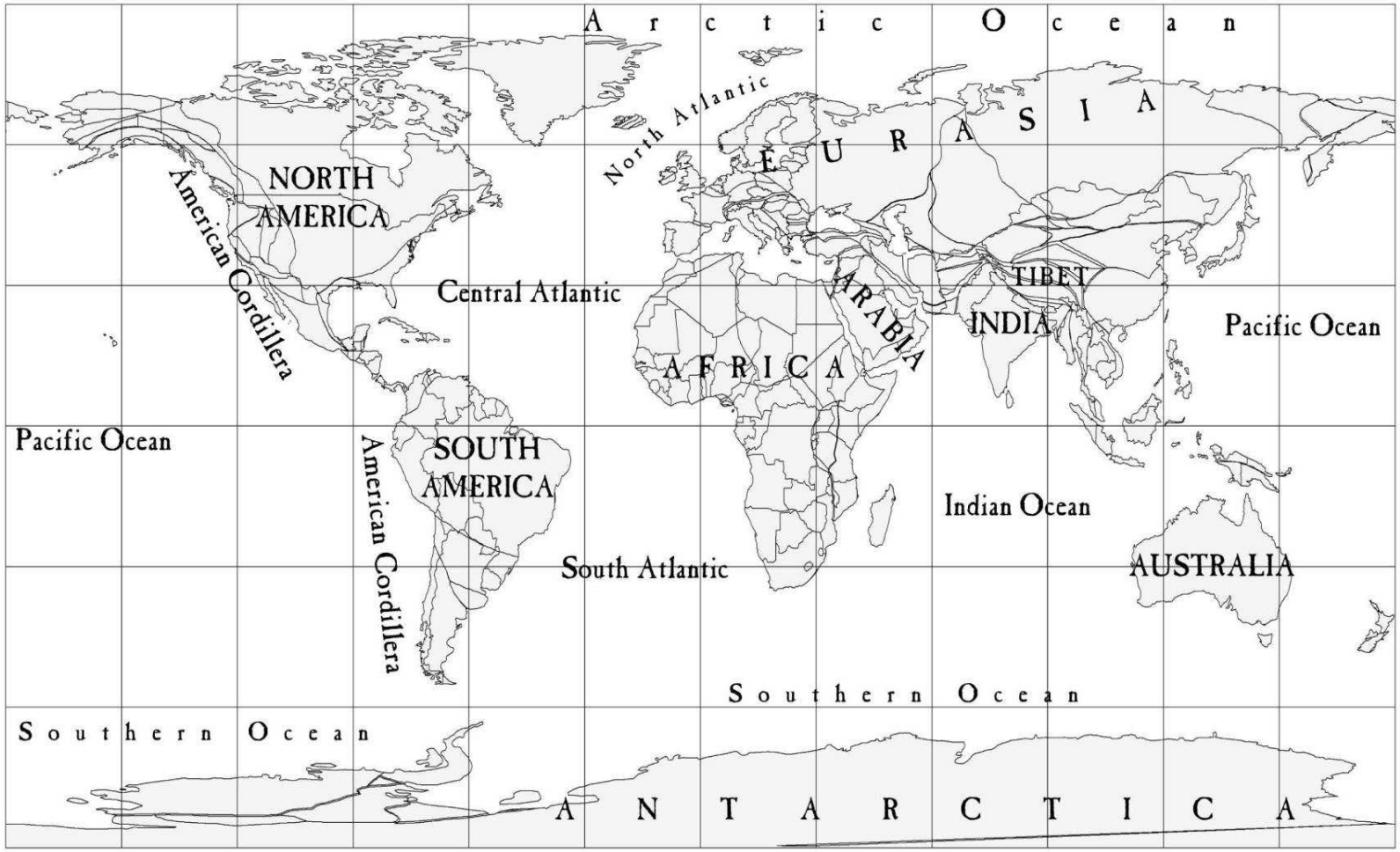

Fig. 7.2 Paleogeographic Base Map for the end of the Miocene. Scotese, 2008

A triple-junction appeared under Ethiopia, beginning to rift open the Gulf of Aden and the Red Sea. Regional uplift associated with the East African Rift formed an orographic barrier.

The Colorado Plateau was rising isostatically in the Late Miocene (Moucha et al., 2008, Moucha et al., 2009). Its eastern boundary had become the failed intra-continental Rio Grande Rift, most active between 16 and 10 Ma (Keller and Cather, 1994). Active extension in the Basin and Range Province, including Trans-Pecos Texas and part of northern Mexico, bordered the Colorado Plateau to the West and South (McQuarrie and Wernicke, 2005, Scotese et al., 2008). Baja California rifted away from the mainland of North America, opening the Gulf of California.

The Central Andes had risen to their present elevation by 6 Ma (Rowley and Garzione, 2007). In the Western Pacific, new backarc basins had formed, opening the Sea of Okhotsk, the South China Sea, and the Sea of Japan.

New Zealand was in the midst of being assembled in the Miocene. The eastern part of South Island moved in a right-lateral sense in relation to the North Island. These landmasses rode opposite sides of an obliquely convergent transverse plate boundary, the Hikurangi Margin. The Pacific Plate was subducted as it moved past the Australian Plate. New Zealand's separate tectonic parts would move hundreds of kilometers, and rotate 4-5°/Myr, in the next six million years (Lamb, 2011).

7.1.2 Paleogeography

In general, the geography of the Messinian world looked much like the present day, though its details varied slightly in most areas, and radically in others. The dessicated Mediterranean Basin is one of the most significant paleogeographic features, as is the development of the Greenland ice sheet. During the Late Messinian, continents became cooler and drier. (Kürschner et al., 2006). CO_2 levels fell, boosting the evolution of C4-pathway photosynthesis plants (Zachos et al., 2001). Extensive grasslands began to spread in the Miocene, replacing broadleaf herbs and ferns as ground cover (Kürschner et al., 2006).

Grasslands transformed the savanna-like habitats of the past into a fully modern savanna (Edwards et al., 2010).

7.1.2.1 Ocean Basins

Paleogeographic reconstructions of the Neogene (Haq et al., 1987, Scotese 2004, 2006, and 2008) show that Miocene sea levels ranged between a highstand of ~100 m above modern sea level, to a lowstand of ~75 m below modern sea level. Plate motions closed oceanic gateways near the Equator (Panama and Indonesia), while the Circum-Antarctic Current grew even stronger. The modern movement of ocean currents had powerful effects on global temperature and precipitation (Scotese et al., 2011). The permanent continental ice sheet grew in the uplands of east-central Greenland, and may have caused the end-Miocene sea level fall (Haq et al., 1987)

7.1.2.2 Evidence for Ice Caps Appears for the First Time In the Arctic

During the Miocene, the Antarctic Circumpolar Current (ACC) flowed unobstructed in the Southern Ocean (Frakes et al., 1992; Ruddiman, 2001; Hays et al., 2005). The North Atlantic Gulf Stream carried warm waters to the Arctic. Dropstones show that these glaciers reached the sea and made icebergs in the Messinian. Tillites in Patagonia also appear in the Late Miocene sedimentary record (Graham, 2011).

Lying at or north of 30 degrees N latitude in the arid and warm temperate climatic zones, Mediterranean Basin waters evaporated quickly. Thus, once isolated, the Mediterranean sea level dropped drastically (Govers, 2009). Ocean waters withdrew into a few separate hypersaline seas in the deepest parts of its basin (Fig 7.1). Gypsum, anhydrite, evaporitic limestone and halite formed in thick (10^3 meters) sequences in these large, Dead Sea-like bodies of concentrated seawater.

Erosion of deep canyons in the Betic-Balearic-Kabiliy Arc opened sluices through which the Atlantic Ocean poured through, rapidly recharging the Mediterranean Sea.

These recharge events may have been repeated as many as 50 times (Hsü et al., 1973) or much less (Michalzik, 1996). Evaporite bodies of roughly the same age have been described across the much shallower Paratethys, but it is not known whether it was completely dessicated and refilled (Krijgsman et al., 2010).

7.1.2.3 Closure of the Panama Oceanic Gateway Linking Atlantic and Pacific Oceans

By the Late Miocene, the Panama Arc blocked currents flowing between the Atlantic and Pacific Basins. Closure of the Panama oceanic gateway diverted west-flowing warm currents in the Central Atlantic and Caribbean into the North Atlantic, carrying warm, saline water. Evaporation of Gulf Stream waters in the Arctic provided more water vapor to the atmosphere, and brought about heavier precipitation of snow in the uplands of East Greenland and Baffin Island. Coincidentally, glaciers began to grow in the northern American Cordillera. On land, as the Miocene merged into the Pliocene, a great number of plant and animal species began crossing between the northern and southern American continents.

7.1.2.4 Australia Closes Pacific-Indian Ocean Gateway

Australia had begun to collide with Indonesia in the mid-Miocene. The landmasses of Indonesia, New Guinea, and Australia blocked the movement of equatorial currents between the Pacific and Indian Oceans. Warm equatorial currents in these two basins became directed to the Southern Ocean, similar to the Gulf Stream in the Northern Hemisphere.

7.1.2.5 Paratethys Sea

The Paratethys Sea was a vast, shallow epicontinental sea that combined the Black and Caspian Seas with the Dacic and Pannonian Basins. Before the Miocene, Paratethys had extended to the Tarim Basin, but had retreated from Central Asia by the late Miocene (Guo et al., 2003). Correlation of Miocene sediments from Paratethys and the Mediterranean has been problematic, so it is not clear if the Mediterranean and Paratethys were connected during the

MSC (Krijgsman et al., 2010). The westward regression of Paratethys in the Miocene completed the desertification of Central Asia.

7.1.2.6 Tibetan Plateau

The South Asian and East Asian monsoons are the result of moisture encountering the Tibetan Plateau (Guo et al., 2003, Zhang et al., 2007). The monsoon-wind dominated climate truncated the arid climate belt that had formerly reached the Pacific coast of East Asia (Zhang et al., 2007). This formidable orographic barrier has caused strong South Asian and East Asian monsoons ever since the Miocene (Zachos et al., 2001, Tang et al., 2011).

7.1.3 Paleoclimate of the Messinian in Context of the Neogene

A cooler, drier world resulted from restricted ocean and air circulation in the Neogene. Oceanic gateways closed that had allowed water to remain in equatorial latitudes. Warm currents were sent toward the poles in the Central Atlantic, West Pacific, and Indian Oceans. These warm currents delivered moisture to the polar regions, and their waters were chilled at the same time. Equatorial seas were cooled by the cold, deep currents returning from the poles.

Atmospheric CO_2 was low in the Miocene, at ~100-200 ppm. At the end of Messinian time, $\delta^{18}O$ dipped as low as it had been at the Eocene-Oligocene Transition, indicating growth of continental ice sheets. Antarctica's ice cap covered the entire continent in the Late Miocene. An ice sheet had existed in the Barents Sea since at least 14 Ma (Knies and Gaina, 2008). Arctic landmasses received increased snowfall, that resulted from increased evaporation from warm Gulf Stream waters. East Greenland's montane glaciers began to combine into an ice cap. Other glaciers and incipient ice caps may have begun to form in Svalbard, Novaya Zemlya, Kolyma, and Alaska. Tibet was high enough to have year-round snows on its heights.

The unusual Boreal Tropical Zone that characterized the Paleogene no longer existed. Abundant forests did exist, covering Southern and Central Europe, and Turkey, with coal deposits of Miocene age. To the East, where lush forests had once covered Central Asia in early

Oligocene time, no evidence of heavy forest cover is found. Central Asia had a fully continental climate, with no large water bodies to regulate its extremes of temperature.

7.2 Discussion of Messinian Paleoclimate Reconstruction

In this section, we review the climatic zones of the Messinian, starting with Equatorial Wet and moving toward the poles. Similar zones, such as the Northern and Southern hemispheres' Arid climatic zones, are discussed in this section.

7.2.1 Description of Climatic Zones

7.2.1.1 Equatorial Wet Climatic Zone

The broadest tropical zone yet seen in the Cenozoic Americas extended from Central Mexico to Minas Gerais in Brazil. Africa's rainforest area had widened markedly since the EOT. Closure of the Indian-Pacific oceanic gateway truncated the southern arid belt, and New Guinea became tropical by Late Miocene time.

7.2.1.1.1 Lithologic and Paleontologic Data for the Equatorial Wet Zone

Coal appears in Mexico, Honduras, Guatemala and Panama, and in the Greater Antilles. Miocene coal, bauxite, and laterites are found in Colombia, Venzuela, Ecuador, Guyana, and Brazil. Africa's tropics are delineated by bauxites, coal, laterite, and kaolinite of Messinian age that appear between ~15N and South latitude.

Coal appears in South India, Indochina, Indonesia and New Guinea. Kaolinite is additional evidence of these areas' Miocene climates.

7.2.1.2 Arid and Semiarid Climatic Zones

As in the EOT, arid to semiarid climates covered the interior western United States—the Rockies and plains to the East. This arid region was in the form of a salient with its point at the Canadian border and opening onto the northern Mexican Pacific coast. During dessicated periods

in the Mediterranean Basin, desert extended from the southern Sahara to Marseilles, Venice, Istanbul, and beyond.

South America and Africa were crossed by arid belts roughly between 15 and 30 degrees away from the Equator. The East Asian arid belt, though, was truncated by the East Asian Monsoon that brought abundant seasonal rains to Asia's Pacific coast.

7.2.1.2.1 Lithologic and Paleontologic Data for the Arid and semiarid Climatic Zones

Evaporites and calcretes of Miocene age appear in North America, Egypt, and Pakistan. Central Asia abounds in evaporite beds. Rifting in the Afar Triple Junction, the incipient Red Sea and Gulf of Aden, laid down thick sequences of evaporites. The story of the Mediterranean Salinity Crisis has been told above. Evaporites ringed the Mediterranean basin, occuring in concentric rings that were deposited as the water receded to accumulate in hypersaline lakes on the abyssal plains. Some evaporites were formed from precipitates in these lakes.

7.2.1.3 Warm Temperate Climatic Zone

Warm temperate climate prevailed in the parts of North America surrounding the arid salient described above. Deciduous/coniferous forested landscape covered southern Canada and that part of Mexico that lay between the tropics and the desert. In South America, a much smaller region of warm temperate forest covered parts of Chile and Argentina. Africa's warm temperate region was restricted to the southern half of the Republic of South Africa.

All of Europe, the parts that were not a salt desert at the bottom of a dessicated ocean basin, was in the warm temperate zone. A zone of comparable size covered parts of Northeast Asia between Mongolia and Japan. All of Australia south of New Guinea was in the Warm Temperate Zone, as was New Zealand.

7.2.1.3.1 Lithologic and Paleontologic Data for the Warm Temperate Climatic Zone

Coal, kaolinite, and occasional crocodilian fossils mark warm temperate environments of Miocene age. Sometimes a mix of coal and evaporites, calcretes and bauxites, appears in the same area, such as in Western North America and Europe.

7.2.1.3 Cool Temperate Climatic Zone

Canada, Alaska, and all but the northeast corner of Greenland were in the Cool Temperate Climatic Zone in Miocene time. Tierra del Fuego and East Asia north of the Amur were the only other Cool Temperate Zones of this time.

7.2.1.3.1 Lithologic and Paleontologic Data for the Cool Temperate Zone

A mix of coal, glendonites, and tillite from montane glaciers mark the Cool Temperate Zone. Kaolinite and fossil plants tell of a cool, dark, rainy Arctic, which was nevertheless forested.

7.2.1.4 Polar Climatic Zone

Greenland's eastern uplands and Russia's Arctic coast had become Polar Climatic Zones by the Messinian. Continental ice sheets began to develop in Greenland and the Russian Far East.

7.2.1.4.1 Lithologic and Paleontologic Data for the Polar Climatic Zone

Ice-rafted debris (IRD) appears in seafloor sediments off Greenland. Tillites mark the passage of glaciers in Antarctica.

7.3 Summary of Messinian Global Climate

In the Late Miocene Ice House world, the Temperate and Arid Climatic Zones were compressed toward the Equator. Dark Boreal Zone forests covered the high latitude landmasses, while steppe grasslands replaced scrub and forest in the temperate zones. Antarctica was fully glaciated as it is today, while continental ice caps were just beginning to cover the northern high-latitude landmasses.

Parts of the Messinian world would have appeared very similar to the modern world if viewed from outer space. East Asia, India, the North American interior West, resembled today's world. Other areas contrasted strongly with today's climatic zones. Australia was green with temperate forests and grasslands. The Mediterranean Basin became a group of hypersaline seas. Greenland still had extensive forests.

The Messinian is relevant to the understanding of Cenozoic climates. Why are climate belts not laid out in even, symmetrical bands? In the Miocene, a globe-circling arid belt was cut by monsoon winds. The winds were deflected by Tibet, a plateau formed by long, slow tectonic uplift.

Which of these variables is more significant—the rate of tectonic uplift, erosion, and evaporation? The Messinian Salinity Crisis showed all these variables were important at the same time, their rhythms sometimes in phase and sometimes out of phase. These minor changes in environmental conditions resulted in an entire ocean basin dessicating and filling repeatedly, probably on the order of tens to thousands of years.

CHAPTER 8

LAST GLACIAL MAXIMUM (LGM) CLIMATE

8.1 Introduction to the LGM

When the Pleistocene was first described as an "Ice Age," it seized human imagination. The question of whether or not our species faces a return of mile-thick ice sheets to the Northern Temperate Zone is an interesting thought-problem. Milutin Milanković (Milanković, 1941) and others (Hays et al., 1976, Rial, 2004, Ruddiman et al., 2008) have argued convincingly that astronomical cycles control the rhythm in which glaciers advance and retreat in an Ice House World. The Earth entered full Ice House conditions in the Miocene (Zachos et al., 2001) as the CO_2 concentration in the atmosphere fell drastically. After a brief warming spell in the Pliocene (Zachos et al., 2001), Arctic ice sheets accumulated and grew to continental scales in the Pleistocene. The Milanković cycles began a rhythm of glacial advance and retreat that has shown no sign of slowing or decreasing up to the present day.

20,000 years ago, the level of atmospheric CO_2 fell lower than any time since the glaciation of Marine Isotope Stage (MIS) 6, which was the previous glacial maximum at 140,000 years ago (Suwa and Bender, 2008). The Last Glacial Maximum (LGM) has a different name in every region in which it is mapped: Wisconsonian in North America, Weichselian in northwestern Europe, Vistulan or Valdaian in Eastern Europe, and other names elsewhere. The LGM encompasses all of these local ice sheets, and includes Antarctic and montane glaciation. Worldwide, the glaciers were largest just before they retreated precipitously at the beginning of the present interglacial stage. The timing of the onset of the glacial retreat varies from ice sheet to ice sheet (~19-20 to ~14.5 ka; Clark et al., 2010). The LGM is defined with respect to its local maximum extent—different ice sheets began to recede at different times (Anderson et al., 2002).

Glacial landforms resulting from the last glacial stage lie unconformably over glacial landforms made during previous ice advances (Rabassa et al., 2010, Murton and Murton, in press). These superimposed landforms are evidence of huge climatic fluctuations in the Ice House World. Secondary glacial landforms, such as loess soils, meltwater lakes and dropstones from rapid, short-lived glacial advances called Heinrich events, extend far beyond the maximum boundary of continental ice (Haberlah et al., 2010). These landforms contain evidence of glacial stage climates. From these landforms, wind directions, sediment sources, and total ice volume can often be estimated (Muhs and Bettis, 2000, Lambeck et al., 2000, Smith et al., 2003).

The LGM is of particular interest to humankind, because our species emerged from its African homeland and expanded throughout the Old World and Australasia during the last glacial advance (Westaway et al., 2009). Eustatic sea level fall exposed continental shelves, and exposed new geographic links between the continents (e.g. Beringia). As soon as melting began, the Americas were peopled as well (Goebel et al., 2008).

8.1.1 Plate Tectonics

Plate boundaries at 20 ka are essentially identical to plate boundaries today (Scotese, 2008). At the maximum speed of Phanerozoic plate movement, 15 cm/yr (Meert et al., 1993), a plate could have only moved 3 km in 20 ka. Ice sheets pressed down on continents, which sank isostatically into the mantle (Rabineau et al., 2006). Global plate tectonic processes were not significantly affected by ice loading, but tectonic regimes up to hundreds of kilometers away were affected by the presence of glaciers (Stewart et al., 2000; Thorson, 2000).

8.1.2 Paleogeography

Antarctic ice sheets covered the entire continent and extended outward as ice shelves into the Southern Ocean. Huge ice sheets covered the Arctic landmasses, extending in several lobes southward to cover the northern portions of of North America, Europe, and Asia. Climatic zones narrowed and were shifted towards the Equator (Anhuf et al., 2006, Kim et al., 2008).

Colder sea surface temperatures (SST) and decreased insolation are two of many causes that resulted in a significantly drier glacial stage climate (Yu et al., 2000, Kim et al., 2008).

8.1.2.1 Sea Level Fluctuation

A profound drop in global sea level of ~125 m (Clark et al., 2009) resulted from the sequestration of water in expanding ice sheets during the last glacial advance. Sea level falls occurred during previous glacial maxima as well; the LGM was only the last of a series of radical sea level fluctuations (Lambeck and Chappell, 2001, Rabineau et al., 2006). As sea level fell, broad marine shelf areas were converted into grasslands, forests, deserts, or tundra, depending on their climatic zone (Prentice et al., 2000, Lambeck and Chappell, 2001, Soulet et al., 2011). This sea level fall drastically reduced shelf area for marine fauna, and contributed to Pleistocene extinctions of benthic fauna (Pandolfi, 1999).

8.1.2.2 Land Bridges Emerge

Beringia, an emerged continental shelf in the Bering Sea, connected Asia to America. Pleistocene species, including humans, crossed this ice-free land bridge (Elias, 1997). Dry land also connected the British Isles to each other and to Europe (Murton & Murton, in press). The Persian Gulf was dry, and the area of the Red Sea and Black Sea were greatly diminished (Lericolais, 2009, Rohling and Zachariasse, 1996). Sri Lanka was connected to India, and the islands of Indonesia were connected by land, as were Australia and New Guinea. Newfoundland was connected to Canada, though covered by the Laurentide ice sheet. The islands of Japan were united by land, and Japan and Sakhalin were connected to mainland Asia. The Yellow Sea was dry land covered in boreal forest, uniting the Korean Peninsula to China (Lambeck and Chappell, 2001). Tasmania was joined to Australia.

8.1.2.3 Loess Deposition

Continental glaciers produced large amounts of sediment, grinding much of it into rock flour. This fine sediment was entrained and deposited by aeolian processes as loess. Loess

deposits accumulated very rapidly, in terms of geologic time, building up tens of meters during and after the LGM (Roberts et al., 2003). Loess covered landscapes in central North America, in China, Europe, South and Central Asia, South America, Australia and New Zealand (Smith et al., 2003, Muhs and Bettis, 2000, Haberlah et al., 2010, Újvári et al., 2010, Suggate and Almond, 2010). Dust also reinforced climate forcing mechanisms already cooling the planet, by blocking solar energy. In the cold, dry LGM world, with glaciers grinding rock into rock flour, dust became a significant constituent in cooling of the global climate (Újvári et al., 2010).

While the mass accumulation rates of loess are impressive, this environment of deposition has none of the visual impact of other aeolian processes, such as dune fields (Muhs et al., 2004). In loess deposition, very fine particles of rock flour settle into forest or other vegetative cover (Timireva and Velichko, 2006). Loess has been observed being deposited today (Muhs et al., 2004). With the exception of occasional dust storms, loess deposition is a quiet, undramatic, continuous fall of very fine grains on the forest litter (Muhs et al., 2004).

8.1.2.4 Ice-Age Tropics

The Inter-Tropical Convergence Zone's (ITCZ) seasonal shift stayed closer to the Equator, and decreased precipitation occurred within it (Otto-Bliesner and Brady, 2006). Decreased precipitation resulted in a greatly restricted zone of rain forests (Prentice et al., 2000; Zhang and Delworth, 2005; Anhuf et al., 2006; Otto-Bliesner and Brady, 2006). Instead of the continent-spanning belts of deep green equatorial rain forest we see from space today, the LGM rain forests were smaller and isolated from each other. The glacial-stage climate in the Northern Hemisphere weakened tropical monsoons (Cosford et al., 2010), favoring semiarid forests, scrubland, and dry savanna. These cooler, drier environments replaced monsoon-dependent vegetation across much of the tropics (Hessler et al., 2010).

8.1.2.5 Enlarged deserts

The dry climate of the LGM resulted in global expansion of deserts and semiarid land area (Ray and Adams, 2001). As in the Eocene/Oligocene Transition and PETM, desert spread across North Africa, South America, and Central Asia. The Great Australian Desert spanned the center of Australia. Smaller deserts appeared in Africa and India—the Kalahari, Ogaden, and Thar deserts.

8.1.2.6 Glacial meltwater lakes

Continental ice sheets grew outward from their core areas until the process of forward motion and melting along the glacial front reached equilibrium. Even at equilibrium, seasonal melting produced large amounts of meltwater. This fresh water accumulated as large meltwater lakes in basins around the perimiters of the ice sheets. Huge lakes such as Lake Agassiz and Lake Missoula were formed thousands of years after the LGM as the ice sheets began to retreat.

8.1.3 Paleoclimate of LGM in Context of the Pleistocene

Pollen from land sources is the primary data from which many LGM biome maps have been made. In a few select environments, a continuous record of pollen deposition has been preserved. These rare locations include lake bottoms, ice sheets, caves and sinkholes, swamp deposits, peat bogs, and moss cushions. Some of these environments of deposition preserve pollen much better than even seafloor cores. Thus, high-resolution pollen-based reconstructions of climatic zones for the LGM are possible.

Because pollen is not a good proxy for all climate signals, Allen et al. (2008) suggested that pollen biome maps should be compared with other climate proxies. Pleistocene glacial landforms are used to estimate precipitation and temperature of the climates in which they were formed (Allen et al., 2008). It is worth noting that with some exceptions, pollen sample sites seem to be concentrated in the developed world (Prentice et al., 2000). The United States, Japan, Russia, China, Europe, and South Africa have approximately as many sample sites as the rest of

the world combined. In contrast, Anhuf et al (2006) had only seven dependable LGM pollen sites in the entire Amazon Basin.

Changes in CO_2 concentration, as well as cooling, influenced shifts in biomes and associated pollen assemblages. (Jolly and Haxeltine, 1997). CO_2 concentration has been estimated by measuring pollen from species that are sensitive to it. Grasses are significantly affected by change in CO_2; mixed C_4 and C_3 grasslands that grew in low-CO_2 LGM climates were replaced by C_3-dominated assemblages as the level of atmospheric CO_2 increased in the Holocene (Fredlund and Tieszen, 1997, Muhs et al., 1999)

8.2 Discussion of LGM Paleoclimatic Reconstruction

In this section, we review the climatic zones of the LGM, starting with Equatorial Wet Zone and moving toward the poles. Other zones, such as the Northern and Southern Arid zones, are discussed in the same section.

8.2.1 Description of Climatic Zones

8.2.1.1 Equatorial Wet Climatic Zone

During full Ice House conditions much of the Tropics were covered by savanna or semiarid forest vegetation. Evergreen and deciduous forest grew in the upper Amazon Basin, but the mouths of the Amazon received far less rainfall than today, and the river ran through a semiarid coastal plain to the sea (Anhuf et al., 2006). Africa's equatorial region looked very different from the present day, with forests in isolated patches in the Congo Basin, East African Rift, and rimming the Guinea Coast and Bight of Biafra. Surrounding these isolated forests were extensive savannas, grasslands, and semiarid forests. This semiarid environment stretched from the Sahara to Zambia, and from the South Atlantic to the Indian Ocean (Anhuf et al., 2006, Ray and Adams, 2001, Elenga et al., 2000). Treelines in tropical mountain forests moved downhill hundreds of meters, owing to the LGM's reduced CO_2 (Jolly and Haxeltine, 1997, Farrera et al., 1999). In Africa, for example, relatively small montane forests clung to the Ethiopian Highlands,

Rwenzori Mountains, Cameroon Range, and Guinea Highlands. Similar forests ringed the highlands in the rest of the world.

8.2.1.1.1 Lithologic and Paleontologic Data for the Equatorial Wet Zone

Pollen of equatorial semiarid forest or savanna is reported in Anhuf et al., (2006), from Kenya southward along the East African Rift, and westward to the Atlantic Ocean. Tropical montane forest pollen is described in peat bogs and swamps in Rwanda and Burundi (Bonnefille and Chalie, 2000).

South America is not yet as well-described. As of 2006, only 7 pollen records in the Amazon Basin had been dated back to LGM time (Anhuf et al., 2006). These samples show pollen of rain forest species concentrated in the western Amazon Basin, divided from the Atlantic by a ~1000 km wide semiarid zone. Savanna grass pollen shows Rondonia to have been much drier than today, possibly receiving 1000 mm/yr less rainfall.

Evidence of reduced alluvial erosion is found in sediments of LGM age in the southern Gangetic Plain (Gibling et al., 2008) indicating a reduced Indian Monsoon at that time. Multiple climate proxies, including $\delta^{18}O$, $\delta^{13}C$, and fluorescence values of speleothems, indicate drier conditions in Java at the LGM (Westaway et al., 2009).

8.2.1.2 Arid and Semiarid Climatic Zones

Arid and semiarid climates were at a maximum during the Pleistocene. Cooler global temperatures reduced the atmosphere's ability to carry water vapor. Dry or semiarid forests emerged where warm temperate woodlands had previously grown. Tropical lowland forests were replaced by tropical grasslands and savannas in the Amazon Basin, Congo Basin, India, and the exposed continental shelf of Southeast Asia. Drier conditions prevailed in the tropical environments of Central Africa, India, Southeast Asia, the Phillipine Archipelago, and lowland forests of Australia and New Guinea (Ray and Adams, 2001, Anhuf et al., 2006).

Semiarid forest and steppe left Eurasia uncharacteristically treeless from Iberia to Hokkaido. Siberia's vast forests were nowhere to be seen (Ray and Adams, 2001).

8.2.1.2.1 Lithologic and Paleontologic Data for the Arid and semiarid Zones

$\delta^{18}O$ from speleothems indicate a weakened East Asian Monsoon between 23 and 20 ka (Cosford et al., 2010). As noted above, the Indian Monsoon also seems to have been diminished (Gibling et al., 2008). Without monsoons to bring moisture deep into South and East Asia, conditions favored more drought-tolerant vegetation

8.2.1.3 Warm Temperate Climatic Zone

In the LGM world, few environments could be characterized as warm temperate. Ray and Adams (2001) show warm temperate forests on the flanks of the southern Andes, and the Mediterranean slope of the Atlas Mountains. But in a biome reconstruction of pollen data from South America at 18 ka, no warm temperate forest equivalent appears (Marchant et al., 2009).

8.2.1.3.1 Lithologic and Paleontologic Data for the Warm Temperate Zone

Macrofossils of deciduous trees have been found in the lower Mississippi Valley in LGM sediments. Fossils of beech have been found throughout the Mississippi and Ohio watersheds, contradicting the harsher climate inferred from pollen maps (Jackson et al., 2000, Loehle, 2007). Deciduous forest pollen has been reported in Japan from 18,000 C^{14} years before the present (Takahara et al., 2000).

8.2.1.3 Cool Temperate Climatic Zone

The colder, drier LGM world shifted climatic zones toward the Equator, and shrank the areal extent of the cool temperate zone. Grasses of the steppe-tundra biome dominated most of the northern landmasses that were not covered by ice. Extensive Boreal or Cool Temperate Zone woodlands were not present across the northern parts of North America and Eurasia. The largest boreal forests were concentrated in the eastern United States, eastern China, and Japan south of

Hokkaido. (Jackson et al., 2000; Ray and Adams, 2001; Hayashi et al., 2010). Open Cool Temperate Zone woodland, sometimes called subalpine parkland, grew throughout North America's Basin and Range and Colorado Plateau (Ray and Adams, 2001).

The eastern United states was dominated by closed-canopy forest, with the exception of Florida and the land adjacent to the ice sheets. The Upper Mississippi Valley supported taiga—here used to mean open boreal forest as in northern Canada today. The Lower Mississippi/Lower Ohio valleys were covered by closed-canopy forest. The northern portion of this area was boreal forest, closest to the ice sheet and its periphery of tundra. A cool temperate temperate forest of mixed coniferous and deciduous species occupied the remainder of the land west of the Appalachians.. Boreal forest grew east of the Appalachians between New Jersey and Georgia (Jackson et al., 2000).

Florida experienced July temperatures up to 28℃ du ring the LGM (Jackson et al., 2000). Pollen of Florida scrub species are mixed with southern pine pollen, indicating warm, wet conditions, and drought-tolerant species such as Ceratiola (sandhill-rosemary) (Jimenez-Moreno et al., 2010)

A rim of boreal forest grew on the south boundary of the ice sheet covering the Alps, and within the triangular center of Transylvania (Ray and Adams, 2001). Much of of Earth's landmass that normally experienced cool temperate conditions became dry steppe and cold desert in the LGM (Crowley, 1995; Ray and Adams, 2001).

8.2.1.3.1 Lithologic and Paleontologic Data for the Cool Temperate Zone

Pollen of steppe and tundra are found throughout the northern latitudes of Eurasia and North America, where cool temperate and boreal forests grow today (Sher et al., 2011). Pollen of denser, cool temperate to boreal forest is found in North America east of the Mississippi and north of Florida (Jackson et al., 2000). The loess deposits of North America, Europe, and China record the cool temperate forest that grew on the loess as it was being deposited. Leaves, nuts,

and macrofossils of plants and animals show the loess hills were mantled by cool temperate forests even as aeolian process continued to build up the loess deposits (Pye, 1995, Begét, 2001).

8.2.1.4 Polar Climatic Zone

Ice House conditions reached their greatest extent at the LGM. Ice sheets 2-3 kilometers thick extended far into today's temperate zones in North America, Europe, and Asia.

In the LGM world, the ice sheets did not advance evenly on every front. Polar desert, tundra, and steppe existed on the same latitude as kilometers-thick ice sheets (Elias et al., 1997, Tarasov et al., 2000). Beringia and the North Sea/English Channel hosted abundant plant and animal life (Elias et al., 1997). The shores of the Arctic Ocean were unglaciated across northeast Asia (Kienast et al., 2005, Gualtieri et al., 2003). An unglaciated coastline may have extended around the Canadian Arctic to Greenland (Adams, 2001)

Terminal moraines mark the southernmost extent of the Laurentide ice sheet in Iowa, Illinois, Indiana, and Ohio. The British Isles were covered by a single ice sheet centered in the Highlands of Scotland, and extending south to the Shannon estuary in Ireland and the Severn in western Britain. A lobe of this ice sheet extended south across the Wash into northern Essex. The Scandinavian ice sheet, flowing outward from the Scandinavian highlands, crossed the Baltic Sea and covered the Baltic States. It extended south into Denmark, northern Germany, and Poland. To the east, the Scandinavian ice sheet covered Finland, Karelia, the Kola Peninsula, and northwestern Russia. For the most part, eastern Russia, Tibet, and the intermontane highlands of Central Asia were dry, cold deserts. These climates were nearly as cold as polar regions, but had greater seasonality because of their lower latitudes. Alpine glaciation introduced polar-like climate conditions in the Rocky Mountains, Andes, Alps, East Asian ranges, and Tibet.

Beringia's climate was modified by the proximity of the North Pacific Ocean. Beringia was warmer and wetter than the intracontinental cold deserts. While still a cold, polar climate, Beringia

was warm enough to support spruce forests [Paleoatlas of Beringia—NOAA] and many species of grasses (Blinnikov et al., 2011).

8.2.1.4.1 Lithologic and Paleontologic Data for the Polar Zone

Terminal moraines of continental glaciers, along with other glacial landforms, show the extent of the LGM ice sheets. Remains of Arctic plants, and paleosols of patterned ground, are evidence of tundra conditions in non-glaciated areas. Pollen of tundra vegetation from the LGM is found in lake sediments, bogs, and long-lived growths of moss in eastern Russia and Alaska (Bigelow et al., 2003). Plant macrofossils are abundant in bogs and river sediments of the Russian Far East and Alaska (Tarasov et al., 2000, Bigelow et al., 2003). Steppe pollen assemblages are found across southern Europe and eastern Russia (Wu et al., 2007). Cold-hardy grasses dominated a “Steppe-Tundra” biome, not found in the present day, which may have covered Beringia and much of eastern Siberia (Blinnikov et al., 2011). Numerous species of grasses grew in this extinct biome, which supported herds of large grazing mammals—horse, rhinoceros, bison, and mammoth.

8.3 Summary of LGM World Climate

In the Pleistocene, paleogeographic configuration, orbital cycles, and greenhouse gas concentration combined to cause an Ice Age characterized by a series of glacial advances and retreats. Once the Earth’s climate had cooled past a climatic threshold, orbital cycles began to significantly affect global climate, initiating growth of massive ice sheets. The Polar Climatic Zone expanded, compressing the other climatic zones toward the Equator. Ice sheets mantled much of the higher latitudes of the continents, advancing and retreating in response to changes in insolation due to orbital cycling.

The LGM world was much colder and drier than any other interval in the Cenozoic. The most significant paleogeographic features of the LGM were the continental ice sheets. Next in

importance were the emerged marine shelf areas, reduced rain forest area, increased grassland area, increased desert area, and large glacial meltwater lakes.

Emerged marine shelves linked islands and continents, and were rapidly colonized by land plants, becoming tundra/grasslands in the case of the North Sea and Beringia. Tropical grassland grew on the new land connecting Indonesia's islands.

Forest area decreased greatly in the Pleistocene, replaced by grassland, semiarid scrubland, tundra, and desert. In the Pleistocene, grasses had moved into every climatic zone, in some cases becoming the dominant flora. Grasses adapted to the cold steppe, the temperate zones, the tropics, tundra and desert climates as well.

Deserts covered more land area than at any other time in the Cenozoic. Large deserts covered continental interiors in South America, Africa, Arabia, India, Asia, and Australia. North America was an exception to this pattern. The desert areas of the American Southwest and Mexico received enough precipitation to support semiarid and even warm temperate biomes. Increased precipitation in landlocked basins near the ice sheets formed pluvial lakes in areas that are now desert. Pluvial lakes formed in the Basin and Range, Dasht-e-Kevir, Tarim Basin, and on the Tibetan Plateau.

8.3.1 Comparison of Quantitative Data with Climate Model

The chief discrepancy between fossil data and computer models is that pollen biomizations indicate a colder climate than most climate models. In some cases this discrepancy is up to 10℃. Computer models such as PMIP and CCS M3 suggest that forests encroached close to the continental glacial boundary. The reason for this disagreement is not known.

CHAPTER 9

SUMMARY AND CONCLUSIONS

9.1 Overview of Past Climate Forcing Mechanisms

Earth's climate transitioned from Hot House to Ice House conditions in the last 65 million years. These reconstructions of the Cenozoic Earth's climatic zones shows the results of the climate forcing mechanisms that shaped the course of Cenozoic climate history.

Continents and oceans change their configuration over geologic time. In each time interval mapped, the continents and oceans were in a configuration unique to that time, that influenced the climate of that time interval. Fluctuations in the more ephemeral but no less powerful radiative forcings (GHG concentration, solar intensity, volcanism and dust, orbital cycles, vegetation cover and albedo) acted in these time intervals to form the global climates of the Cenozoic Earth.

Plate tectonics influenced sea level as ocean basins closed and new basins rifted open, and by changes in seafloor spreading rates. Continental collisions raised orographic barriers, dividing adjacent land surfaces into areas of rainforest and desert. Plate tectonics closed and opened oceanic gateways, changing patterns of oceanic circulation, which in turn affected climate in the Cenozoic. Prior to the Eocene/Oligocene Transition, world oceans were connected in low latitudes. After the EOT, low-latitude ocean gateways began to close, while the Antarctic and Arctic oceans became much more important to global ocean circulation.

Atmospheric and oceanic climate forcing mechanisms played an equally important role in forming Cenozoic climates. Greenhouse gas concentration varied greatly across the Cenozoic. High concentrations of GHG were a crucial factor that caused a super-greenhouse world at the

PETM. Low GHG concentrations in the Miocene and the LGM were a significant factor in the growth of Arctic ice sheets.

Albedo played an important role in forcing Cenozoic climates. Forest cover darkened Cretaceous and Paleogene polar landmasses, causing heightened absorption of solar energy. Dust generated in the dry, glacial environment of the LGM decreased insolation, contributing to the already-cold climate. Grassland, tundra, and ice raised the albedo of high-latitude landmasses, increasing the amount of solar energy that was reflected back into space, and contributing to global cooling.

Orbital forcing (Milanković, 1941) is a climate variable that is always present, but which can only affect climates that have crossed a certain threshold. Orbital forcing had affected climate during the early Eocene, and at other times in the Early and Middle Cenozoic (Bijl et al., 2009; Scher et al., 2011). Orbital forcing began to strongly influence regional insolation in the late Pliocene, after other factors had significantly cooled global climate. The polar ice caps that formed after the EOT affected sea level, ocean circulation, and planetary albedo. Orbital forcing has continued to affect the Earth's climate to this day (Milanković, 1941).

9.2 K/T

Wide oceanic gateways in the equatorial and temperate zones permitted warm ocean currents to circle the globe in the Late Cretaceous Hot House World. Equatorial ocean basins, such as the Central Atlantic and Central Pacific, were the source areas for warm deep ocean currents. These conditions resulted in a shallow temperature gradient between the Equator and the poles. Oceans that surrounded the dispersed continents moderated their interior climates. Shallow epicontinental seas moderated climate across Europe and southern Eurasia. Polar ocean basins were separated from each other, or entirely cut off from the world ocean.

Cool temperate forests grew across the Arctic and Antarctic landmasses, absorbing much more heat from the sun than bare soil (Upchurch et al., 1999). This helped warm the Hot

House poles, preventing accumulation of sea ice, or continental ice other than alpine snowfields and seasonal snowfall.

The orographic barriers that would rise in the Cenozoic were still low or nonexistent. Crustal shortening and uplift along the American Cordilleras had only begun. Tibet and the Himalayas did not yet exist, so no massive barrier to airflow caused monsoon climates in Asia. No high Andes blocked equatorial easterlies to water the Amazon Basin and dessicate the Atacama Desert as severely as it is today. The K/T world did not have the continent-spanning deserts in Africa, Asia, and Australia that were to develop in the Cenozoic. Instead, warm temperate forest, or dry scrubland, covered much of the Earth's landmass.

9.3 PETM

A tremendous release of greenhouse gases, possibly the result of clathrate decompression, causing global change in atmospheric and oceanic temperature and chemistry, caused the geologically brief PETM. Warm climatic zones expanded poleward from the Equator, reducing or eliminating entirely the cooler zones surrounding the poles. Lithologic evidence shows warm to temperate, rainy conditions prevailed over much of North America, northern Eurasia, and Australia. Wet, tropical climates were established north of the northern arid belt in North America and Eurasia. The equatorial wet climatic zone was greatly enlarged. Tropical rainforest covered most of the equatorial landmasses. Extensive deserts formed in the arid belts. These deserts extended into Spain, France, and northern China in the Northern Hemisphere, and crossed South America and South Africa in the Southern Hemisphere.

The PETM marks the highest average global temperatures and highest sea levels of the Cenozoic. With the possible exception of montane snowfields, or polar seasonal snowfall, no ice existed on Earth. The PETM Hot House world would continue into the Eocene, though with less extreme conditions.

9.4 Eocene/Oligocene Transition

Isolated at the South Pole, Antarctica became encircled by the Southern Ocean as new ocean floor broadened the Tasman Sea and Drake Passage. A mantle of continental ice grew in Antarctica, covering the frozen continent and dramatically cooling the Southern Hemisphere. Deep, cool bottom water now began to be formed by cold Antarctic waters sinking, rather than from dense, hypersaline water in the equatorial oceans.

India had collided with Eurasia, raising Tibet as a huge plateau. Tibet blocked wind currents in every direction, causing the Indian, East Asian, and Southeast Asian monsoons to begin. The monsoons watered eastern China, which has not been a desert since this time. Tethys had closed in the preceding 20 million years, blocking one of the three oceanic gateways for warm equatorial currents.

Central America, approaching its modern position, limited exchange of warm water between the Atlantic and Pacific Oceans.

The North Atlantic had opened wide enough to end the isolation of the Arctic Ocean. Cooling Northern Hemisphere climate may have resulted in some glaciation in Northern Alaska and Arctic Canada, Greenland and the highlands of Russia east of the Verkhoyansk Mountains.

Southern Eurasia was now mountainous, cutting off Paratethys from the world's oceans.

9.5 Late Miocene (Messinian)

At the end of the Eocene Hot House, the Southern Hemisphere cooled dramatically into the Oligocene Ice House. But in the Northern Hemisphere, a long interval of intermediate conditions, neither Hot House nor fully Ice House, lasted until the Late Miocene. The Late Miocene marked the beginning of full bipolar Ice House conditions. Central America had closed the oceanic gateway between the Atlantic and Pacific Oceans. The Pacific and Indian Oceans were now essentially cut off from each other by Indonesia and Australasia. The currents that once

passed between them now flowed toward cooler latitudes, dissipating heat from equatorial waters. Cut off by the collision of Africa and Eurasia, the Mediterranean Basin dessicated repeatedly—sometimes, perhaps, completely.

Permanent glaciers now formed all around the Arctic Ocean, in East Greenland, and in Arctic Canada. As these Northern Hemisphere glaciers grew, Late Miocene sea level dropped. The extent of these glaciers cannot be precisely known, because the glacial features they made have long since been scoured away by Quaternary glaciation.

Grasslands—a new type of biome—spread over temperate and tropical landmasses, replacing forest and scrubland. Grasslands absorb less solar heat than forest cover; the widespread success of this new biome helped cool the Earth's climate.

9.6 Last Glacial Maximum

The climate forcing mechanisms that had brought Earth into full Ice House conditions continued affecting the planet through the Pliocene and Quaternary. At the end of the Pliocene, Earth was cool enough for Milanković cycles to become a dominant forcing mechanism. The resulting ice caps were large enough to draw down sea level hundreds of meters, exposing wide areas of continental shelf.

This coldest Ice House of all was cool enough to greatly reduce the amount of evaporation, and thus rainfall, around the world. Deserts spanned continents in South America, Africa and Arabia, South and Central Asia, and Australia. Much of Eurasia, and western North America, were dry, cold steppe. Boreal forests grew in eastern North America, China, and Japan. The broad rainforests of previous ages had greatly shrunk; tropical grassland, scrubland, and seasonal dry forest covered much of the tropics.

APPENDIX A

PLATES

See Supplementary File.

REFERENCES

Abels, H.A., Dupont-Nivet, G., Xiao, G., Bosboom, R., and Krijgsman, W., 2011, Step-wise change of Asian interior climate preceding the Eocene–Oligocene Transition (EOT): Palaeogeography, Palaeoclimatology, Palaeoecology, v. 299, no. 3-4, p. 399-412.

Abelson, A., Agnon, A., Almogi-Labin, A., 2008, Indications for control of the Iceland plume on the Eocene–Oligocene "greenhouse–icehouse" climate transition: Earth and Planetary Science Letters, v. 265, p. 33-48.

Akhmetiev, M.A., 2010, Paleocene and Eocene floristic and climatic change in Russia and Northern Kazakhstan: Bulletin of Geosciences, v.85 no. 1 p. 77-94,

Akhmetiev, M.A., and Beniamovski, V.N., 2009, Paleogene floral assemblages around epicontinental seas and straits in Northern Central Eurasia: proxies for climatic and paleogeographic evolution: Geologica Acta, v. 7, no. 1-2, p. 297-309.

Allen, M.B., and Armstrong, H.A., 2011, Reconciling the Intertropical Convergence Zone, Himalayan/Tibetan tectonics, and the onset of the Asian monsoon system: Journal of Asian Earth Sciences, v. 44, p. 36-47.

Allen, R., Siegert, M.J., and Payne, A.J., 2008, Reconstructing glacier-based climates of LGM Europe and Russia – Part 2: A dataset of LGM precipitation/temperature relations derived from degree-day modelling of palaeo glaciers: Climate of the Past, v. 4, no. 4, p. 249-263.

Allen, R., Siegert, M. J., and Payne, A. J., 2008, Reconstructing glacier-based climates of LGM Europe and Russia – Part 3: Comparison with previous climate reconstructions: Climate of the Past, v. 4, no. 4, p. 265-280.

Alvarez, L.W., Alvarez, W., Asaro, F., Michel, H.V., 1980, Extraterrestrial Cause for the Cretaceous-Tertiary Extinction: Science, v. 208, no. 4448, p. 1095-1108.

Anderson, J.B., Shipp, S.S., Lowe, A.L., Wellner, J.S., and Mosola, A.B., 2002, The Antarctic Ice Sheet during the Last Glacial Maximum and its subsequent retreat history: a review: Quaternary Science Reviews, v. 21, p. 49-70.

Anderson, J.B., Warny, S., Askin, R.A., Wellner, J.S., Bohaty, S.M., Kirshner, A.E., Livsey, D.N., Simms, A.R., Smith, T.R., Ehrmann, W., Lawver, L.A., Barbeau, D., Wise, S.W., Kulhenek, D.K., 2011, Progressive Cenozoic cooling and the demise of Antarctica's last refugium: Proceedings of the National Academy of Sciences of the United States of America, vol. 108, no. 28, p. 11356-11360.

Anhuf, D., Ledru, M.P., Behling, H., Da Cruz Jr., F.W., Cordeiro, R.C., Van der Hammen, T., Karmann, I., Marengo, J.A., De Oliveira, P.E., and Pessenda, L., 2006, Paleo-environmental change in Amazonian and African rainforest during the LGM: Palaeogeography, Palaeoclimatology, Palaeoecology, v. 239, no. 3-4, p. 510-527.

Aragón, E., Goin, F.J., Aguilera, Y.E., Woodburne, M.O., Carlini, A.A., and Roggiero, M.F., 2011, Palaeogeography and palaeoenvironments of northern Patagonia from the Late Cretaceous to the Miocene: the Palaeogene Andean gap and the rise of the North Patagonian High Plateau: Biological Journal of the Linnean Society, v. 103, p. 305-315.

Arpe, K., Leroy, S.A.G., and Mikolajewicz, U., 2011, A comparison of climate simulations for the last glacial maximum with three different versions of the ECHAM model and implications for summer-green tree refugia: Climate of the Past, v. 7, no. 1, p. 91-114.

Askin, R.A., 1990, Campanian to Paleocene spore and pollen assemblages of Seymour Island: Review of Palaeobotany and Palynology, v. 65, no. 1–4, p. 105-113.

Bartoli, G., Sarnthein, M., Weinalt, M., Erlenkeuser, H., Garbe-Schönberg, D., Lea, D.W., 2005, Final closure of Panama and the onset of northern hemisphere glaciation: Earth and Planetary Science Letters, v. 237, p. 33-44.

Beerling, D.J., Lomax, B.H., Royer, D.L., Upchurch, G.R., and Kump, L.R., 2002, An atmospheric pCO_2 reconstruction across the Cretaceous-Tertiary boundary from leaf megafossils: Proceedings of the National Academy of Sciences of the United States of America, v. 99, no. 12, p. 7836-7840.

Begét, J.E., 2001, Continuous Late Quaternary proxy climate records from loess in Beringia: Quaternary Science Reviews, v. 20, p. 499-507.

Berner, R.A., 1994, GEOCARB II: A revised model for atmospheric CO2 over Phanerozoic time: American Journal of Science, v. 294, p. 56-91.

Bice, K.L., Marotzke, J., 2002, Could changing ocean circulation have destabilized methane hydrate at the Paleocene/Eocene boundary?: Paleoceanography, v. 17, p. 1–12.

Bigelow, N.H., 2003, Climate change and Arctic ecosystems: 1. Vegetation changes north of 55°N between the last glacial maximum, mid-Holocene , and present: Journal of Geophysical Research, v. 108, no. D19, p. ALT 11-1-ALT 11-25.

Bijl, P.K., Schouten, S., Sluijs, A., Reichart, G.J., Zachos, J.C., and Brinkhuis, H., 2009, Early Palaeogene temperature evolution of the southwest Pacific Ocean: Nature, v. 461, no. 7265, p. 776-779.

Blinnikov, M.S., Gaglioti, B.V., Walker, D.A., Wooller, M.J., and Zazula, G.D., 2011, Pleistocene graminoid-dominated ecosystems in the Arctic: Quaternary Science Reviews, v. 30, no. 21-22, p. 2906-2929.

Bonnefille, R., and Chalie, F., 2000, Pollen-inferred precipitation time-series from equatorial mountains, Africa, the last 40 kyr BP: Global and Planetary Change, v. 26, no. 1-3, p. 25-50.

Boucot, A.J., and Gray, J., 2001, A critique of Phanerozoic climatic models involving changes in the CO_2 content of the atmosphere: Earth-Science Reviews, v. 56, p. 1-159.

Boucot, A.J., Xu, C., Scotese, C.R., Morley, R.J., 2012, Phanerozoic Atlas of Climatic Indicators.

Bowen, G.J., and Zachos, J.C., 2010, Rapid carbon sequestration at the termination of the Palaeocene–Eocene Thermal Maximum: Nature Geoscience, v. 3, no. 12, p. 866-869.

Brady, P.V., and Gislason, S.R., 1997, Seafloor Weathering Controls on Atmospheric CO2 and Global Climate: Geochimica et Cosmochimica Acta, v.61, no. 5, p. 965-973.

Brinkhuis, H., Schouten, S., Collinson, M.E., Sluijs, A., Damsté, J.S.S., Dickens, G.R., Huber, M., Cronin, T.M., Onodera, J., Takahashi, K., Bujak, J.P., Stein, R., van der Burgh, J., Eldrett, J.S., & the Expedition 302 Scientists, 2006, Episodic fresh surface waters in the Eocene Arctic Ocean: Nature, v. 441, no. 7093, p. 606-609.

Bryant, J.D., Froelich, P.N., Showers, W.J., and Genna, B.J., 1996, Biologic and climatic signals in the oxygen isotopic composition of Eocene-Oligocene equid enamel phosphate: Palaeogeography, Palaeoclimatology, Palaeoecology, v. 126, p. 75-89.

Clark, P.U., Dyke, A.S., Shakun, J.D., Carlson, A.E., Clark, J., Wohlfarth, B., Mitrovica, J.X., Hostetler, S.W., and McCabe, A.M., 2009, The Last Glacial Maximum: Science, v. 325, no. 5941, p. 710-714.

Collins, W.D., Bitz, C.M., Blackmon, M.L., Bonan, G.B., Bretherton, C.S., Carton, J.A., Chang, P., Doney, S.C., Hack, J.J., Henderson, T.B., Kiehl, J.T., Large, W.G., McKenna, D.S., Santer, B.D., Smith, R.D., 2006, The Community Climate System Model Version 3 (CCSM3): Journal of Climate, v. 19, no. 11, p. 2545-2143.

Cooper, A.K., O'Brien, P.E., and Richter, C., eds., 2004, 1. Leg 188 Synthesis: Transitions in the Glacial History of the Prydz Bay Region, East Antarctica, from ODP Drilling: *in* Proceedings of the Ocean Drilling Program, Scientific Results, v. 188, p. 1-42.

Cope, J.T., and Winguth, A., 2009, On the sensitivity of ocean circulation to arctic freshwater input during the Paleocene/Eocene Thermal Maximum: Palaeogeography, Palaeoclimatology, Palaeoecology, v. 306, no. 1–2, p. 82-94.

Cosford, J., Qing, H., Lin, Y., Eglington, B., Mattey, D., Chen, Y.G., Zhang, M., and Cheng, H., 2010, The East Asian monsoon during MIS 2 expressed in a speleothem $\delta^{18}O$ record from Jintanwan Cave, Hunan, China: Quaternary Research, v. 73, no. 3, p. 541-549.

Coxall, H.K., Wilson, P.A., Pälike, H., Lear, C.H., and Backman, J., 2005, Rapid stepwise onset of Antarctic glaciation and deeper calcite compensation in the Pacifi c Ocean: Nature, v. 433, p. 53–57.

Crouch, E.M., Utrecht, C.D., Morgans, H.E.G., and Rogers, K.M., 2001, Global dinoflagellate event associated with the late Paleocene thermal maximum: Geology, v.29, no. 4, p. 315-318.

Crowley, T.J., 1995, Ice age terrestrial carbon changes revisited: Global Biogeochem Cycles, v.9, p. 377–389.

Currie, B.S., Rowley, D.B., and Tabor, N.J., 2005, Middle Miocene paleoaltimetry of southern Tibet: Implications for the role of mantle thickening and delamination in the Himalayan orogen: Geology, v. 33, no. 3, p. 181.

Dawson, M. R.,West, R. M., and Langston,W., 1976, Paleogene terrestrial vertebrates: Northernmost occurrence, Ellesmere Island, Canada: Science, v. 192, p. 781–782.

Dettmann, M.E., 1989, Antarctica: Cretaceous cradle of austral temperate rainforests?, *in* Crame, .A. ed., Origins and Evolutionof the Antarctic Biota: Geological Society Special Publication, vol. 47, p. 89–105.

Dickens, G.R., O'Neil, J.R., Rea, D.K., and Owen, R.M., 1995, Dissociation of oceanic methane hydrate as a cause of the carbon isotope excursion at the end of the Paleocene: Paleoceanography, v. 10, no. 6, p. 965.

Diester-Haass, L., and Zahn, R., 1996, Eocene–Oligocene transition in the Southern Ocean: History of water mass circulation and biological productivity: Geology, v. 24, p. 163–166.

Donnadieu, Y., Pierrehumbert, R., Jacob, R., and Fluteau, F., 2006, Modelling the primary control of paleogeography on Cretaceous climate: Earth and Planetary Science Letters, v. 248, no. 1-2, p. 426-437.

Duggen, S., Hoernle, K., Van Den Bogaard, P., Rupke, L. and Morgan, J.P., 2003, Deep roots of the Messinian salinity crisis: Nature, v. 422, p. 602–606.

Dworkin, S.I., Nordt, L., and Atchley, S., 2005, Determining terrestrial paleotemperatures using the oxygen isotopic composition of pedogenic carbonate: Earth and Planetary Science Letters, v. 237, no. 1-2, p. 56-68.

Edwards, E.J., Osborne, C.P., Strömberg, C.A.E., Smith, S.A, Members of the C_4 Grasses Consortium, 2010, The origins of C4 grasslands: integrating evolutionary and ecosystem science: Science, v. 328, no. 5978, p. 587-591.

Ehrmann, W.U., and Mackensen, A., 1992, Sedimentological evidence for the formation of an East Antarctic ice sheet in Eocene/Oligocene time: Palaeogeography, Palaeoclimatology, Palaeoecology, v. 93, no. 1-2, p. 85-112.

Eldrett, J.S., Greenwood, D.R., Harding, I.C., and Huber, M., 2009, Increased seasonality through the Eocene to Oligocene transition in northern high latitudes: Nature, v. 459, no. 7249, p. 969-973.

Eldrett, J.S., Harding, I.C., Wilson, P.A., Butler, E., and Roberts, A.P., 2007, Continental ice in Greenland during the Eocene and Oligocene: Nature, v. 446, no. 7132, p. 176-179.

Elenga, H., Peyron, O., Bonnefille, R., Jolly, D., Cheddadi, R., Guiot, J., Andrieu, V., Bottema, S., Buchet, G., de Beaulieu, J.L., Hamilton, A.C., Maley, J., Marchant, R., Perez-Obiol, R., Reille, M., Riollet, G., Scott, L., Straka, H., Taylor, D., Van Campo, E., Vincens, A., Laarif, F., Jonson, H., 2000, Pollen-based biome reconstructions for southern Europe and Africa 18,000 yr BP: Journal of Biogeography, v. 27, p.621–634.

Elias, S.A., Short, S.K., and Birks, H.H., 1997, Late Wisconsin environments of the Bering Land Bridge: Palaeogeography, Palaeoclimatology, Palaeoecology, v. 136, p. 293-308.

Eros, J.M., Montanez, I.P., Osleger, D.A., Davydov, V.I., Nemyrovska, T.I., Poletaev, V.I., Zhykalyak, M.V., 2012, Sequence stratigraphy and onlap history of the Donets Basin,

Ukraine: Insight into Carboniferous icehouse dynamics: Palaeogeography, Palaeoclimatology, Palaeoecology, v. 313-314, p. 1-25.

Farrera, I., Harrison, S.P., Prentice, I.C., Ramstein, G., Guiot, J., Bartlein, P.J., Bonnefille, R., Bush, M., Cramer, W., von Grafenstein, U., Holmgren, K., Hooghiemstra, H., Hope, G., Jolly, D., Lauritzen, S.E., Ono, Y., Pinot, S., Stute, M., Yu, G., 1999, Tropical climates at the Last Glacial Maximum: a new synthesis of terrestrial palaeoclimate data. I. Vegetation, lake-levels and geochemistry: Climate Dynamics, v. 15, no. 11, p. 823-856.

Flecker, R., and Ellam, R.M., 2006, Identifying Late Miocene episodes of connection and isolation in the Mediterranean–Paratethyan realm using Sr isotopes: Sedimentary Geology, v.188–189, p. 189-203.

van de Flierdt, T., Goldstien, S.L., Hemming, S.R., Roy, M., Frank, M., Halliday, A.N., 2007, Global neodymium–hafnium isotope systematics — revisited: Earth and Planetary Science Letters, v. 259, no. 3–4, p. 432-441.

Flögel, S., and Wagner, T., 2006, Insolation-control on the Late Cretaceous hydrological cycle and tropical African climate—global climate modelling linked to marine climate records: Palaeogeography, Palaeoclimatology, Palaeoecology, v. 235, p. 288-304.

Flögel, S., Wallmann, K., and Kuhnt, W., 2011, Cool episodes in the Cretaceous — Exploring the effects of physical forcings on Antarctic snow accumulation: Earth and Planetary Science Letters, v. 307, no. 3-4, p. 279-288.

Frakes, L.A., 1999, Estimating the global thermal state from Cretaceous sea surface and continental temperature data, *in* Barrera, E., Johnson, C.C. eds., Evolution of the Cretaceous Ocean-Climate System: Geological Society of America Special Paper 332, p. 49–57.

Francis, J., 2002, Cretaceous and early Tertiary climates of Antarctica: evidence from fossil wood: Palaeogeography, Palaeoclimatology, Palaeoecology, v. 182, no. 1-2, p. 47-64.

Francis, J.E., Ashworth, A., Cantrill, D.J., Crame, J.A., Howe, J., Stephens, R., and Thorn, V., 2008, 100 Million Years of Antarctic Climate Evolution: Evidence from Fossil Plants: *in* Cooper, A.K., Barrett, P.J., Stagg, H., Storey, B., Stump, E., Wise, W., and the 10th ISAES editorial team, eds., Antarctica: A Keystone in a Changing World. Proceedings of the 10th International Symposium on Antarctic Earth Sciences. Washington, DC: The National Academies Press, p. 19-27.

Fredlund, G.G.,and Tieszen, L.L., 1997, Calibrating grass phytolith assemblages in climatic terms: Application to late Pleistocene assemblages from Kansas and Nebraska: Palaeogeography, Palaeoclimatology, Palaeoecology, v. 136, p. 199-211.

Garcia-Castellanos, D., Estrada, F., Jiménez-Munt, I., Gorini, C., Fernàndez, M., Vergés, J., and De Vicente, R., 2009, Catastrophic flood of the Mediterranean after the Messinian salinity crisis: Nature, v. 462, no. 7274, p. 778-781.

Gibling, M.R., Sinha, R., Roy, N.G., Tandon, S.K., and Jain, M., 2008, Quaternary fluvial and eolian deposits on the Belan river, India: paleoclimatic setting of Paleolithic to Neolithic archeological sites over the past 85,000 years: Quaternary Science Reviews, v. 27, no. 3-4, p. 391-410.

Goebel, T., Waters, M.R., and O'Rourke, D.H., 2008, The late Pleistocene dispersal of modern humans in the Americas: Science, v. 319, no. 5869, p. 1497-1502.

Govers, R., 2009, Choking the Mediterranean to dehydration: The Messinian salinity crisis: Geology, v. 37, no. 2, p. 167-170.

Guo, Z.T., Ruddiman, W.F., Hao, Q.Z., Wu, H.B., and Qiao, Y.S., 2002, Onset of Asian desertification by 22 Myr ago inferred from loess deposits in China: Nature, v. 416, p. 159-163.

Haberlah, D., Williams, M.A.J., Halverson, G., McTainsh, G.H., Hill, S.M., Hrstka, T., Jaime, P., Butcher, A.R., and Glasby, P., 2010, Loess and floods: High-resolution multi-proxy data of Last Glacial Maximum (LGM) slackwater deposition in the Flinders Ranges, semi-arid South Australia: Quaternary Science Reviews, v. 29, no. 19-20, p. 2673-2693.

Habib, D., and Saeedi, F., 2007, The Manumiella seelandica global spike: Cooling during regression at the close of the Maastrichtian: Palaeogeography, Palaeoclimatology, Palaeoecology, v. 255, no. 1-2, p. 87-97.

Haq, B.U., Hardenbol, J., Vail, P.R., 1987, Chronology of fluctuating sea levels since the Triassic: Science, v. 235, v. 1156-1167.

Hardie, L.A., and Lowenstein, T.K., 2004, Did the Mediterranean Sea Dry Out During the Miocene? A Reassessment of the Evaporite Evidence from DSDP Legs 13 and 42A Cores: Journal of Sedimentary Research, v. 74, no. 4, p. 453-461.

Haug, G.H., and Tiedemann, R., 1998, Effect of the formation of the Isthmus of Panama on Atlantic Ocean thermohaline circulation: Nature, v. 393, p. 673-676.

Hayashi, R., Takahara, H., Hayashida, A., and Takemura, K., 2010, Millennial-scale vegetation changes during the last 40,000 yr based on a pollen record from Lake Biwa, Japan: Quaternary Research, v. 74, no. 1, p. 91-99.

Hayes, P. A., J. E. Francis, and D. J. Cantrill, 2006, Palaeoclimate of Late Cretaceous Angiosperm leaf floras, James Ross Island, Antarctic. *in* Francis, J. E., Pirrie, D., and Crame, J. A., eds., Cretaceous-Tertiary High Latitude Palaeoenvironments, James Ross Basin: Geological Society London Special Publication 258: p. 49-62.

Hays, J.D., Imbrie, J., and Shackleton, N.J., 1976, Variations in the Earth's Orbit: Pacemaker of the Ice Ages: Science, v. 194, no. 4270, p. 1121-1132.

Heinemann, M., Jungclaus, H.H., Marotzke, J., 2009, Warm Paleocene/Eocene Climate as Simulated in ECHAM5/MPI-OM: Climate of the Past, v. 5, p. 785-802.

Herman, A., Spicer, R.A., 1996, Palaeobotanical evidence for a warm Cretaceous Arctic ocean: Nature v. 380, p. 330-333.

Herman, A.B., Akhmetiev, M.A., Kodrul, T.M., Moiseeva, M.G., and Iakovleva, A.I., 2009, Flora development in Northeastern Asia and Northern Alaska during the Cretaceous-Paleogene transitional epoch: Stratigraphy and Geological Correlation, v. 17, no. 1, p. 79-97.

Hessler, I., Dupont, L., Bonnefille, R., Behling, H., González, C., Helmens, K.F., Hooghiemstra, H., Lebamba, J., Ledru, M.P., Lézine, A.M., Maley, J., Marret, F., and Vincens, A., 2010, Millennial-scale changes in vegetation records from tropical Africa and South America during the last glacial: Quaternary Science Reviews, v. 29, no. 21-22, p.

Horrell, M. A., 1991, Phytogeography and paleoclimatic interpretation of the Maestrichtian: Palaeogeography, Palaeoclimatology, Palaeoecology, v. 86, p. 87-138.

Hsü, K.J., Cita, M.B., Ryan, W.B.F.,1973, The origin of the Mediterranean evaporites, *in* Kaneps, A. G., ed., Initial Reports of the Deep Sea Drilling Project 42, p. 1203–1231.

Huber, M., and Caballero, R., 2003, Eocene El Niño: evidence for robust tropical dynamics in the "hothouse": Science, v. 299, no. 5608, p. 877-881.

Huber, M., and Sloan, L.C., 2001, Heat transport, deep waters, and thermal gradients: Coupled simulation of an Eocene "greenhouse" climate: Geophysical Research Letters, v. 28, p. 3481–3484.

Jackson, S.T., Webb, R.S., Anderson, K.H., Overpeck, J.T., Webb, T., Williams, J.W., and Hansen, B.C.S., 2000, Vegetation and environment in Eastern North America during the Last Glacial Maximum: Quaternary Science Reviews, v. 19, p. 489-508

Jacob, R., Schafer, C., Foster, I., Tobis, M., and Anderson, J., 2001, Computational Design and Performance of the Fast Ocean Atmosphere Model, Version One, *in* Proceedings, 2001 International Conference on Computational Science, Alexandrov, V.N., Dongarra, J. J., and Tan, C. J. K., eds., Berlin, Germany, Springer-Verlag, p. 175–184,.

Jaramillo, C., Ochoa, D., Contreras, L., Pagani, M., Carvajal-ortiz, H., Pratt, L.M., Krishnan, S., Cardona, A., Romero, M., Quiroz, L., Rodriguez, G., and Rueda, M.J., 2010, Effects of Rapid Global Warming at the Paleocene-Eocene Boundary on Neotropical Vegetation: Science, v. 330, p. 957-961 .

Jiménez-Moreno, G., Anderson, R.S., Desprat, S., Grigg, L.D., Grimm, E.C., Heusser, L.E., Jacobs, B.F., López-Martínez, C., Whitlock, C.L., and Willard, D. a., 2010, Millennial-scale variability during the last glacial in vegetation records from North America: Quaternary Science Reviews, v. 29, no. 21-22, p. 2865-2881.

Jolly, D., 1997, Effect of Low Glacial Atmospheric CO_2 on Tropical African Montane Vegetation: Science, v. 276, no. 5313, p. 786-788.

Jolly, D., Haxeltine, A., 1997, Effect of low glacial CO_2 on tropical African montane vegetation: Science, v. 276, p. 786–787.

Kashiwagi, H., Ogawa, Y., and Shikazono, N., 2008, Relationship between weathering, mountain uplift, and climate during the Cenozoic as deduced from the global carbon-strontium cycle model: Palaeogeography, Palaeoclimatology, Palaeoecology, v. 270, p. 139-149.

Katz, M.E., Cramer, B.S., Toggweiler, J.R., Esmay, G., Liu, C., Miller, K.G., Rosenthal, Y., Wade, B.S., and Wright, J.D., 2011, Impact of Antarctic Circumpolar Current development on late Paleogene ocean structure: Science (New York, N.Y.), v. 332, no. 6033, p. 1076-1079.

Kazmin, V.G., and Napatov, L.M. editors, 1998, The Paleogeographic Atlas of Northern Eurasia. Institute of Tectonics of the Lithospheric Plates. Russian Academy of Natural Sciences, Moscow, Russia.

Keigwin, L., 1982, Isotopic Paleoceanography of the Caribbean and East Pacific: Role of Panama Uplift in Late Neogene Time: Science, v. 217, p. 350-353.

Keller, G. R., and Cather, S. M., editors, Basins of the Rio Grande Rift; structure, stratigraphy, and tectonic setting: Boulder, Colorado, Geological Society of America, Special Paper 291, p. 83-112.

Kelly, D.C., Bralower, T.J., Zachos, J.C., Silva, I.P., and Milano, U., 1996, Rapid diversification of planktonic foraminifera in the tropical Pacific (ODP Site 865) during the late Paleocene thermal maximum: Geology, v. 24, p. 423-426.

Kennett, J. P., and Stott, L. D., 1991, Abrupt deep-sea warming, palaeoceanographic changes and benthic extinctions at the end of the Palaeocene: Nature, v. 353, p. 225-229.

Kent, D.V., Muttoni, 2008. Equatorial convergence of India and early Cenozoic climate trends: Proceedings of the National Academy of Sciences of the U.S.A., v. 105, no. 42, p. 16,065-16,070.

Kim, S.J., Crowley, T.J., Erickson, D.J., Govindasamy, B., Duffy, P.B., and Lee, B.Y., 2007, High-resolution climate simulation of the last glacial maximum: Climate Dynamics, v. 31, no. 1, p. 1-16.

Knies, J., and Gaina, C., 2008, Middle Miocene ice sheet expansion in the Arctic: Views from the Barents Sea: Geochemistry, Geophysics, Geosystems, v. 9, no. 2., p. 1-8.

Kürschner, W.M., Kvaček, Z., Dilcher, D.L., 2008. The impact of Miocene atmospheric carbon dioxide fluctuations and the evolution of terrestrial ecosystems: Proceedings of the National Academy of Sciences of the U.S.A., v. 105, p. 449–453.

Lamb, S., 2011, Cenozoic tectonic evolution of the New Zealand plate-boundary zone: A paleomagnetic perspective: Tectonophysics, v. 509, no. 3-4, p. 135-164.

Lambeck, K., and Chappell, J., 2001, Sea level change through the last glacial cycle: Science, v. 292, no. 5517, p. 679-686.

Lambeck, K., Yokoyama, Y., Johnston, P., and Purcell, A., 2000, Global ice volumes at the Last Glacial Maximum and early Lateglacial: Earth and Planetary Science Letters, v. 181, p. 513-527

Lasaga, A. C., Berner, R. A., Garrels, R. M., 1984, An improved geochemical model of atmospheric CO2 fluctuations over the past 100 million years, *in* Proceedings of the Chapman Conference on Natural Variations in Carbon Dioxide and the Carbon Cycle, Tarpon Springs, FL, May 1985: Washington, D.C., American Geophysical Union, p. 397-411.

Lawver, L., 2003, Evolution of Cenozoic seaways in the circum-Antarctic region: Palaeogeography, Palaeoclimatology, Palaeoecology, v. 198, no. 1-2, p. 11-37.

Leng, Q., Langlois, G.A., and Yang, H., 2010, Early Paleogene Arctic terrestrial ecosystems affected by the change of polar hydrology under global warming: Implications for modern climate change at high latitudes: Science China Earth Sciences, v. 53, no. 7, p. 933-944.

Leon-Rodriguez, L., and Dickens, G.R., 2010, Constraints on ocean acidification associated with rapid and massive carbon injections: The early Paleogene record at ocean drilling program site 1215, equatorial Pacific Ocean: Palaeogeography, Palaeoclimatology, Palaeoecology, v. 298, no. 3-4, p. 409-420.

Lericolais, G., Bulois, C., Gillet, H., and Guichard, F., 2009, High frequency sea level fluctuations recorded in the Black Sea since the LGM: Global and Planetary Change, v. 66, no. 1-2, p. 65-75.

Liu, L., Eronen, J.T., and Fortelius, M., 2009, Significant mid-latitude aridity in the middle Miocene of East Asia: Palaeogeography, Palaeoclimatology, Palaeoecology, v. 279, no. 3-4, p. 201-206.

Liu, Z., Pagani, M., Zinniker, D., Deconto, R., Huber, M., Brinkhuis, H., Shah, S.R., Leckie, R.M., and Pearson, A., 2009, Eocene-Oligocene Climate Transition: Science, v. 323, p. 1187-1190.

Livermore, R., Nankivell, A., Eagles, G., and Morris, P., 2005, Paleogene opening of Drake Passage: Earth and Planetary Science Letters, v. 236, no. 1-2, p. 459-470.

Loehle, C., 2007, Predicting Pleistocene climate from vegetation in North America: Climate Of The Past, v. 3, p. 109-118.

Lomax, B., Beerling, D., Upchurch, G., and Otto-Bliesner, B., 2001, Rapid (10-yr) recovery of terrestrial productivity in a simulation study of the terminal Cretaceous impact event: Earth and Planetary Science Letters, v. 192, no. 2, p. 137-144.

Lourens, L.J., Sluijs, A., Kroon, D., Zachos, J.C., Thomas, E., Röhl, U., Bowles, J., and Raffi, I., 2005, Astronomical pacing of late Palaeocene to early Eocene global warming events: Nature, v. 435, no. 7045, p. 1083-1087.

McIver, E.E., Basinger, J.F., 1999. Early Tertiary floral evolution in the Canadian high Arctic. Annals of the Missouri Botanical Garden, v. 86, p. 523– 545.

Marchant, R., Cleef, A., Harrison, S.P., Hooghiemstra, H., Markgraf, V., van Boxel, J., Ager, T., Almeida, L., Anderson, R., Baied, C., Behling, H., Berrio, J.C., Burbridge, R., Björck, S., Byrne, R., Bush, M., Duivenvoorden, J., Flenley, J., De Oliveira, P., van Geel, B., Graf, K., Gosling, W. D., Harbele, S., van der Hammen, T., Hansen, B., Horn, S., Kuhry, P., Ledru, M.P., Mayle, F., Leyden, B., Lozano-García, S., Melief, A. M., Moreno, P., Moar, N. T., Prieto, A., van Reenen, G., Salgado-Labouriau, M., Schäbitz, F., Schreve-Brinkman, E. J., Wille, M., 2009, Pollen-based biome reconstructions for Latin America at 0, 6000 and 18 000 radiocarbon years ago: Climate of the Past, v. 5, no. 4, p. 725-767.

Markwick, P. J., 1997: Fossil crocodilians as indicators of Late Cretaceous and Cenozoic climates: Implications for using palaeontological data in reconstructing palaeoclimate. Palaeogeography, Palaeoclimatology, Palaeoecology, v. 137, p. 205–271.

Markwick, P.J., 2007. The paleogeographic and paleoclimatic significance of climate proxies for data–model comparisons, in Williams, M., Haywood, A.M., Gregory, F.J., Schmidt, D.N. eds., Deep-Time Perspectives on Climate Change: Marrying the Signal from Computer Models and Biological Proxies: The Micropaleontological Society Special Publications 002, The Geological Society, London, p. 251–312.

McQuarrie, N., and B. P. Wernicke, 2005, An animated tectonic reconstruction of southwestern North America since 36 Ma: Geosphere, v. 1, p. 147– 172

Mateer, N. J., Chen Pei-ji, 1992, A review of the nonmarine Cretaceous-Tertiary transition in China: Cretaceous Research, v. 13, no. 1, p. 81-90

Meert, J.G., Van der Voo, R., Powell, C. McA., Li, Z.X., McElhinny, M.W., Chen, Z. and D.T.A. Symons, 1993, A plate tectonic speed limit?: Nature, v. 363, p. 216-217.

Michalzik, D., 1996, Lithofacies, diagenetic spectra and sedimentary cycles of Messinian (Late Miocene) evaporites in SE Spain: Sedimentary Geology, v. 106, p. 203-222.

Micheels, A., Bruch, A.A., Uhl, D., Utescher, T., and Mosbrugger, V., 2007, A Late Miocene climate model simulation with ECHAM4/ML and its quantitative validation with terrestrial proxy data: Palaeogeography, Palaeoclimatology, Palaeoecology, v. 253, no. 1-2, p. 251-270.

Mikolajewicz, U., Maier-Reimer, E., Crowley, T.J., Kim, K., 1993, Effect of Drake and Panamanian Gateways on the circulation of an ocean model: Paleoceanography, v. 8, no. 4, p. 409-426.

Milanković, M. 1941, Kanon der Erdbestrahlung und seine Anwendung auf das Eiszeitproblem. 1998 English translation: Belgrade, Textbook Publishing Company, 634 pages.

Miller, K. G., Janacek, T. R., Katz, M. E., and Keil, D. J., 1987, Abyssal circulation and benthic foraminiferal changes near the Paleocene/Eocene boundary: Paleoceanography, v. 2, p. 741–761.

Miller, K.G., Wright, J.D., Katz, M.E., Browning, J.V., Cramer, B.S., Wade, B.S., Mizintseva, S.F., 2008, A view of Antarctic ice-sheet evolution from sea-level and deep-sea isotope changes during the Late Cretaceous–Cenozoic. *in*: Cooper, A.K., Barrett, P.J., Stagg, H., Storey, B., Stump, E., Wise, W., the 10th ISAES editorial team, eds., Antarctica: a Keystone in a Changing World: Proceedings of the 10th International Symposium on Antarctic Earth Sciences, Washington, DC ,The National Academies Press, p. 55–70.

Moucha, R., Forte, A.M., Rowley, D.B., Mitrovica, J.X., Simmons, N.A., and Grand, S.P., 2009, Deep mantle forces and the uplift of the Colorado Plateau: Geophysical Research Letters, v. 36, no. 19, p. 1-6.

Moucha, R., Forte, A.M., Rowley, D.B., Mitrovica, J.X., Simmons, N.A., and Grand, S.P., 2008, Mantle convection and the recent evolution of the Colorado Plateau and the Rio Grande Rift valley: Geology, v. 36, no. 6, p. 439.

Muhs, D. R., Aleinikoff, J. N., Stafford, T. W., Jr., Kihl, R., Been, J., Mahan, S. A., and Cowherd, S. (1999). Late Quaternary loess in northeastern Colorado: Part I—Age and paleoclimatic significance: GSA Bulletin, v. 111, no. 12, p. 1861-1875.

Muhs, D.R., and Bettis, E.A., 2000, Geochemical Variations in Peoria Loess of Western Iowa Indicate Paleowinds of Midcontinental North America during Last Glaciation: Quaternary Research, v. 53, no. 1, p. 49-61.

Muhs, D.R., McGeehin, J.P., Beann, J., and Fisher, E., 2004, Holocene loess deposition and soil formation as competing processes, Matanuska Valley, southern Alaska: Quaternary Research, v. 61, no. 3, p. 265-276.

Murphy, B.H., Farley, K.A., and Zachos, J.C., 2010, An extraterrestrial ^{3}He-based timescale for the Paleocene–Eocene thermal maximum (PETM) from Walvis Ridge, IODP Site 1266: Geochimica et Cosmochimica Acta, v. 74, no. 17, p. 5098-5108.

Murton, D.K., and Murton, J.B., 2011, Middle and Late Pleistocene glacial lakes of lowland Britain and the southern North Sea Basin: Quaternary International, (in press).

National Aeronautics and Space Administration (NASA), 2012, Blue Marble: http://earthobservatory.nasa.gov/Features/BlueMarble/ (accessed 2010-2012).

National Oceanic and Atmospheric Administration (NOAA), 2012, Paleoenvironmental Atlas of Beringia: http://www.ncdc.noaa.gov/paleo/parcs/atlas/beringia/ (accessed 2011-2012)

Nunes, F., and Norris, R.D., 2006, Abrupt reversal in ocean overturning during the Palaeocene/Eocene warm period: Nature, v. 439, no. 7072, p. 60-63.

Osborne, C.P., 2008, Atmosphere, ecology and evolution: what drove the Miocene expansion of C_4 grasslands?: The Journal of Ecology, v. 96, no. 1, p. 35-45.

Osborne, C.P. & Beerling, D.J. 2006, Nature's green revolution: the remarkable evolutionary rise of C_4 plants: Philosophical Transactions of the Royal Society of London B, v. 361, p. 173–194.

Otto-Bliesner, B., and Brady, E.C., 2006, Last Glacial Maximum and Holocene Climate in CCSM3: Journal of Climate, v. 19, p. 2526-2544.

Pak D. K. and Miller K. G., 1992, Paleocene to Eocene benthic foraminiferal isotopes and assemblages: implications for deepwater circulation: Paleoceanography, v. 7, p. 405–422.

Pancost, R.D., Steart, D.S., Handley, L., Collinson, M.E., Hooker, J.J., Scott, A.C., Grassineau, N.V., and Glasspool, I.J., 2007, Increased terrestrial methane cycling at the Palaeocene-Eocene thermal maximum: Nature, v. 449, no. 7160, p. 332-335.

Pandolfi, J.M., 1999, Response of Pleistocene Coral Reefs to Environmental Change Over Long Temporal Scales: Integrative and Comparative Biology, v. 39, no. 1, p. 113-130.

Parrish, J.T., Spicer, R.A., 1988, North Polar Late Cretaceous temperature curve:evidence from plant fossils: Geology, v. 16, p. 22–25.

Peppe, D.J., Royer, D.L., Cariglino, B., Oliver, S.Y., Newman, S., Leight, E., Enikolopov, G., Fernandez-Burgos, M., Herrera, F.M. Adams, J.M., Correa, E., Currano, E.D., Erickson, J.M., Hinojosa, L.F., Hoganson, J.W., Iglesias, A., Jaramillo, C.A., Johnson, K.R., Jordan, G.J., Kraft, N.J.B., Lovelock, E.C., Lusk, C.H., Niinemets, U., Penuelas, J., Rapson, G.,

Wing, S.L., Wright, I.J., 2011, Sensitivity of leaf size and shape to climate: global patterns and paleoclimatic applications: New Phytologist, v. 190, no. 3, p. 724-739.

Peters, S.E., Carlson, A. E., Kelly, D.C., and Gingerich, P.D., 2010, Large-scale glaciation and deglaciation of Antarctica during the Late Eocene: Geology, v. 38, no. 8, p. 723-726.

Poole, I., Cantrill, D., and Utescher, T., 2005, A multi-proxy approach to determine Antarctic terrestrial palaeoclimate during the Late Cretaceous and Early Tertiary: Palaeogeography, Palaeoclimatology, Palaeoecology, v. 222, no. 1-2, p. 95-121.

Prentice, I.C., and Jolly, D., 2000, Mid-Holocene and glacial-maximum vegetation geography of the northern continents and Africa: Journal of Biogeography, v. 27, no. 3, p. 507-519.

Pucéat, E., Lécuyer, C., Donnadieu, Y., Naveau, P., Cappetta, H., Ramstein, G., Huber, B.T., and Kriwet, J., 2007, Fish tooth $\delta^{18}O$ revising Late Cretaceous meridional upper ocean water temperature gradients: Geology, v. 35, no. 2, p. 107.

Rabassa, J., Coronato, A., and Martínez, O., 2011, Late Cenozoic glaciations in Patagonia and Tierra del Fuego: an updated review: Biological Journal of the Linnean Society, v. 103, p. 316–335.

Rabineau, M., Berné, S., Olivet, J.-L., Aslanian, D., Guillocheau, F., and Joseph, P., 2006, Paleo sea levels reconsidered from direct observation of paleoshoreline position during Glacial Maxima (for the last 500,000 yr): Earth and Planetary Science Letters, v. 252, no. 1-2, p. 119-137.

Rasmussen, S.O., Seierstad, I.K., Andersen, K.K., Bigler, M., Dahl-Jensen, D., and Johnsen, S.J., 2008, Synchronization of the NGRIP, GRIP, and GISP2 ice cores across MIS 2 and palaeoclimatic implications: Quaternary Science Reviews, v. 27, no. 1-2, p. 18-28.

Richter, S., Johnson, A, Dranoff, M., Lepage, B., and Williams, C., 2008, Oxygen isotope ratios in fossil wood cellulose: Isotopic composition of Eocene- to Holocene-aged cellulose: Geochimica et Cosmochimica Acta, v. 72, no. 12, p. 2744-2753.

Robert, C., and Kennett, J. P. 1994 Antarctic subtropical humid episode at the Paleocene-Eocene boundary: Clay-mineral evidence: Geology, v. 22, p. 211-214

Robinson, S.A., 2010, Shallow-water carbonate record of the Paleocene-Eocene Thermal Maximum from a Pacific Ocean guyot: Geology, v. 39, no. 1, p. 51-54.

Roeckner, E., Bäuml, G., Bonaventura, L., Brokopf, R., Esch, M., Giorgetta, M., Hagemann, S., Kirchner, I., Kornblueh, L., Manzini, E., Rhodin, A., Schlese, U., Schulzweida, U., Tompkins, A., 2003, The Atmospheric General Circulation Model ECHAM5, Part I, Model Description: Max-Planck-Institut für Meteorologie, Report No. 349, p. 1-127.

Rowley, D.B., and Garzione, C.N., 2007, Stable Isotope-Based Paleoaltimetry: Annual Review of Earth and Planetary Sciences, v. 35, no. 1, p. 463-508.

Ruddiman, W.F., 2006, What is the timing of orbital-scale monsoon changes?: Quaternary Science Reviews, v. 25, no. 7-8, p. 657-658.

Rohling and Zachariasse, 1996, Red Sea outflow during the Last Glacial Maximum: Quaternary International, v. 31, p. 77-83.

Scher, H.D., Bohaty, S.M., Zachos, J.C., and Delaney, M.L., 2011, Two-stepping into the icehouse: East Antarctic weathering during progressive ice-sheet expansion at the Eocene-Oligocene transition: Geology, v. 39, no. 4, p. 383-386.

Scher, H.D., and Martin, E.E., 2006, Timing and Climatic Consequences of the Opening of Drake Passage: Science, v. 312, p. 428-432.

Schmitz, B., Speijer, R.P., and Aubry, M.P., 1996, Latest Paleocene benthic extinction event on the southern Tethyan shelf (Egypt): Foraminiferal stable isotopic ($\delta^{13}C$, $\delta^{18}O$) records: Geology, v. 24, no. 4, p. 347-350.

Scotese, C.R., 2008, The PALEOMAP Project PaleoAtlas for ArcGIS, Cenozoic Paleogeographic and Plate Tectonic Reconstructions: PALEOMAP Project, Arlington, Texas, Volumes 1-6.

Scotese, C.R., Boucot, A.J., McKerrow W.S., 1999, Gondwanan palaeogeography and palaeoclimatology: Journal of African Earth Sciences, v 28, no. 1, p. 99-114.

Scotese, C.R., Illich, H., Zumberge, J, and Brown, S., 2007, The GANDOLPH Project: Year One Report: Paleogeographic and Paleoclimatic Controls on Hydrocarbon Source Rock Deposition, A Report on the Methods Employed, the Results of the Paleoclimate Simulations (FOAM), and Oils/Source Rock Compilation, Conclusions at the End of Year One, February, Houston, Texas, GeoMark Research Ltd, 142 pp.

Sewall, J.O., van de Wal, R.S.W., van der Zwan, K., van Oosterhout, C., Dijkstra, H.A., and Scotese, C.R., 2007, Climate model boundary conditions for four Cretaceous time slices: Climate of the Past, v. 3, no. 4, p. 647-657.

Sluijs, A., Bijl, P.K., Schouten, S., Röhl, U., Reichart, G.J., and Brinkhuis, H., 2011, Southern ocean warming, sea level and hydrological change during the Paleocene-Eocene thermal maximum: Climate of the Past, v. 7, no. 1, p. 47-61.

Sluijs, A., Schouten, S., Pagani, M., Woltering, M., Brinkhuis, H., Damsté, J.S.S., Dickens, G.R., Huber, M., Reichart, G.J., Stein, R., Matthiessen, J., Lourens, L.J., Pedentchouk, N., Backman, J., Moran, K., and the Expedition 302 scientists, 2006, Subtropical Arctic Ocean temperatures during the Palaeocene/Eocene thermal maximum: Nature, v. 441, no. 7093, p. 610-613.

Smith, J., Vance, D., Kemp, R.A, Archer, C., Toms, P., King, M., and Zárate, M., 2003, Isotopic constraints on the source of Argentinian loess – with implications for atmospheric circulation and the provenance of Antarctic dust during recent glacial maxima: Earth and Planetary Science Letters, v. 212, no. 1-2, p. 181-196.

Smith, F., Wing, S., and Freeman, K., 2007, Magnitude of the carbon isotope excursion at the Paleocene–Eocene thermal maximum: The role of plant community change: Earth and Planetary Science Letters, v. 262, no. 1-2, p. 50-65.

Smith, F. A., Wing, S. L., Freeman, K. H., 2007, Magnitude of the carbon isotope excursion at the Paleocene–Eocene thermal maximum: The role of plant community change: Earth and Planetary Science Letters, v. 262, p. 50-65.

Soulet, G., Ménot, G., Garreta, V., Rostek, F., Zaragosi, S., Lericolais, G., and Bard, E., 2011, Black Sea "Lake" reservoir age evolution since the Last Glacial — Hydrologic and climatic implications: Earth and Planetary Science Letters, v. 308, no. 1-2, p. 245-258.

Spicer, R.A., Ahlberg, A.., Herman, A. B., Hofmann, C. C., Raikevich, M., Valdes, P.J., Markwick, P.J., 2008. The Late Cretaceous continental interior of Siberia: A challenge for climate models: Earth andPlanetary Science Letters, v. 267, p. 228–235.

Spicer, R. A., and Herman, A.B., 2010, The Late Cretaceous environment of the Arctic: A quantitative reassessment based on plant fossils: Palaeogeography, Palaeoclimatology, Palaeoecology, v. 295, no. 3-4, p. 423-442.

Spicer, R. A., Ahlberg, A., Herman, A.B., Hofmann, C.C., Raikevich, M., Valdes, P.J., and Markwick, P.J., 2008, The Late Cretaceous continental interior of Siberia: A challenge for climate models: Earth and Planetary Science Letters, v. 267, no. 1-2, p. 228-235.

Spielhagen, R.F., and Tripati, A., 2009, Evidence from Svalbard for near-freezing temperatures and climate oscillations in the Arctic during the Paleocene and Eocene: Palaeogeography, Palaeoclimatology, Palaeoecology, v. 278, no. 1-4, p. 48-56.

Stap, L., Lourens, L.J., Thomas, E., Sluijs, A., Bohaty, S., and Zachos, J.C., 2010, High-resolution deep-sea carbon and oxygen isotope records of Eocene Thermal Maximum 2 and H2: Geology, v. 38, no. 7, p. 607-610.

Stehlin, H.G., 1910. Remarques sur les faunules de Mammifères des couches Éocènes et Oligocènes du Bassin de Paris. Bulletin de la Societe Geologique de France v. 9, no. 4, p. 488–520.

Sun, X., and Wang, P., 2005, How old is the Asian monsoon system?—Palaeobotanical records from China: Palaeogeography, Palaeoclimatology, Palaeoecology, v. 222, no. 3-4, p. 181-222.

Suwa, M., and Bender, M.L., 2008, Chronology of the Vostok ice core constrained by O2/N2 ratios of occluded air, and its implication for the Vostok climate records: Quaternary Science Reviews, v. 27, no. 11-12, p. 1093-1106.

Tajika, E., 1998, Climate change during the last 150 million years: reconstruction from a carbon cycle model: Earth and Planetary Science Letters, v. 160, p. 695-707.

Takahara, H., Sugita, S., Harrison, S. P., Miyoshi, N., Morita, Y.& Uchiyama, T., 2000, Pollen-based reconstruction of Japanese biomes at 0, 6000 and 18,000 ^{14}C yr bp: Journal of Biogeography, v. 27, p. 665–683.

Tang, H., Micheels, A., Eronen, J., and Fortelius, M., 2011, Regional climate model experiments to investigate the Asian monsoon in the Late Miocene: Climate of the Past Discussions, v. 7, no. 2, p. 841-886.

Tarasov, P.E., Volkova, V.S., Webb, T., Guiot, J., Andreev, A.A., Bezusko, L.G., Bezusko, T.V., Bykova, G.V., Dorofeyuk, N.I., Kvavadze, E.V., Osipova, I.M., Panova, N.K., and Sevastyanov, D.V., 2000, Last glacial maximum biomes reconstructed from pollen and plant macrofossil data from northern Eurasia: Journal of Biogeography, v. 27, no. 3, p. 609-620.

Thomas, D.J., Bralower, T.J., and Jones, C.E., 2003, Neodymium isotopic reconstruction of late Paleocene–early Eocene thermohaline circulation: Earth and Planetary Science Letters, v. 209, no. 3-4, p. 309-322.

Thorn, V.C., and DeConto, R., 2006, Antarctic climate at the Eocene/Oligocene boundary — climate model sensitivity to high latitude vegetation type and comparisons with the palaeobotanical record: Palaeogeography, Palaeoclimatology, Palaeoecology, v. 231, no. 1-2, p. 134-157.

Timireva, S., and Velichko, A., 2006, Depositional environments of the Pleistocene loess-soil series inferred from sand grain morphoscopy—A case study of the East European Plain: Quaternary International, v. 152-153, p. 136-145.

Tripati, A., and Elderfield, H., 2005, Deep-Sea Temperature and Circulation Changes at the Paleocene-Eocene ThermalMaximum: Science, v. 308, p. 1894-1898.

Tripati, A., Zachos, J., Marincovich, L., and Bice, K., 2001, Late Paleocene Arctic coastal climate inferred from molluscan stable and radiogenic isotope ratios: Palaeogeography, Palaeoclimatology, Palaeoecology, v. 170, no. 1-2, p. 101-113.

Újvári, G., Kovács, J., Varga, G., Raucsik, B., Marković, S.B., 2010, Dust flux estimates for the Last Glacial Period in East Central Europe based on terrestrial records of loess deposits: a review: Quaternary Science Reviews, v. 29, p. 3157-3166.

Upchurch, G. R. Jr., Lomax, B. H., and Beerling, D. J., 2007, Paleobotanical Evidence for Climatic Change across the Cretaceous–Tertiary Boundary, North America: Twenty Years After Wolfe and Upchurch: Courier Forschungsinstitut Senckenberg, v. 258, p. 57–74.

Upchurch, G. R., Otto-Bliesner, B.L., Scotese, C.R., 1999, Upchurch et al, 1999, Terrestrial vegetation and its effects on climate during the latest Cretaceous, *in* Barrera, E, and Johnson, C. C., eds., Evolution of the Cretaceous Ocean-Climate System: Geological Society of America Special Paper 332, p. 407-436.

Utescher, T., and Mosbrugger, V., 2007, Eocene vegetation patterns reconstructed from plant diversity — A global perspective: Palaeogeography, Palaeoclimatology, Palaeoecology, v. 247, no. 3-4, p. 243-271.

Van der Ham, R. W. J. M., van Konijnenburg-van Cittert, J.H.A., Dortangs, R.W., Herngreen, G.F.W., van der Burgh, J., 2003, Brachyphyllum patens (Miquel) comb. nov. (Cheirolepidiaceae?): remarkable conifer foliage from the Maastrichtian type area (Late Cretaceous, NE Belgium, SE Netherlands): Review of Palaeobotany and Palynology, v. 127 p. 77-97

Warwick, P. D., and Shakoor, T., 1993, Lithofacies and Depositional Environments of the Coal-Bearing Paleocene Patala Formation, Salt Range Coal Field, Northern Pakistan *in* Warwick,

P. D., and Bruce R. Wardlaw, B. R., eds., Regional Studies of the Potwar Plateau Area, Northern Pakistan: U.S. Geological Survey Bulletin 2078–I, p. 1-23

Westaway, K.E., Morwood, M.J., Sutikna, T., Moore, M.W., Rokus, A.D., van den Bergh, G.D., Roberts, R.G., and Saptomo, E.W., 2009, Homo floresiensis and the late Pleistocene environments of eastern Indonesia: defining the nature of the relationship: Quaternary Science Reviews, v. 28, no. 25-26, p. 2897-2912.

Wheeler, E. A., and Lehman, T.M., 2005, Upper Cretaceous–Paleocene conifer woods from Big Bend National Park, Texas: Palaeogeography, Palaeoclimatology, Palaeoecology, v. 226, no. 3-4, p. 233-258.

Williams, C.J., Trostle, K.D., and Sunderlin, D., 2010, Fossil wood in coal-forming environments of the late Paleocene–early Eocene Chickaloon Formation: Palaeogeography, Palaeoclimatology, Palaeoecology, v. 295, no. 3-4, p. 363-375.

Wilson, D. S., Jamieson, S. S. R., Barrett, P. J., Leitchenkov, G., Gohl, K., Larter, R. D., 2011, Antarctic topography at the Eocene–Oligocene boundary: Palaeogeography, Palaeoclimatology, Palaeoecology, (in press).

Wing, S.L., and Harrington, G.J., 2001, Floral response to rapid warming in the earliest Eocene and implications for concurrent faunal change: Paleobiology, v. 27, no. 3, p. 539-563.

Winguth, A., Shellito, C., Shields, C., and Winguth, C., 2010, Climate Response at the Paleocene–Eocene Thermal Maximum to Greenhouse Gas Forcing—A Model Study with CCSM3: Journal of Climate, v. 23, no. 10, p. 2562-2584.

Wolfe, J. A., 1987, Late Cretaceous-Cenozoic history of diciduousness and the terminal Cretaceous event: Paleobiology, v. 13, p. 215-226.

Wolfe, J. A., 1994, Alaskan Palaeogene climates as inferred from the CLAMP database: NATO ASI Series, v. 127, p. 223-237.

Wolfe, J. A., and Upchurch, G. R., 1987, North American non-marine climates and vegetation during the Late Cretaceous. Palaeogeography, Palaeoclimatology, Palaeoecology, v. 61, p. 33-77.

Wu, H., Guiot, J., Brewer, S., and Guo, Z., 2007, Climatic changes in Eurasia and Africa at the last glacial maximum and mid-Holocene: reconstruction from pollen data using inverse vegetation modelling: Climate Dynamics, v. 29, no. 2-3, p. 211-229.

Yin, A., 2010, Cenozoic tectonic evolution of Asia: A preliminary synthesis: Tectonophysics, v. 488, p. 293-325.

Yu, G., Chen, X., Ni, J., Cheddadi, R., Guiot, J., Han, H., Harrison, S.P., Huang, C., Ke, M. Kong, Z., Li, S., Li, W., Liew, P., Liu, G., Liu, J., Liu, Q, Liu, K., Prentice, I. C., Qui, W., Ren, G., Song, C., Sugita, S., Sun, X., Tang, L., Van Campo, E., Xia, Y., Xu, Q., Yan, S.,Yang, X., Zhao, J., and Zheng, Z., 2000, Palaeovegetation of China: a pollen data-based synthesis for the mid-Holocene and last glacial maximum: Journal of Biogeography, v. 27, p. 635–664.

Zachos, J.C., Berggren, W.A., Aubry, M., Mackensen, A., 1992, ISOTOPE AND TRACE ELEMENT GEOCHEMISTRY OF EOCENE AND OLIGOCENE FORAMINIFERS FROM SITE 748, KERGUELEN PLATEAU, *in* Barbu, E., ed., Proceedings of the Ocean Drilling Program, Scientific Results, Vol. 120. Part 1, Central Kerguelen Plateau, p. 839-854.

Zachos, J.C., Dickens, G.R., Zeebe, R.E., 2008, An early Cenozoic perspective on greenhouse warming and carbon-cycle dynamics: Nature, v. 45, no. 17, p. 279-283.

Zachos, J.C., McCarren, H., Murphy, B., Röhl, U., and Westerhold, T., 2010, Tempo and scale of late Paleocene and early Eocene carbon isotope cycles: Implications for the origin of hyperthermals: Earth and Planetary Science Letters, v. 299, no. 1-2, p. 242-249.

Zachos, J., Pagani, M., Sloan, L., Thomas, E., and Billups, K., 2001, Trends, rhythms, and aberrations in global climate 65 Ma to present: Science, v. 292, no. 5517, p. 686-93.

Zachos, J.C., Röhl, U., Schellenberg, S.A, Sluijs, A., Hodell, D.A, Kelly, D.C., Thomas, E., Nicolo, M., Raffi, I., Lourens, L.J., McCarren, H., and Kroon, D., 2005, Rapid acidification of the ocean during the Paleocene-Eocene thermal maximum: Science, v. 308, no. 5728, p. 1611-5.

Zachos, J.C., Schouten, S., Bohaty, S., Quattlebaum, T., Sluijs, A., Brinkhuis, H., Gibbs, S.J., and Bralower, T.J., 2006, Extreme warming of mid-latitude coastal ocean during the Paleocene-Eocene Thermal Maximum: Inferences from TEX_{86} and isotope data: Geology, v. 34, no. 9, p. 737.

Zachos, J.C., Wara, M.W., Bohaty, S., Delaney, M.L., Petrizzo, M.R., Brill, A., Bralower, T.J., and Premoli-Silva, I., 2003, A transient rise in tropical sea surface temperature during the Paleocene-Eocene thermal maximum: Science, v. 302, no. 5650, p. 1551-1554.

Zhang, R., and Delworth, T.L., 2005, Simulated Tropical Response to a Substantial Weakening of the Atlantic Thermohaline Circulation: Journal of Climate, v. 18, no. 12, p. 1853-1860.

Zhang, Z., Nisancioglu, K.H., Flatøy, F., Bentsen, M., Bethke, I., and Wang, H., 2011, Tropical seaways played a more important role than high latitude seaways in Cenozoic cooling: Climate of the Past, v. 7, no. 3, p. 801-813.

Zonenshayn., L. P., Kuzmin, M. I., and Natapov, L. M., editors,1990, Geology of the USSR; a plate-tectonic synthesis, *in* Page, B., M., ed., Geodynamics series: Washington, D. C., American Geophysical Union.

BIOGRAPHICAL INFORMATION

Clinton Crowley is a geologist and natural history artist living in Fort Worth, Texas. He holds a Bachelor of Science in Geology from New Mexico Institute of Mining and Technology. His illustrations have been published in local and international scientific journals including the National Geographic and PALAIOS, and in news publications around the world. He is employed at Joint Resources Company, and oil & gas exploration company, and is a member of the Fort Worth Geological Society.

Clinton has worked at oil & gas companies as a mudlogger and geotech, and has worked at Joint Resources Company for six years. He intends to work as an exploration geologist in onshore oil & gas plays. He maintains a strong, lifelong interest in paleogeography, and will continue to work with Dr. Scotese and the PALEOMAP Project as well.